보건학박사 학위논문

Characteristics of Atmospheric Wet Deposition of Total Mercury in Seoul, Korea

: Identification of Possible Source Locations using Receptor Model

서울시 대기 중 총 수은의
습식침적량 특성에 관한 연구
: 수용모델을 이용한 오염 가능 지역 위치 파악

2013 년 2월

서울대학교 대학원

보건학과 환경보건학 전공

서 용 석

Characteristics of Atmospheric Wet Deposition of Total Mercury in Seoul, Korea

: Identification of Possible Source Locations using Receptor Model

A dissertation submitted in partial fulfillment of
the requirement for the degree of
Doctor of Philosophy in Public Health

To the Faculty of the Graduate School of Public Health
at
Seoul National University

by

Seo, Yong-Seok

Data approved: December, 2012

Kyung-Duk Zoh

Kyungho Choi

Domyung Paek

Young-Ji Han

Seung-Muk Yi

서울시 대기 중 총 수은의 습식침적량 특성에 관한 연구

: 수용모델을 이용한 오염 가능 지역 위치 파악

지도교수 이 승 묵

이 논문을 보건학박사 학위논문으로 제출함
2012년 10월

서울대학교 대학원
보건학과 환경보건 전공
서 용 석

서용석의 보건학박사 학위논문을 인준함
2012년 12월

위 원 장	조 경 덕	(인)
부위원장	최 경 호	(인)
위 원	백 도 명	(인)
위 원	한 영 지	(인)
위 원	이 승 묵	(인)

ABSTRACT

Precipitation samples for total mercury (TM) were collected with a modified MIC-B sampler concurrent with atmospheric gaseous oxidized mercury (GOM) and particulate bound mercury (PBM) concentrations on the roof of Graduate School of Public Health building in Seoul, Korea from January 2006 to December 2009.

These samples were used to determine the seasonal variations in TM wet deposition, to determine the contribution of GOM and PBM scavenging to mercury wet deposition, and to identify source areas contributing to the high TM wet deposition using a Lagrangian particle dispersion model (LPDM).

The volume weighted mean (VWM) TM concentrations in 2006, 2007, 2008, and 2009 were 10.1 ± 17.0 ng L^{-1}, 16.3 ± 16.5 ng L^{-1}, 14.3 ± 11.9 ng L^{-1}, and 10.2 ± 14.8 ng L^{-1}, respectively and the TM wet deposition flux in 2006, 2007, 2008, and 2009 were 16.8 μg m^{-2}, 20.2 μg m^{-2}, 18.5 μg m^{-2} and 16.4 μg m^{-2}, respectively.

During the sampling period, the VWM TM concentration was highest in winter, followed by spring, fall, and summer while the wet deposition flux was highest in summer, followed by spring, fall, and winter.

Nonparametric Mann-Whitney test revealed that there were statistical differences in VWM TM concentration between winter and other seasons ($p<0.01$) and there were statistical differences in wet deposition flux between summer and other seasons ($p<0.01$) except winter ($p=0.09$). The high VWM TM concentration in winter was associated with the combined effect of the low rainfall depth and high speciated mercury (GOM and PBM) concentrations. In addition, the high VWM TM concentration in spring was due to the yellow sand events suggesting that GOM and PBM present in the rain were long-range transported from China during this period. Yellow sand events occurred immediately prior to wet deposition events in 2006 and in 2007. During those periods GOM and PBM concentrations were elevated resulting in high VWM TM concentrations.

The high TM wet deposition flux in summer (53% of total TM wet deposition flux) was primarily due to the high precipitation rate in summer (77% of total rainfall depth).

Multiple linear regression showed that scavenging coefficient (SC) for GOM was much higher than SC for PBM suggesting that GOM was more effectively scavenged by wet deposition than PBM (SC_{GOM} = 715 and SC_{PBM} = 407).

Joint-probability LPDM (JP-LPDM) indicated that the main sources of TM wet deposition were Guizhou, Guangdong, Liaoning, Hunan,

Shaanxi, Nei Mongol and Gobi Desert. This suggests that both anthropogenic sources such as industrial areas and natural source areas such as deserts contributed to the high TM concentration in Seoul, Korea.

Key words: total mercury (TM), gasoues oxidized mercury (GOM), particulate bound mercury (PBM), wet deposition, scavenging coefficient, Joint-probability LPDM (JP-LPDM)

Student number: 2005-31234

TABLE OF CONTENTS

ABSTRACT i

TABLE OF CONTENTS iv

LIST OF TABLES vi

LIST OF FIGURES vii

Chapter 1. Introduction

1.1. Backgrounds 1

1.2. Overviews 5

1.3. Objectives 5

References 7

Chapter 2. Theoretical background

2.1. Physical and chemical properties of mercury 11

2.2. Mercury in the environment 13

2.3. Atmospheric wet deposition of mercury 24

2.4. Sources of mercury 42

2.5. Health effects of mercury 46

2.6. Model description 52

References 60

Chapter 3. Characteristics of total mercury (TM) wet deposition: Scavenging of atmospheric mercury species

Abstract....76

3.1. Introduction....78

3.2. Materials and methods....81

3.3. Results and discussion....87

3.4. Conclusions....101

References....103

Chapter 4. Source identification of total mercury (TM) wet deposition using Lagrangian particle dispersion model (LPDM)

Abstract....109

4.1. Introduction....111

4.2. Materials and methods....113

4.3. Model description....117

4.4. Comparison between emission inventories and LPDM results....123

4.5. Results and Discussion....123

References....140

Supporting Information....147

Chapter 5. Conclusions....153

국문초록....156

LIST OF TABLES

Table 2-1. Physical/chemical properties of mercury and its compounds...12

Table 2-2. Summary of monitoring networks for mercury wet deposition 30

Table 2-3. Summary of TM wet deposition in Asia 41

Table 3-1. Summary of atmospheric speciated mercury concentrations....93

Table 3-2. Comparisons with previous studies for TM wet deposition flux 96

Table 4-1. Summary of TM wet deposition in this study.....124

Table 4-2. Summary of atmospheric speciated mercury concentrations

.....128

Table 4-3. Comparisons with previous studies for TM wet deposition flux 130

Table 4-4. Spatial correlation index (r) between LPDM results and emissions inventory.....137

LIST OF FIGURES

Figure 2-1. Mercury oxidation, reduction, and mass transfer processes in the atmosphere 13

Figure 2-2. Mercury chemistry in droplets 27

Figure 2-3. Locations of the UMAQL Great Lakes Atmospheric Monitoring Sites, NADP Mercury Deposition Network Sites, NADP Air Mercury Network Sites and AMNet ambient air mercury speciation sites 32

Figure 2-4. Total mercury concentration and wet deposition annual gradient maps from the MDN program for the year 2011 35

Figure 2-5. Mercury measurement sites within the EMEP network as of 2009 39

Figure 3-1. Location of sampling site in this study (Seoul, Korea) 81

Figure 3-2. Seasonal variation of VWM TM concentration, wet deposition flux, and rainfall depth in 2006 and 2007 88

Figure 3-3. Relationship between rainfall depth and VWM TM concentration by season 97

Figure 3-4. Relationship between rainfall depth and TM wet deposition flux by season 99

Figure 4-1. The location of sampling site in this study (Seoul, Korea) 114

Figure 4-2. Relationship between rainfall depth and VWM TM concentration. 132

Figure 4-3. JP-LPDM result calculated from Approach 5 for VWM TM concentration 136

Chapter 1

Introduction

1.1. Backgrounds

Mercury (Hg), a well-known environmental toxic pollutant, is among the most highly bioaccumulative trace metals in the food chain (Meili, 1991) and is now classified as a persistent bioaccumulative and toxic (PBT) chemical by the United States Environmental Protection Agency (U.S. EPA, 1997). Mercury continuously goes through the emission and deposition cycle after its release, and therefore the atmosphere plays an important role in the environmental cycling of mercury. Mercury can be distributed long distances from sources through atmospheric transport in its gaseous elemental form (Bullock et al., 1998; Mason et al., 1994; Mason and Sheu, 2002; Petersen et al., 1995) so the relationship between source and environmental effects is complex.

Mercury has various physical and chemical forms including different oxidation states making its behavior complex. After release into the environment mercury can be transformed from one species to another via photo-oxidation, photo-reduction, reactions with halides, and other

oxidation/reduction reactions. Therefore these transformations are very important because various species of mercury have different characteristics with respect to solubility, volatility, and deposition velocities (Bullock and Brehme, 2002; Fitzgerald et al., 1998; Grigal, 2002; Schroeder and Munthe, 1998; Xu et al., 2000).

Gaseous elemental mercury (GEM) is the predominant form in ambient air (> 95%) and its residence time is 0.5 ~ 2 years due to its low solubility and inertness (Schroeder and Munthe, 1998) which does not allow it to be efficiently incorporated into wet deposition.

On the other hand, gaseous oxidized mercury (GOM) is very water soluble, with relatively strong surface adhesion properties (Han et al., 2005) and can be scavenged by rain within precipitating clouds and below clouds (Lin and Pehkonen, 1999). GOM has a significantly larger scavenging ratio and deposition velocity than GEM (Lindberg and Stratton, 1998).

Particulate bound mercury (PBM) can be wet deposited relatively efficiently if its host particles are in or below precipitating clouds (Cohen et al., 2004). As a result, the predominant form of mercury in wet deposition is in the oxidized (GOM) or particulate forms (PBM).

Mercury is emitted from both natural sources such as volcanoes, weathering of rock, oceans, biomass burning, vegetation, geothermal sources and topsoil enriched in mercury, and from anthropogenic sources such as fossil fuel combustion, cement production, chlor-alkali

facilities, ferrous and non-ferrous metals manufacturing facilities, ore processing facilities, incinerators, industrial uses (batteries, electrical apparatus, etc.), chemical production facilities and re-emission of previously deposited anthropogenic mercury (Pirrone et al., 2010; UNEP, 2002).

Pacyna et al. (2006) reported that much of the worldwide atmospheric mercury in 2000 originated from coal combustion (65%), gold production (11%), non-ferrous smelters (7%), and cement production (6%). Selin et al. (2007) also suggested that anthropogenic sources contribute approximately 60% to total global emissions, which is almost 1.5 times the contribution of natural sources.

Atmospheric transport, fate, and bioaccumulation of mercury and methylmercury (MeHg) are critical contamination issues. Especially, mercury contamination of fish is a widespread problem with important public health concerns (Fitzgerald and Clarkson, 1991; Lindqvist et al. 1991; Weiner and Stokes, 1990). Previous studies reported high concentrations of methylmercury in fish in non-industrial areas such as the Arctic (Wagemann et al., 1996; Evers et al., 1998; Muir et al., 2001).

The increasing concentration of mercury, principally as MeHg, in higher trophic levels of the aquatic food chain contrasts sharply with that of other trace metals whose concentrations remain constant or decrease with increasing levels in the aquatic food web (Mason et al.,

1995). Although low levels of mercury are present in the ambient air, atmospheric mercury can be transported over long distances because of the long lifetime of GEM. Therefore, mercury can affect ecosystems on local, regional, and global scales.

Mercury exposure can induce serious neurological conditions in humans such as paresthesia, memory loss, slurred speech, tremors, and cerebellar ataxia, even at low concentrations (Cranmer et al., 1996).

Seigneur et al. (2004) estimated that 21% of total mercury wet deposition in the United States originated from China. According to Weiss-Penzias et al. (2007), 31% of Hg^0 high concentration events at Mt. Bachelor Observatory, a remote location on the West Coast of the U.S. were due to long-range transport from East Asia, including China.

Many studies have attempted to characterize mercury wet deposition (Glass and Sorensen, 1999; Guo et al., 2008; Huang and Gustin, 2012; Keeler et al., 2006; Lai et al., 2007; Mason et al., 2000; Prestbo and Gay, 2009; Risch et al., 2011; Sakata and Marumoto, 2005; Selin and Jacob, 2008) and there have been a few prior studies that used a Lagrangian Particle Dispersion Model (LPDM) to obtain the source-receptor relationships. However, there have been no studies involving mercury wet deposition data.

1.2. Overviews

This dissertation consists of 5 chapters. Chapter 1 presents an introduction that reviews related research backgrounds, and associated details of the objectives of this study. Chapter 2 presents a theoretical background of the fundamental knowledge about mercury compounds and receptor models. Chapter 3 and Chapter 4 discuss the "Characteristics of total mercury (TM) wet deposition: Scavenging of atmospheric mercury species" and "Source identification of total mercury (TM) wet deposition using a Lagrangian Particle Dispersion Model (LPDM), respectively. Chapter 5 summarized the major findings in this study.

1.3. Objectives

The overall objectives of this study were to determine the seasonal variations in atmospheric wet deposition of total mercury (TM), and identify the possible source locations using receptor model. To accomplish these objectives, total mercury wet deposition was measured and combined with calculated back-trajectories and back-dispersion.

The specific objectives of this study were summarized as follows:

1. To determine the seasonal variations in atmospheric wet deposition of total mercury (TM) in Seoul, Korea
2. To identify the relationship of total mercury in precipitation among the variables (e.g. rainfall depth, volume-weighted mean concentration, flux)
3. To identify the source locations of TM wet deposition in Seoul, Korea. The modeling results were compared with a recent emissions inventory.

References

Bullock, O. R., Brehme, K. A., Mapp, G. R., 1998. Lagrangian modeling of mercury air emission, transport and deposition: an analysis of model sensitivity to emissions uncertainty. Science of the Total Environment 213, 1-12.

Bullock, O. R. and Brehme, K. A., 2002. Atmospheric mercury simulation using the CMAQ model: formulation description and analysis of wet deposition results. Atmospheric Environment 36, 2135-2146.

Cohen, M., Artz, R., Draxler, R., Miller, P., Niemi, D., Ratte, D., Deslauriers, M., Duvar, R., Laurin, R., Slotnick, J., Nettesheim, T., McDonald, J., 2004. Modeling the atmospheric transport and deposition of mercury to the Great Lakes. Environmental Research 95, 247-265.

Cranmer, M., Gilbert, S., Cranmer, J., 1996. Neurotoxicity of mercury indicators and effects of low-level exposure: overview. Neurotoxicology 17, 9–14.

Evers, D. C., Kaplan, J. D., Meyer, M. W., Reaman, P. S., Braselton,W.E., Major, A., Burgess, N., Scheuhammer, A.M., 1998. Geographic trends in mercury measured in common loon feathers and blood. Environmental Toxicology and Chemistry 17, 173–183.

Fitzgerald, W. F. and Clarkson, T. W., 1991. Mercury and monomethylmercury: present and future concerns. Environmental Health Perspectives 96, 159-166.

Fitzgerald, W. F., Engstrom, D. R., Mason, R. P., Nater, E.A., 1998. The case for atmospheric mercury contamination in remote areas. Environmental Science and Technology 32, 1-7.

Glass, G. E., Sorensen, J. A., 1999. Six-year trend (1990-1995) of wet mercury deposition in the Upper Midwest, U. S. A. Environmental Science and Technology 33, 3303-3312.

Grigal, D. F., 2002. Inputs and outputs of mercury from terrestrial watersheds: a review. Environmental Reviews 10, 1-39.

Guo, Y., Feng, X., Li, Z., He, T., Yan, H., Meng, B., Zhang, J., Qiu, G., 2008. Distribution and wet deposition fluxes of total and methyl

mercury in Wujiang River Basin, Guizhou, China. Atmospheric Environment 42, 7096-7103.

Han, Y. J., Holsen, T. M., Hopke, P. K., Yi, S. M., 2005. Comparison between back-trajectory based modeling and Lagrangian backward dispersion modeling for locating sources of reactive gaseous mercury. Environmental Science and Technology 39, 1715-1723.

Huang, J. and Gustin, M. S., 2012. Evidence for a free troposphere source of mercury in wet deposition in the western United States. Environmental Science and Technology 46, 6621-6629.

Keeler, G. J., Landis, M. S., Norris, G. A., Christianson, E. M., Dvonch, J. T., 2006. Sources of mercury wet deposition in eastern Ohio, USA. Environmental Science and Technology 40, 5874-5881.

Lai, S. O., Holsen, T. M., Hopke, P. K., Liu, P., 2007. Wet deposition of mercury at a New York state rural site: Concentrations, fluxes, and source areas. Atmospheric Environment 41, 4337-4348.

Lin, C.-J. and Pehkonen, S.O., 1999. The chemistry of atmospheric mercury: a review. Atmospheric Environment 33, 2067–2679.

Lindberg, S. E. and Stratton, W. J., 1998, Atmospheric mercury speciation: concentrations and behavior of reactive gaseous mercury in ambient air. Environmental Science and Technology 32, 49-57.

Lindqvist, O., Aastrup, M., Andersson, A., Bringmark, L., Hovsenius, G., Hakanson, L., Iverfeldt, Å., Meili, M. and Timm, B. 1991. Mercury in the Swedish environment: recent research on causes, consequences and corrective methods. Water, Air, and Soil Pollution 55, 143-177.

Mason, R. P., Fitzgerald, W. F., Morel, F. M. M., 1994. The biogeochemical cycling of elemental mercury: Anthropogenic influences. Geochimica et Cosmochimica Acta 58 3191-3198, 1994.

Mason, R. P., Reinfelder, J. R., Morel, F. M. M., 1995. Bioaccumulation of mercury and methylmercury. Water, Air, and Soil Pollution 80 915-921, 1995.

Mason, R. P., Lawson, N. M., Sheu, G. R., 2000. Annual and seasonal trends in mercury deposition in Maryland. Atmospheric Environment 34, 1691-1701.

Mason, R. P. and Sheu, G.-R., 2002. Role of the ocean in the global

mercury cycle. Global Biogeochemical Cycles 16, 1093. doi:10.1029/2001GB001440.

Meili, M, 1991. The coupling of mercury and organic matter in the biogeochemical cycle - towards a mechanistic model for the boreal zone. Water, Air, and Soil Pollution 56, 333-347.

Muir, D., Fisk, A., Kwan, M., 2001. Temporal trends of persistent organic pollutants and metals in ringed seals from the Canadian Arctic. In: Kalhok, S. (Ed.), Synopsis of Research Conducted Under the 2000–2001 Northern Contaminants Program. Indian and Northern Affairs Canada, Ottawa, ON, Canada, pp. 208–214.

Pacyna, E. G., Pacyna, J. M., Steenhuisen, F., Wilson, S., 2006. Global anthropogenic mercury emission inventory for 2000. Atmospheric Environment 40, 4048–4063.

Petersen, G., Iverfeldt, A., Munthe, J., 1995. Atmospheric mercury species over central and northern Europe - model calculations and comparison with observations from the Nordic air and precipitation network for 1987 and 1988. Atmospheric Environment 29, 47-67.

Pirrone, N., Costa, P., Pacyna, J.M., Ferrara, R., 2001. Mercury emissions to the atmosphere from natural and anthropogenic sources in the Mediterranean region. Atmospheric Environment 35, 2997-3006.

Pirrone, N., Cinnirella, S., Feng, X., Finkelman, R. B., Friedli, H. R., Leaner, J., Mason, R., Mukherjee, A. B., Stracher, G. B., Streets, D. G., Telmer, K., 2010. Global mercury emissions to the atmosphere from anthropogenic and natural sources. Atmospheric Chemistry and Physics 10, 5951-5964.

Prestbo, E. M. and Gay, D. A., 2009. Wet deposition of mercury in the U.S and Canada, 1996-2005: Results and analysis of the NADP mercury deposition network (MDN).

Risch, M. R., Gay, D. A., Fowler, K. K., Keeler, G. J., Backus, S. M., Blanchard, P., Barres, J. A., Dvonch, J. T., 2011. Spatial pattern and temporal trends in mercury concentrations, precipitation depth, and mercury wet deposition in the North American Great Lakes region, 2002-2008. Environmental pollution 161, 261-271.

Sakata, M. and Marumoto, K., 2005. Wet and dry deposition fluxes of mercury in Japan. Atmospheric Environment 39, 3139-3146.

Schroeder, W. H. and Munthe, J., 1998. Atmospheric mercury - An overview. Atmospheric Environment 32, 809-822.

Seigneur, C., Vijayaraghavan, K., Lohman, K., Karamchandani, P., Scott, C., 2004. Global source attribution for mercury deposition in the United States. Environmental Science and Technology 38, 555-569.

Selin, N. E., Jacob, D. J., Park, R. J., Yantosca, R. M., Strode, S., Jaegle, L., Jaffe, D., 2007. Chemical cycling and deposition of atmospheric mercury: global constraints from observations. Journal of Geophysical Research 112, D02308.

Selin, N. E. and Jacob, D. J., 2008. Seasonal and spatial patterns of mercury wet deposition in the Unites States: Constraints on the contribution from North American anthropogenic sources. Atmospheric Environment 42, 5193-5204.

UNEP, 2002. Chemicals: Global Mercury Assessment Available from: http://www.chem.unep.ch/Mercury/Report/GMA-report-TOC.htm.

U.S. EPA, 1997. Persistent, bioaccumulative and toxic chemical program, http://www.epa.gov/pbt.

Wagemann, R., Innes, S., Richard, P. R., 1996. Overview and regional and temporal differences of heavy metals in Arctic whales and ringed seals in the Canadian Arctic. Science of the Total Environment 186, 41–67.

Weiner, J. G and Stokes, P. M., 1990. Enhanced bioaccumulation of mercury, cadmium and lead in low-alkalinity waters: An emerging regional environmental problem. Environmental Toxicology and Chemistry

Xu, X., Yang, X., Miller, D. R., Helble, J. J., Carley, R. J., 2000. A regional scale modeling study of atmospheric transport and transformation of mercury. II. Simulation results for the northeast United States. Atmospheric Environment 34, 4945-4955.

Chapter 2

Theoretical background

2.1. Physical and chemical properties of mercury

Mercury (Hg) is a chemical element with atomic number 80 and atomic weight 200.59. Mercury is the only metal that is liquid at standard condition for temperature and pressure. Mercury has a high surface tension, high specific gravity (13.55 at 20^{o}C), low electrical resistance, and a constant volume of expansion over the entire temperature range of its liquid state (Schroeder and Munthe, 1998).

As mentioned before, Mercury is capable of existing in three oxidation states: 0, + 1 and + 2. In the atmospheric environment, mercury exists predominantly in the elemental form (oxidation state 0) and in the + 2 oxidation state, with the + 1 oxidation state being very rare, if it exists at all.

The physical and chemical properties of mercury and mercury compounds are summarized in Table 2-1.

Table 2-1. Physical/chemical properties of mercury and its compounds

Property	Hg^0	$HgCl_2$	HgO	HgS	CH_3HgCl	$(CH_3)_2Hg$
Melting point (°C)	-39	277	decomp. @+500°C	584 (sublim.)	167 (sublim.)	-
Boiling point (°C)	357 @1atm	303 @1atm	-	-	-	96
Vapor pressure (Pa)	0.180 @20°C	8.99×10^{-3} @20°C	9.2×10^{-12} @25°C	n.d.	1.76 @25°C	8.3×10^{3} @25°C
Water solubility (g/l)	49.4×10^{-6} @20°C	66 @20°C	5.3×10^{-2} @25°C	~2×10^{-24} @25°C	~5-6 @25°C	2.95 @24°C
Henry's law coefficient (dimensionless)	0.30[a] @20°C 0.32 [a] @25°C 0.18 [a] @5°C	3.69×10^{-5} @20°C	3.76×10^{-11} @25°C	n.d.	1.6×10^{-5} [a] @15°C and pH=5.2	646 @25°C 0.31[a] @25°C 0.15@0°C
Octanol - water partition coefficient	4.2[a]	0.5[a]	-	n.d.	2.5[a]	180[a]

The atmospheric chemistry of mercury involves partitioning between gaseous, aqueous and solid phases, and chemical reactions in the gaseous and aqueous phases. Photochemistry is also significant in the oxidation and reduction of mercury in the environment. The interaction between mercury atmospheric processes and chemistry is shown in Figure 2-1.

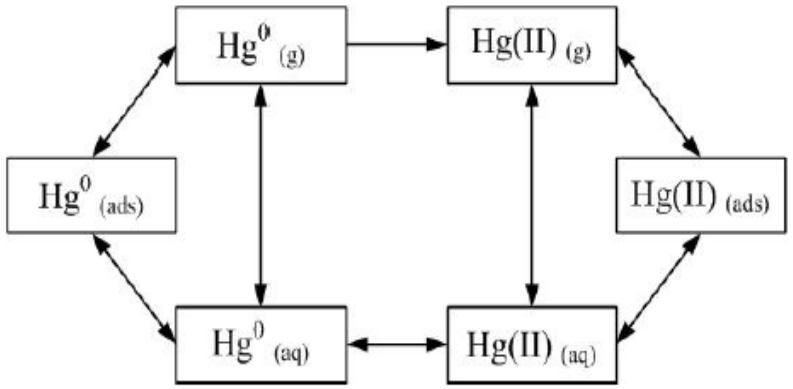

Source: Pirrone et al. (2001a)

Figure 2-1. Mercury oxidation, reduction, and mass transfer processes in the atmosphere

2.2. Mercury in the environment

Most of the mercury found in the environment is in the form of elemental (metallic) mercury and inorganic mercury compounds. Elemental and inorganic mercury enters the air from mining deposits of ores that contain mercury, from the emissions of coal-fired power

plants, from burning municipal and medical waste, from the production of cement, and from uncontrolled releases in factories that use mercury. Metallic mercury is a liquid at room temperature, but some of the metal will evaporate into the air and can be carried long distances. In air, the mercury vapor can be changed into other forms of mercury, and can be further transported to water or soil in rain or snow. Inorganic mercury may also enter water or soil from the weathering of rocks that contain mercury, from factories or water treatment facilities that release water contaminated with mercury, and from incineration of municipal garbage that contains mercury (for example, in thermometers, electrical switches, or batteries that have been thrown away). Inorganic or organic compounds of mercury may be released to the water or soil if mercury-containing fungicides are used. Microorganisms (bacteria, phytoplankton in the ocean, and fungi) convert inorganic mercury to methylmercury. Methylmercury released from microorganisms can enter the water or soil and remain there for a long time, particularly if the methylmercury becomes attached to small particles in the soil or water. Mercury usually stays on the surface of sediments or soil and does not move through the soil to underground water. If mercury enters the water in any form, it is likely to settle to the bottom where it can remain for a long time.

The relationship between source and environmental effect is complex because mercury is redistributed over long distances via the atmosphere (Bullock et al., 1997, 1998; Petersen et al., 1995; Mason et al., 1994; U.S. EPA, 1993, 1996; U.S. DOE, 1996). Because of different physicochemical characteristics, each mercury species behaves differently in various environmental media, and undergo wet and dry deposition, evasion from soil, and sedimentation in aquatic and terrestrial ecosystems to different extents (Mason et al., 2005).

Deposition of natural and anthropogenic mercury is its main pathway to most aquatic systems, either as direct deposition to the water surface or as indirect deposition in runoff from the watershed (Mason et al., 1994; Miller et al., 2005; Pirrone et al., 2001; Pirrone et al., 2010; Risch et al., 2011). There is a significant portion of mercury in wet deposition which originates from the global transport of elemental mercury through its chemical conversion to the divalent form, aerosol scavenging and subsequent incorporation into precipitation (Dastoor and Larocque, 2004). Therefore, the understanding of mercury speciation and chemistry are important to atmospheric deposition.

2.2.1. Mercury in air

2.2.1.1. Gaseous elemental mercury (GEM)

Gaseous elemental mercury (GEM) is the predominant form in

ambient air (> 95%) and its residence time is relatively long (0.5 ~ 2 years) due to its low solubility and inertness (Slemr et al., 1985; Tokos et al., 1998) which does not allow it to be efficiently incorporated into wet deposition. Vegetation is an important sink for GEM as are direct dry deposition and homogeneous/heterogeneous oxidation reactions (Ericksen et al., 2003; Gustin, 2011; Lin et al., 2006; Lin et al., 2007)

GEM is vertically well mixed in the troposphere and its typical concentration is reported as ~1-4 ng m^{-3} at background sites (Lin and Pehkonen, 1999; Slemr and Langer, 1992), however, GEM concentrations can be elevated to be as high as 10 ng m^{-3} in urban or industrial areas (Chen et al., 2004; Fthenakis et al., 1995). Consequently, GEM predominates in the atmosphere, and is thought to be relatively inert resulting in global transport (Schroeder and Munthe, 1998).

2.2.1.2. Gaseous oxidized mercury (GOM)

Mercurous mercury (Hg^{+}) is rarely stable under environmental conditions as it is rapidly oxidized to mercuric forms (Hg^{2+}) by hydrolysis (Schroeder and Munthe, 1998; U.S. EPA, 1997). Gaseous oxidized mercury (GOM) (Hg^{2+}), therefore, is the most common form of oxidized mercury.

Gaseous oxidized mercury (GOM) is very water soluble, with relatively strong surface adhesion properties (Han et al., 2005) and can be scavenged by rain within precipitating clouds and below clouds (Lin and Pehkonen, 1999). It has very high dry deposition velocity which is similar to HNO_3 (1~5 cm sec^{-1}) if it is assumed that all GOM is $HgCl_2$ (Petersen et al., 1995). Therefore the contribution of GOM in total deposition to surfaces is probably very high even though its concentration is typically less than 5% of total gas phase mercury.

Once released to the atmosphere, GEM (Hg^0) is oxidized to GOM (Hg^{2+}) via gas-phase or aqueous phase reactions (Lin and Pehkonen, 1999; Schroeder et al., 1991; Seigneur et al., 1994), and Hg^{2+} is further associated with organic or inorganic compounds, existing as gases (e.g., $HgCl_2$ or $Hg(OH)_2$), aqueous phase (e.g., $HgCl_2$, $Hg(OH)_2$ or sulfites) or particulate phase (e.g., HgO or HgS) (Lindqvist and Rodhe, 1985; Schroeder et al., 1991).

GOM is efficiently absorbed by cloud droplets during rain formation (Petersen et al., 1995), scavenged in precipitation and dry-deposited over 100 times more readily than GEM (Lindberg, et al., 1992). These rapid removal processes result in a relatively short atmospheric residence times (~days) with a transport of tens to hundreds of kilometers from source areas (Slemr et al., 1985; Tokos et al., 1998). The travel distance of GOM depends on the characteristics of sources

such as emission height and meteorological conditions (Fthenakis et al., 1995), oxidant levels (Poissant et al., 2005).

2.2.1.3. Particulate bound mercury (PBM)

It is well known that vapor phase mercury constitutes the vast majority of the atmospheric mercury burden, but particulate bound mercury (PBM) (Hg_p) may actually play a disproportionately large role in the amount of mercury in the various environmental compartments (Keeler et al., 1995) especially for mercury deposition into terrestrial and aquatic ecosystems. PBM is associated with airborne particles such as dust, soot, sea-salt aerosols, ice crystal (Lu and Schroeder, 2004) or is likely produced by adsorption of GOM species (e.g. $HgCl_2$) onto atmospheric particles (Sakata and Marumoto, 2002 ; Gauchard et al., 2005; Lu and Schroeder, 2004). A previous study reported that PBM concentrations were correlated to the amount of particles in the atmosphere (Hall et al., 2006).

Schroeder et al. (1991) indicated that atmospheric PBM can be represented by the following compounds such as HgO, HgS, $HgCl_2$, $HgSO_4$, $Hg(NO_3)_2$. Particulate bound mercury (PBM) can be wet deposited relatively efficiently if it is associated with particles in or below precipitating clouds (Cohen et al., 2004). PBM is removed fast from the atmosphere although the dry and wet deposition velocities are

not as high as that of GOM. Background concentrations of PBM have been shown to be 0.2-0.9% of TGM (Slemr et al., 1985), but it accounts for 71% of the total atmospheric mercury load in the Artic has been observed during the elevated episodes (Lu and Schroeder, 2004).

Atmospheric transport of PBM is significantly affected by its particle size distribution and ranges from hours to many days (Schroeder and Munthe, 1998), and it is likely to be deposited at intermediate distances contributing significantly, like GOM, to both wet and dry deposition (Lynam and Keeler, 2002). PBM transported from source areas in Central Europe 500-800 km northward (Wängberg et al., 2001), and regional coal combustion might lead to an elevation of PBM in winter (Zielonka et al., 2005). Typical background levels of PBM range between 1 and 100 pg m^{-3} (Keeler et al., 1995; Wängberg et al., 2001).

2.2.2. Mercury in water

GEM (Hg^0) is predominant in the atmosphere. GEM is deposited by wet deposition after it is converted to GOM (Hg^{2+}) through oxidant-mediated reactions mainly in cloud droplet.

Mercury exist in different chemical forms in freshwater including dissolved gaseous mercury (DGM, Hg^0), dissolved reactive mercury (DRM, Hg^{2+}), and organic mercury, mainly in the form of methylmercury (MeHg) (CH_3Hg^+) (Morel et al., 1998). The majority of

mercury in aquatic ecosystems is in the inorganic form (about 95 to 99 %) (Krabbenhoft, 1998), however, a high level of mercury in fish tissues is observed when dissolved mercury in natural water systems exists mostly in organic forms (Gill and Bruland, 1990). Major oxidation pathways of Hg^0 in aqueous phase are as follows (Finlayson-Pitts and Pitts, 1986; Lin and Pehkonen, 1997; Munthe, 1992; Zepp et al., 1987).

$$Hg^0_{(aq)} + O_{3(aq)} + 2H^+ \longrightarrow Hg^{2+}_{(aq)} + H_2O + O_{2(aq)} \quad (2\text{-}1)$$

$$Hg^0_{(aq)} + \bullet OH_{(aq)} \longrightarrow Hg^+_{(aq)} + OH^-_{(aq)} \quad (2\text{-}2)$$

$$Hg^+_{(aq)} + \bullet OH_{(aq)} \longrightarrow Hg^{2+}_{(aq)} + OH^-_{(aq)} \quad (2\text{-}3)$$

$$HOCl_{(aq)} + Hg^0_{(aq)} \longrightarrow Hg^{2+}_{(aq)} + Cl^-_{(aq)} + OH^-_{(aq)} \quad (2\text{-}4)$$

Hg^0 can be oxidized by chlorine (Cl_2) in the aqueous phase (Kobayashi, 1987). Before the oxidation of Hg^0 by aqueous chlorine can take place, Cl_2 must be scavenged into the aqueous phase. The previous studies reported that the Hg^0 oxidation rate increase with the presence of chloride ions (Amyot et al., 1997; Lalonde et al., 2001), and sunlight (Amyot et al., 1994; Lalonde et al., 2001, 2004)

GOM is mainly deposited from air to water by dry and wet deposition (Fitzgerald et al., 1991; Keeler, 1994), and it has two fates; ⅰ) adsorption to sediments where it may be transformed to MeHg,

which is the most toxic environmental mercury species, ii) reduction to DGM (Slemr et al., 1985; Tokos et al., 1998). DGM is volatile and therefore it is rapidly emitted to the atmosphere, or it may be oxidized to DRM and potentially methylated to be bioavailable in the food chain.

Once GOM is deposited into surface water, it tends to be reemitted after reduction to elemental mercury. The important reduction pathways are as follows (Pleijel and Munthe, 1995; Pehkonen and Lin, 1998).

$$Hg(II)_{(aq)} + SO_3^{2-} \longrightarrow HgSO_{3(aq)} \quad (2\text{-}5)$$

$$HgSO_{3\,(aq)} \longrightarrow Hg^0_{(aq)} + S(VI) \quad (2\text{-}6)$$

$$HO_2\bullet_{(aq)} + Hg(II)_{(aq)} \longrightarrow Hg(I)_{(aq)} + O_{2(aq)} + H^+_{(aq)} \quad (2\text{-}7)$$

$$HO_2\bullet_{(aq)} + Hg(I)_{\,(aq)} \longrightarrow Hg^0(aq) + O_{2(aq)} + H^+_{(aq)} \quad (2\text{-}8)$$

After oxidation of Hg^0 to Hg^{2+} or direct deposition of Hg^{2+} in water column and sediments, Hg^{2+} is methylated by microbes to methylmercury compounds with higher mobility and solubility under primarily anaerobic conditions (Stein et al., 1996).

The oxidation state of mercury in aqueous environments is affected by the temperature, dissolved oxygen, conductivity, pH, and oxidation-reduction potential (ORP) (O'Driscoll et al., 2003). Hg^0 prefers the vapor phase more than at lower temperatures.

This is likely due to changes in the Henry's Law constant for elemental mercury, which decreases as temperature decreases (Sanemasa, 1975). For example, the Henry's law constant changes from 0.33 at 23 ℃ to 0.28 at 16 ℃ due to its temperature dependence (Schroeder et al., 1991; Amyot et al., 2000). In addition, the concentration of dissolved organic carbon (DOC) and pH have a strong effect on the ultimate fate of mercury in an ecosystem. The previous studies have shown that for the same species of fish taken from the same region, increasing the acidity of the water (decreasing pH) and/or the DOC content generally results in higher mercury levels in fish, an indicator of greater net methylation. Higher acidity and DOC levels enhance the mobility of mercury in the environment, thus making it more likely to enter the food chain (Driscoll et al., 1995).

Mercury and methylmercury exposure to sunlight (specifically UV) has an overall detoxifying effect. Sunlight can break down methylmercury to Hg^{2+} or Hg^{0}, which can leave the aquatic environment and reenter the atmosphere as a gas (Sellers et al, 1996).

2.2.3. Mercury in soil

The previous studies suggest that emissions of mercury from the soils play a significant and integral part in global and regional mercury budgets (Gustin et al., 2000; Lindberg et al., 1995; Schroeder and

Munthe, 1998). Soils are highly complex natural systems with important characteristics that affect soil mercury emissions. They host a various microbial communities that can influence on mercury biotic transformations. In addition, they have extremely large inorganic and organic surface areas. Therefore, both abiotic and biotic surface reactions play very important roles in the fate of mercury deposited to the soil surface (Zhang and Lindberg, 1999).

Mercury in soils is predominantly in the form of oxidized mercury, however the majority of the gaseous mercury emitted from soils is Hg^0 (Schlüter, 2000). Therefore, mercury must be reduced from Hg^{2+} to Hg^0 in order to be released. This reduction can be occurred in water or soils by biotic processes (Barkay et al., 2003; Rogers, 1979; Rogers and McFarlane, 1979; Schlüter, 2000) or abiotic processes including photolysis and redox reactions with fulvic or humic acids (Alberts et al., 1974; Allard and Arsenie, 1991; Costa and Liss, 1999, 2000; Schlüter, 2000; Skogerboe and Wilson, 1981; Zhang and Lindberg, 2001).

The previous studies report that Hg^0 emissions from soil are positively correlated with ambient air temperature, soil surface temperature, and solar radiation, resulting in a diurnal pattern with a maximum during the afternoon. It is negatively correlated with relative humidity and soil wetness (Carpi and Lindberg, 1997, 1998; Gabriel et al., 2006; Gustin and Lindberg, 2000; Gustin et al., 1997, 1999; Kim et

al., 1995; Leonard et al., 1998; Moore and Carpi, 2005; Wallschläger et al., 1999, 2000; Wang et al., 2005). Mercury emission from the soil containing less than 1 μg Hg g^{-1} and low in organic matter is dominated by biological processes, whereas soils with higher organic matter contents favor abiotic mediated evaporation (Rogers, 1979; Rogers and McFarlane, 1979; Schlüter, 2000).

Consequently, the soils are regarded as a net sink for wet and dry deposition of atmospheric mercury and important mercury sources due to its large surface area (Nater and Grigal, 1992; Carpi and Lindberg, 1998).

2.3. Atmospheric wet deposition of mercury

Mercury wet deposition is one of the most useful measurements of mercury that can be made to evaluate mercury input to sensitive ecosystems and monitor long-term trends. With proper trace metal clean techniques, a high quality laboratory and relatively inexpensive equipment, wet deposition of mercury can be measured routinely.

Experts have demonstrated that four key components are required for accurate mercury wet deposition measurements: (1) a trace clean sample train with an HCl preservative in the collection bottle, (2) a temperature-controlled collector with an automated rain sensor, (3) a rain gauge to verify the rainfall depth collected, and (4) a cold vapor

atomic fluorescence spectrometer (CVAFS) system to measure the mercury concentration (Landis and Keeler, 1997; Mason et al. 2000; Vermette et al. 1995). In addition, manual event-based mercury wet deposition sampling, which requires the presence of an operator to install and/or uncover the sample train for individual precipitation events, is also a possible technique for use in intensive studies (Dvonch et al. 1998; White et al., 2009).

However, atmospheric wet and/or dry deposition of mercury is complex due to the combination of global and synoptic-scale transport, synoptic meteorological systems, and chemical reactions along the transport, and therefore mercury deposition can be originated from local, regional and/or global scales (Dastoor and Larocque, 2004).

Deposition of natural and anthropogenic mercury is its main pathway to most aquatic systems, either as direct deposition to the water surface or as indirect deposition in runoff from the watershed (Mason et al., 1994; Miller et al., 2005; Pirrone et al., 2001; Pirrone et al., 2010; Risch et al., 2011).

In general, mercury deposits in the form of GOM and/or PBM due to their high scavenging ratio and dry deposition velocity. GEM can indirectly be scavenged after chemical oxidation reaction.

Wet deposition is the removal of pollutants from the atmosphere through atmospheric hydrometeors, such as cloud, fog drops, rain and snow. The overall wet deposition flux of a contaminant is the sum of its

transfer from cloud to rain (washout or in-cloud scavenging) and scavenging by falling hydrometeors (rainout or below-cloud scavenging) (Seinfeld and Pandis, 1998).

Wet deposition of mercury is generally composed of scavenging of GOM and PBM by precipitation. In addition, homogeneous and heterogeneous oxidations of GEM to GOM can occur as both in-cloud and during air mass transport (Mason et al., 1992, 1997, 2000; Pleijel and Munthe, 1995). Precipitation generally effectively scavenges particles during the initial rainfall period, followed by smaller washout (Mason et al., 1997) with relatively similar mercury concentrations over increasing rainfall amount.

Figure 2-2 shows the chemical reactions of mercury in droplets, where both oxidation and reduction reactions concurrently occur (Lindqvist et al., 1991; Pleijel and Munthe, 1995).

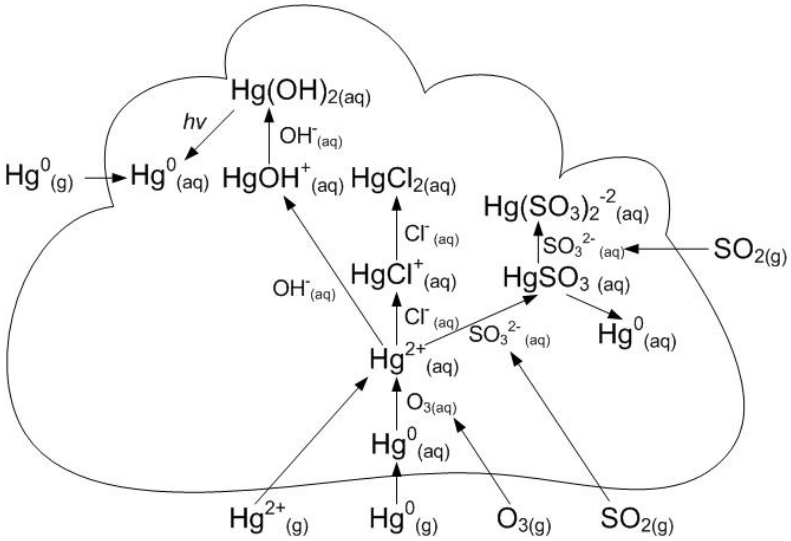

Source: Lindqvist et al., 1991; Pleijel and Munthe, 1995

Figure 2-2. Mercury chemistry in droplets

Precipitation generally effectively scavenges particles during the initial rainfall period, followed by smaller washout (Mason et al., 1997) with relatively similar mercury concentrations with increasing rainfall amounts. GOM is more readily scavenged than PBM (Bullock et al., 1998; Seo et al., 2012).

A seasonal variation in mercury wet deposition flux is evident with a maximum in summer and minimum in winter in several North America (Burke et al., 1995; Mason et al., 2000; Glass and Sorensen, 1999; Guentzel et al., 1995; Hoyer et al., 1995; Sorensen et al., 1994; Watras et al., 2000). Mason et al. (2000) indicated 40–50% and 15–20% of total mercury wet deposition fluxes were measured in summer and

winter, respectively. Smaller fractions of winter flux were also found in Minnesota and Wisconsin (< 5%; Mason et al., 2000), and Michigan (7–15%; Hoyer et al., 1995). The combination of larger mercury concentration and rainfall amount and faster photo-oxidation reaction rates in higher temperature enhanced the largest mercury wet deposition in summer, whereas smaller efficiency of particulate scavenging by snow and slower atmospheric reactions in low temperature, and less precipitation amount resulted in the smallest winter flux (Mason et al., 2000).

Local emission sources could contribute significantly to the spatial and temporal variation of the mercury wet deposition (Dvonch et al., 1998; Glass and Sorensen, 1999; Hoyer et al., 1995; Sorensen et al., 1994). The urban impacts with higher soot particle concentrations, higher O_3 levels, and higher emission rates on the mercury wet deposition were observed in the San Francisco Bay area (Steding and Flegal, 2002). On the other hand, the regional and global impacts on mercury wet deposition were evident (Guentzel et al., 2001; Hoyer et al., 1995; Steding and Flegal, 2002). The long-range transport of GOM coupled with strong convective thunderstorm activity contributing >50% of the mercury deposition has been observed in southern Florida (Guentzel et al., 2001). The direct and indirect (forming reactive halogen species) oxidation of GEM via O_3 destruction led to an increase of GOM concentration in rain contained in storms which

transported mercury across the Pacific to coastal California (Steding and Flegal, 2002). Overall, the factors influencing mercury concentration include precipitation (type, strength and duration), emission source (type, strength and distance), oxidant concentration, in-cloud processes (in-cloud temperature, turbulence, and physical/chemical properties of particles), and meteorological conditions (Hoyer et al., 1995).

In the past two decades, coordinated monitoring networks and long-term monitoring sites have been established in a number of regions and countries for the measurement of mercury in ambient air and wet deposition. Europe and North America have multiple sites with high quality continuous monitoring of mercury in air and wet deposition for greater than 15 years. Notable areas with shorter, high quality continuous mercury air monitoring sites can be found in East Asian Countries and South Africa. Regions with few or no records of high quality, continuous mercury monitoring sites include all of Southern Asia, Africa, South America and Australia. International efforts are now underway to establish long-term monitoring sites with expanded global coverage. Table 2-2 shows a summary of the existing networks for mercury wet deposition.

Table 2-2. Summary of monitoring networks for mercury wet deposition

Location	Program	Region	Duration	Measurements	References	Website
Europe	EMEP	Continental	from 1987	Weekly to monthly ; bulk and wet-only collection	Wangberg et al. (2007)	www.emep.int/
USA	NADP-MDN	National	from 1999	Weekly ; wet-only collection	Butler et al. (2008) ; Prestbo and Gay (2009) ; Risch et al. (2012)	http://nadp.isws.illinois.edu/MDN/
	UMAQL	Midwest / Northeast	from 1992	Daily-event ; wet-only collection	Burke et al. (1995) ; Landis et al. (2002) ; Keeler and Dvonch (2005) ; Keeler et al. (2006) ; White et al.(2009) ; Gratz et al. (2009) ; Gratz and Keeler (2011)	
	UMAQL	Florida	from 1992	Daily-event ; wet-only collection	Dvonch et al. (1998) ; Dvonch et al. (1999) ; Dvonch et al. (2012)	
Canada	CAMNet / CAPMoN	National	from 1996	Weekly ; wet-only collection	Prestbo and Gay (2009) ; Risch et al. (2012)	www.ec.gc.ca/rs-mn/
Global	GMOS	Global	From 2011	Weekly ; wet-only and bulk collection	Sprovieri et al. (2012)	www.gmos.eu/

2.3.1. North America

Long-term measurements of mercury wet deposition in the U.S. and Canada largely commenced in the mid-1990s following the Clean Air Act Amendments of 1990, which mandated monitoring of several hazardous air pollutants, including mercury. A number of monitoring sites were established (Figure 2-3), several of which are still operational today, producing nearly two decades of mercury wet deposition records. In the Great Waters region, which includes the Great Lakes, Chesapeake Bay, and Lake Champlain basins, monitoring sites in Dexter, Michigan (MI) and Underhill, Vermont (VT) began in 1992 under the supervision of the University of Michigan Air Quality Laboratory. Additional sites were added in Pellston and Eagle Harbor, MI in 1993, creating the foundations for the Michigan Mercury Monitoring Network that expanded over time to include other sites in Michigan, Ohio, and Illinois (Keeler and Dvonch 2005).

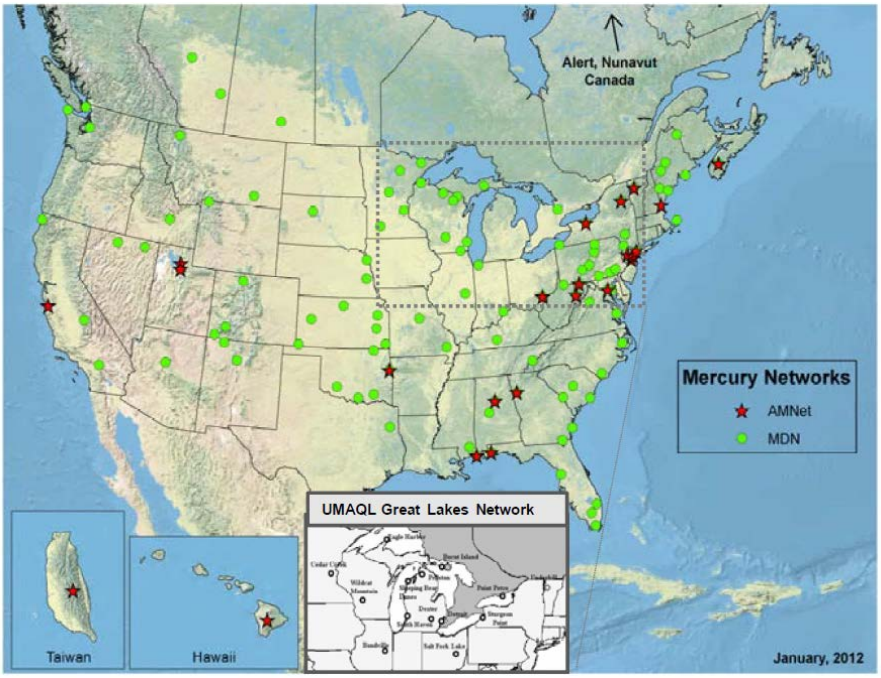

Figure 2-3. Locations of the UMAQL Great Lakes Atmospheric Monitoring Sites (Keeler and Dvonch 2005, inset), NADP Mercury Deposition Network Sites (MDN, green circles, http://nadp.isws.illinois.edu/MDN/), NADP Air Mercury Network Sites and AMNet ambient air mercury speciation sites (red stars, http://nadp.isws.illinois.edu/amn/)

In the United States and Canada, mercury wet deposition has been measured as part of the National Atmospheric Deposition Program (NADP) - Mercury Deposition Network (MDN) at 169 sites (112 currently active). The MDN program has also worked closely with the Canadian monitoring programs, including Canadian Atmospheric Monitoring Network (CAMNet) and Canadian Air and Precipitation Monitoring Network (CAPMoN), to develop consistent sample collection and analysis procedures. All precipitation samples from both

the MDN and CAPMoN programs are analyzed at a common laboratory in the U.S. (Frontier Global Sciences) to ensure consistent analytical results. In more recent years, new sites have also been established in Mexico. As a result, the U.S. and Canadian monitoring networks have generated a long-term record of mercury wet deposition throughout North America over the past 20 years. Reported annual mercury wet deposition ranges from 3 to 25 μg m^{-2} for the United States with values for the western United States being at the lower end (Prestbo and Gay, 2009).

Keeler and Dvonch (2005) reported ten years (1994-2003) of atmospheric mercury observations in the Great Lakes region, where daily-event precipitation samples were collected for mercury and trace elements (Landis and Keeler 1997). Results from three sites in Michigan (Eagle Harbor, Pellston, Dexter) demonstrated a strong decreasing north-south gradient in the amount of mercury wet deposition. An obvious trend in annual deposition over time was not observed, suggesting that despite efforts to control mercury emissions, emission sources in the southern Great Lakes region continually impacted the levels of mercury wet deposition. Similar measurements of event-based mercury wet deposition in the Chicago (Landis et al., 2002; Landis and Keeler, 2002) and Detroit urban areas, as well as the highly industrialized Ohio River Valley (Keeler et al., 2006; White et al., 2009) have further demonstrated the significant contribution from

local and regional anthropogenic sources to the observed levels of mercury in wet deposition in the Great Lakes basin.

Prestbo and Gay (2009) recently summarized 10 years (1996-2005) of weekly mercury wet deposition measurements from NADP-MDN sites in the U.S. and Canada. Results indicated regional differences in precipitation, concentration, and deposition over time. Total mercury deposition was highest in the southeastern U.S., and in all regions mercury wet deposition was greatest during the summer. Several sites in the northeastern U.S. and along the east coast displayed decreasing trends in concentration (1-2% per year). This trend was not observed in the U.S. Midwest or in much of the southeast. Most Midwest sites displayed no significant trend in concentration or deposition, while several sites in the southeast displayed significant increases in wet deposition. Four sites in the region between the Midwest and Northeast U.S. displayed patterns of decreasing concentration, increasing precipitation amount, and consequently no significant trend in deposition. These varying trends could be attributed to regional differences in meteorology and source emission impacts. Figure 2-4 shows the most recently available total mercury concentration and wet deposition annual gradient maps from the MDN program for the year 2011.

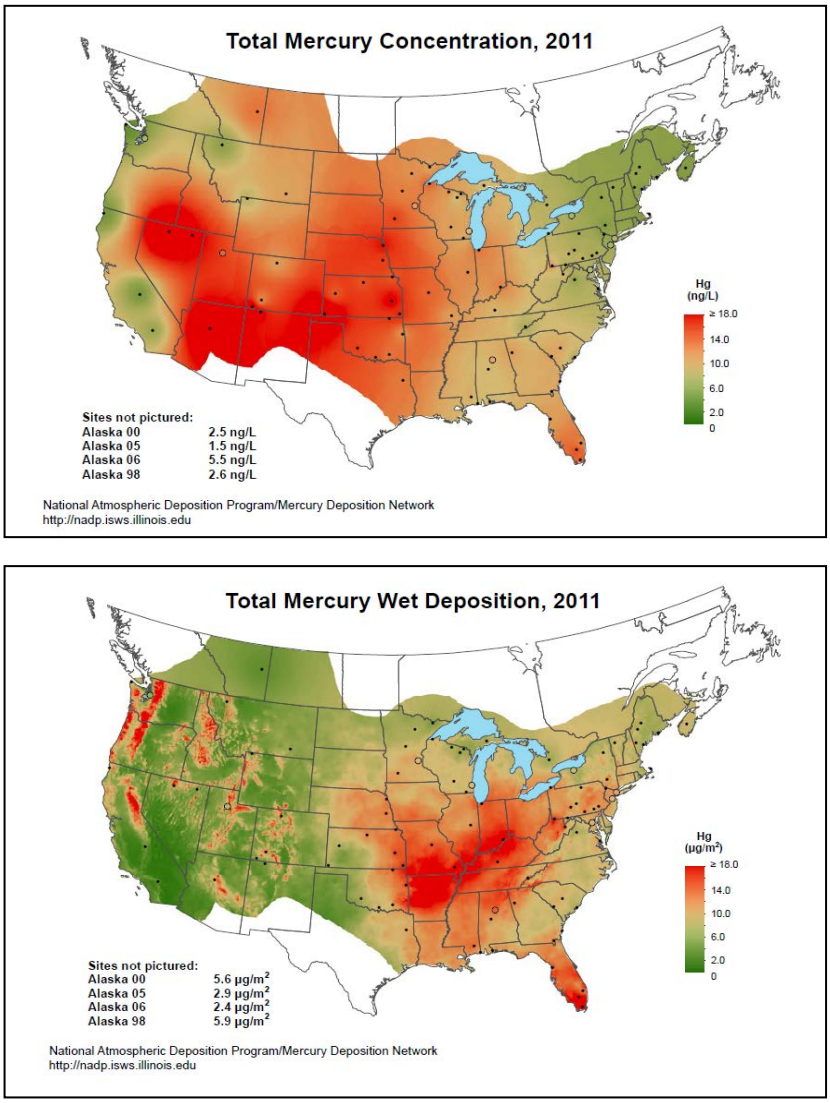

Figure 2-4. Total mercury concentration and wet deposition annual gradient maps from the MDN program for the year 2011

Daily-event precipitation samples collected in Underhill, VT from 1995-2006 were analyzed for total mercury and trace element concentrations (Gratz et al., 2009; Gratz and Keeler 2011).

Measurements from this site comprise one of the longest running mercury wet deposition datasets in the world. A statistically significant trend in annual mercury wet deposition over time was not detected, despite emissions reductions in the U.S. in the late 1990s with the implementation of stack controls on municipal and medical waste incinerators. In contrast, annual volume-weighted mean (VWM) mercury concentration declined in conjunction with an increase in the total annual precipitation amount. The declines in concentration appeared to be related to local scale meteorological and climatological variability rather than to a reduction in emissions of mercury to the atmosphere (Gratz et al., 2009). Multivariate and hybrid receptor modeling analyses further revealed that, of the nearly 80% of measured deposition accounted for by the PMF multivariate statistical receptor model, coal combustion consistently contributed to approximately 60% of mercury wet deposition. Using back-trajectory cluster analysis and hybrid receptor modeling techniques, the majority of mercury deposition at Underhill was linked to transport from the U.S. Midwest and east coast where the density of coal-fired utility boilers in the U.S. is largest (Gratz et al., 2009; Gratz and Keeler 2011).

Risch et al. (2012) recently reported on mercury wet deposition at 37 sites in the North American Great Lakes region from 2002 to 2008. A decreasing trend in mercury concentration was observed at 8 sites, and increasing trends in concentration were observed at 6 sites. Much of the

region saw an increase in annual precipitation depth during this period. Over the course of the study, mercury wet deposition was largely unchanged in the Great Lakes region and surrounding areas, and any significant trends in deposition did not correspond with trends in concentration. Overall, it was suggested that any observed declines in concentration were offset by increases in precipitation depth, and as such the total wet deposition amount remained largely unchanged. These studies revealed regional differences in concentration, precipitation, and deposition patterns in the U.S. and Canada, and over time a large-scale decline in deposition has not been observed. Continued long-term monitoring in this part of the world will demonstrate whether new legislation, such as the recently issued Mercury and Air Toxics Standards that regulate mercury emissions from utility boilers and other sources, have a significant impact on the amount of mercury deposited to the environment.

2.3.2. Europe

The European Monitoring and Evaluation Program (EMEP) was one of the first international environmental measurement networks established in Europe. Over the past 40 years, a number of atmospheric measurements, such as sulfur, nitrogen compounds, and ozone, have been made across 11 countries in Europe. In more recent years, EMEP has also expanded to include heavy metals, mercury, and some

persistent organic pollutants (POPs). Heavy metals were officially included in EMEP's monitoring program beginning in 1999. A number of countries have also been measuring and reporting on heavy metals within the EMEP area in connection with different national and international programmers such as the Arctic Monitoring and Assessment Programme (AMAP), the Commission of the Convention on the Protection of the Marine Environment of the Baltic Sea Area (HELCOM), the Commission for the Protection of the Marine Environment of the North-East Atlantic (OSPARCOM), the World Meteorological Organization Global Atmosphere Watch (WMO/GAW), and the United Nations Framework Convention on Climate Change. EMEP continues to interact with and make use of research activities performed by the scientific community, particularly through the establishment of "supersites" within other concurrent monitoring programs.

The EMEP monitoring stations, however, are not uniformly distributed throughout Europe. Most sites are located in the northern, western and central parts of Europe, while only a few sites measure heavy metals in the southern and eastern parts of Europe. Mercury measurement data from EMEP are largely available only from north and north-west Europe. The locations of the mercury measurement sites within the EMEP network as of 2009 are shown in Figure 2-5.

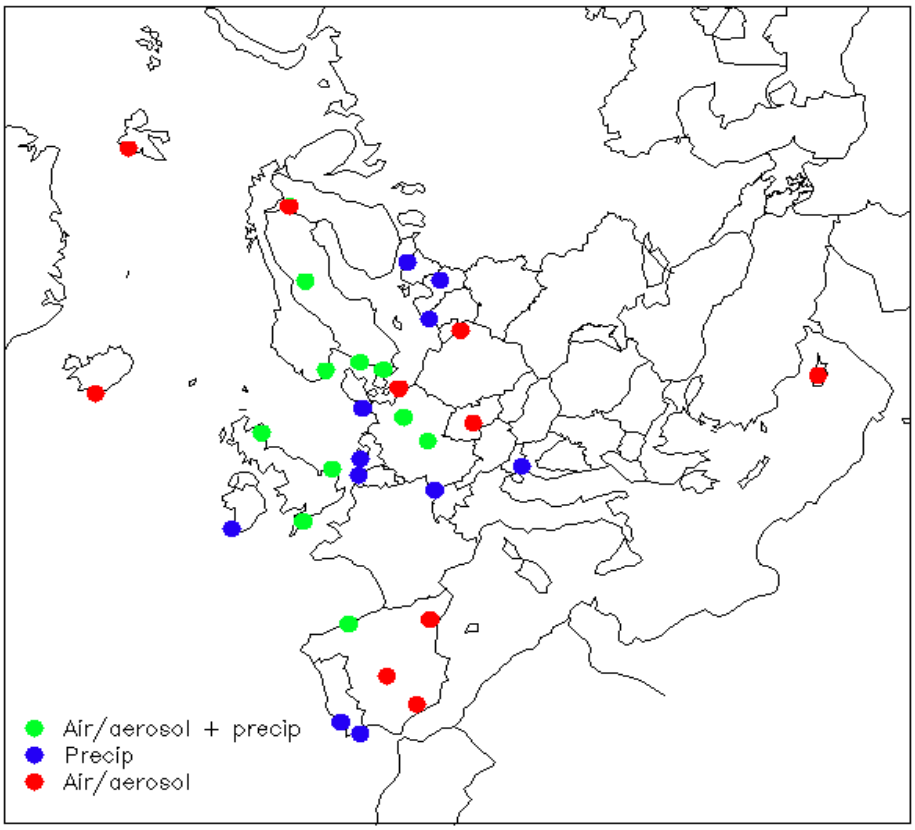

Figure 2-5. Mercury measurement sites within the EMEP network as of 2009

2.3.3. Asia

Table 2-3 shows a summary of TM concentrations in precipitation and wet deposition flux in Asia. TM concentrations obtained from urban and remote areas of Asia were in the ranges of 7.8-30.7 ng L^{-1} and 4.0-36.0 ng L^{-1}, respectively. TM wet deposition flux in urban and remote areas of Asia were in the ranges of 13.1-20.2 μg m^{-2} and 5.8-26.1 μg m^{-2}, respectively. Total mercury concentrations in precipitation

and wet deposition flux in Asia are higher than those observed in urban areas of North America (Guentzel et al., 2001; Keeler et al., 2006; Landis and Keeler 1997). VWM TM concentrations in urban areas of China were much higher than those in Japan and South Korea. This was mostly attributed to the elevated PBM and GOM concentrations in urban areas, which may be readily scavenged by precipitation.

TM concentrations in precipitation and wet deposition flux in remote areas of Asia were comparable to those obtained from the U.S. and Canadian NADP monitoring sites (Prestbo and Gay 2009). The VWM TM concentrations and wet deposition flux in Wujiang were much higher than other studies in remote areas of Asia (Guo et al., 2008), however, this may be due to the collection of monthly-integrated bulk precipitation samples in those studies, and given the generally elevated levels of ambient PBM and GOM concentrations in China it is likely that dry deposition of PBM and GOM substantially contributed to the TM in bulk precipitation samples.

Table 2-3. Summary of TM wet deposition in Asia

Site	Location	Sampling period	Precipitation depth (mm)	VWM conc. (ng L^{-1})	Wet deposition flux (μg m^{-2})	Representation	Reference
Wujiang River, Guizhou	China	Jan. 2006 ~ Dec. 2006	963	36.0	34.7	Rural	Guo et al. (2008) and reference cited therein
Mt.Leigong	China	May 2008 ~ May 2009	1533	4.0	6.1	Remote	Fu et al. (2010a)
Mt. Gongga	China	May 2006 ~ Apr. 2007	1818	14.3	26.1	Remote	Fu et al. (2010b)
Hokkaido	Japan	Dec. 2002 ~ Nov. 2003	882	8.0	7.1	Rural	Sakata and Marumoto (2005)
Aichi	Japan	Dec. 2002 ~ Nov. 2003	1679	7.8	13.1	Urban	Sakata and Marumoto (2005)
Hyogo	Japan	Dec. 2002 ~ Nov. 2003	1481	9.5	14.0	Urban	Sakata and Marumoto (2005)
Tokyo	Japan	Dec. 2002 ~ Nov. 2003	1912	8.7	16.7	Urban	Sakata and Marumoto (2005)
Seoul	Korea	Jan. 2006 ~ Dec. 2006	1645	10.1	16.8	Urban	This study
Seoul	Korea	Jan. 2007 ~ Dec. 2007	1235	16.3	20.2	Urban	This study
Seoul	Korea	Jan. 2008 ~ Dec. 2008	1291	16.1	18.5	Urban	This study
Seoul	Korea	Jan. 2009 ~ Dec. 2009	1822	10.2	16.4	Urban	This study

2.4. Sources of mercury

2.4.1. Natural sources

Mercury is emitted from both natural and anthropogenic sources (Lindqvist et al., 1991; Nriagu and Pacyna, 1988; Nriagu, 1989; Pacyna and Pacyna, 2002). Mercury is released or re-emitted into the atmosphere by a number of natural sources, including outgassing from mercuriferous and non-mercuriferous soils, evasion from water surfaces, vegetation, wildfires, volcanoes and geothermal sources (Lindqvist et al., 1991; Schroeder et al., 1992; Varekamp and Buseck, 1986). The natural sources emit mercury mostly as GEM (Pai et al., 2000), while anthropogenic sources primarily release mercury in three forms: GEM, GOM, and PBM. Re-emission involves gaseous evasion of previously deposited mercury from anthropogenic and natural sources (Lindberg and Turner, 1977). The re-emission of mercury, however, is included as a different category from natural sources because a significant portion of natural sources actually come from the previous anthropogenic sources. In this process, anthropogenically emitted mercury is deposited to the surface as Hg^{2+} and then reduced to volatile Hg^{0} and re-emitted. As a result of reemission, current levels of mercury emitted to the atmosphere by natural processes are elevated relative to pre-industrial levels (U. S. EPA, 1997). The previous studies of mercury emissions have been aimed primarily to assess the

contributions from anthropogenic sources (Nriagu and Pacyna, 1988; Pacyna et al., 2003, 2006; Pirrone et al., 1996, 1998), especially from coal, oil and wood combustion as well as from solid waste incineration and pyrometallurgical processes. However, mercury re-emissions must also be investigated because natural sources including re-emission of previously deposited anthropogenic emissions can be equal to anthropogenic sources when integrated spatially (Fitzgerald, 1995; Mason et al., 1994).

The previous study also suggested the importance of the air-water exchange of mercury as well as biologically mediated volatilization in both marine and terrestrial environments (U. S. EPA, 1997). These sources represent a relatively constant flux to the atmosphere and may comprise 30 to 50 percent of the total natural emissions, however, volcanic, geothermal, and burning biomass burning are widely variable temporally and spatially. In particular, volcanic eruptions can cause massive perturbations in atmospheric trace metal cycles. Volcanic activity alone may comprise 40 to 50 percent of the total natural mercury emissions at times (Nriagu, 1989).

Consequently, the mercury cycle is more complicated than previously thought and mercury emissions from natural sources are more significant than formerly understood (Engle et al., 2001; Engle and Gustin, 2002; Gustin et al., 1999; Gustin et al., 2000)

2.4.2. Anthropogenic sources

Anthropogenic mercury emissions mean the mobilization or release of geologically bound mercury by human activities, with mass transfer of mercury to the atmosphere (U. S. EPA, 1997), or the intentional use of mercury as a process or product ingredient, and incidental release of mercury as a by-product of industrial activities, such as the combustion of fossil fuels (UNEP, 2002). Anthropogenic mercury emissions can be divided into area and point sources. Area sources include electric uses such as fluorescent lamp, thermometers, thermostats, barometers, landfills, mobile emissions, paint use and are typically small and numerous and usually cannot be readily located geographically. On the other hand, point sources are those anthropogenic sources that are associated with a fixed geographic location. These point sources are divided into combustion, manufacturing and miscellaneous source categories (U.S. EPA, 1997).

Anthropogenic mercury emissions were estimated to contribute 50–80% of total mercury emissions (Mason et al., 1994; Nriagu, 1990; U.S. EPA, 1997). UNEP (2002) reported that fossil fuel (e.g. coal) combustion and waste incineration account for approximately 70 % of total anthropogenic mercury emissions.

Because of the increasing energy demands all around the world, mercury emissions have been globally increasing. Slemr and Langer (1992) reported an annual mercury emission rate increased 1.2 to 1.5%

between 1977 and 1990. Other studies suggested that anthropogenic mercury emissions have increased atmospheric mercury levels about three to five fold since the last century (Fitzgerald, 1995; Mason et al., 1994). In particular, Asia contributed about 30 % to the total mercury emissions in 1990, compared to 56 % in 1995 (Pirrone et al., 2001). However, anthropogenic mercury emissions have slightly decreased during the last decade in North America and Europe due to reduction efforts, such as the installation of air pollution control devices (Mukherjee et al., 2000; Pirrone et al., 1996; U.S. EPA, 1997). A decrease of mercury emissions has been observed in Central and Eastern Europe from 1990 to 1995 due to a general decrease of industrial activities and consumption of raw materials with high mercury contents (UNEP, 2002). On the other hand, Boutron (1986) found no clear trend for changes in mercury concentration over the last 800 years.

Pacyna and Pacyna (2002) reported that global atmospheric mercury speciation were 53% as GEM, 37% as GOM, and 10% as PBM. Similarly, Walcek et al. (2003) also suggested that global atmospheric mercury speciation were 47% as GEM, 35% as GOM, and 18% as PBM in eastern North America.

A recent study emphasized on the importance of long-range transport of mercury from Northern Hemisphere including Europe, Asia, and North America (Travnikov, 2005). It indicated that about half the

mercury deposition to such a remote region as the Arctic is due to the transport from anthropogenic emission sources contributed by Asia (33%) and Europe (22%)., The local sources contribute to the background concentration of mercury, however, the global background concentration of mercury contributes significantly to the mercury burden at most locations. Globally, Europe, Asia (particularly China and Japan) and North America were the three major source areas (Dastoor and Larocque, 2004).

2.5. Health effects of mercury

Mercury (Hg) is a well-known environmental toxic pollutant and highly bioaccumulative trace metals in the food chain (Meili, 1991) that has systematic acute and chronic effects on body of various organ systems including central nervous system, skin, motor system, digestive system, cardiovascular system, immune system, reproductive system, skin and oral tissues (Pizzichini et al., 2002; Quig, 1998; Thronhill and Pemverton, 2003; Zahira et al., 2005). Mercury is highly toxic to human health, especially posing a risk to the development of the child in utero and early in life. It occurs naturally and exists in various forms: elemental (or metallic); inorganic (e.g. mercuric chloride); and organic (e.g., methyl- and ethylmercury). The organic form is most toxic as it passes the blood brain barrier owing to its lipid solubility (Zahir et al.,

2005). These forms all have different toxicities and implications for health and for measures to prevent exposure (IPCS, 2000). All mercury compounds usually accumulate in muscles, liver and kidney of fishes, birds, whales and polar bears (Dietz et al., 1996; Kenow et al., 2007).

In general population, fish consumption is the primary pathway of mercury exposure (ATSDR, 1999; National Research Council, 2000). People are mainly exposed to methylmercury, an organic compound, when they eat fish and shellfish that contain methylmercury. About 95% methlymercury ingested in fish was absorbed into the bloodstream (WHO, 1990) and it is distributed throughout the body by the blood stream and accumulates in fat or organs (Chien et al., 2010).

Whether an exposure to the various forms of mercury will harm a person's health depends on a number of factors. Almost all people have at least trace amounts of methylmercury in their tissues, reflecting methylmercury's widespread presence in the environment and people's exposure through the consumption of fish and shellfish. People may be exposed to mercury in any of its forms under different circumstances. The factors that determine how severe the health effects are from mercury exposure include these;

- the chemical form of mercury, the dose, the age of the person;
- the dose;
- the age of the person exposed (the fetus is the most susceptible);

- the duration of exposure;
- the route of exposure such as inhalation, ingestion, dermal contact; and
- the health of the person exposed

Mercury exists in three chemical forms such as methylmercury, elemental mercury, and other mercury compounds (inorganic and organic). They each have following specific effects on human health.

2.5.1. Methylmercury effects

When mercury combines with carbon, the compounds formed are called "organic" mercury compounds or organomercurials. There is a potentially large number of organic mercury compounds; however, by far the most common organic mercury compound in the environment is methylmercury (also known as monomethylmercury). In the past, an organic mercury compound called phenylmercury was used in some commercial products. Another organic mercury compound called dimethylmercury is also used in small amounts as a reference standard for some chemical tests. Dimethylmercury is the only organic mercury compound that has been identified at hazardous waste sites. It was only found in extremely small amounts at two hazardous waste sites

nationwide, but it is very harmful to people and animals. Like the inorganic mercury compounds, both methylmercury and phenylmercury exist as "salts" (for example, methylmercuric chloride or phenylmercuric acetate). When pure, most forms of methylmercury and phenylmercury are white crystalline solids. Dimethylmercury, however, is a colorless liquid.

Methylmercury is produced primarily by microorganisms (bacteria and fungi) in the environment, rather than by human activity. Until the 1970s, methylmercury and ethylmercury compounds were used to protect seed grains from fungal infections. Once the adverse health effects of methylmercury were known, the use of methymercury- and ethylmercury as fungicides was banned.

For fetuses, infants, and children, the primary health effect of methylmercury is impaired neurological development. Methylmercury exposure in the womb, which can result from a mother's consumption of fish and shellfish that contain methylmercury, can adversely affect a baby's growing brain and nervous system. Impacts on cognitive thinking, memory, attention, language, and fine motor and visual spatial skills have been seen in children exposed to methylmercury in the womb. A previous study reports that most people have blood mercury levels below a level associated with possible health effects (Jones et al., 2004).

Outbreaks of methylmercury poisonings have made it clear that adults, children, and developing fetuses are at risk from ingestion exposure to methylmercury. During these poisoning outbreaks some mothers with no symptoms of nervous system damage gave birth to infants with severe disabilities, it became clear that the developing nervous system of the fetus may be more vulnerable to methylmercury than is the adult nervous system. In addition to the subtle impairments noted above, symptoms of methylmercury poisoning may include, impairment of the peripheral vision, disturbances in sensations ("pins and needles" feelings, usually in the hands, feet, and around the mouth), lack of coordination of movements, impairment of speech, hearing, walking, and muscle weakness.

No human data indicate that exposure to any form of mercury causes cancer, but the human data currently available are very limited. Mercuric chloride has caused increases in several types of tumors in rats and mice, and methylmercury has caused kidney tumors in male mice. When EPA revised its ‘Cancer Guidelines’ in 2005, the EPA concluded that neither inorganic mercury nor methylmercury from environmental exposures are likely to cause cancer in humans.

2.5.2. Elemental mercury effects

Elemental (metallic) mercury primarily causes health effects when it is breathed as a vapor where it can be absorbed through the lungs. These exposures can occur when elemental mercury is spilled or products that contain elemental mercury break and expose mercury to the air, particularly in warm or poorly-ventilated indoor spaces.

The symptoms include tremors, emotional changes (e.g., mood swings, irritability, nervousness and excessive shyness), insomnia, neuromuscular changes (such as weakness, muscle atrophy, twitching), headaches, disturbances in sensations, changes in nerve responses, performance deficits on tests of cognitive function. At higher exposures there may be kidney effects, respiratory failure and death.

2.5.3. Effects of other mercury compounds

Inorganic mercury compounds occur when mercury combines with elements such as chlorine, sulfur, or oxygen. These mercury compounds are also called mercury salts. Most inorganic mercury compounds are white powders or crystals, except for mercuric sulfide (also known as cinnabar) which is red and turns black after exposure to light. High exposures to inorganic mercury may result in damage to the gastrointestinal tract, the nervous system, and the kidneys. Both inorganic and organic mercury compounds are absorbed through the

gastrointestinal tract and affect other systems via this route. However, organic mercury compounds are more readily absorbed via ingestion than inorganic mercury compounds. Symptoms of high exposures to inorganic mercury include, skin rashes and dermatitis, mood swings, memory loss, mental disturbances, and muscle weakness.

2.6. Model description

2.6.1. Trajectories

Trajectories are defined as the paths of small particles of air at a certain point in space at a given time and can be traced forward or backward in time (Stohl et al., 2002). The HYSPLIT (HYbrid Single-Particle Lagrangian Integrated Trajectory) model is a complete system for computing simple air parcel trajectories to complex dispersion and deposition simulations (Draxler and Hess, 2005). Therefore, they are often used to explain the chemical measurement data at sampling sites in order to identify the source-receptor relationships (Stohl, 1998).

There are two approaches to compute the time history of air pollutant concentrations. Eulerian models, which solve the advection-diffusion equation on a fixed grid, and Lagrangian models, in which the advection and diffusion components are calculated independently (Draxler et al., 1998). While the Eulerian method is the common way of treating heat and mass transfer phenomena, the Lagrangian approach

is used to interpret the concentration or position changes relative to the moving fluid (Seinfeld et al., 1998). The HYSPLIT model developed by National Oceanic and Atmospheric Administration (NOAA) that was used in this study is a hybrid between Eulerian and Lagrangian approaches, which advection and diffusion calculations are made in a Lagrangian framework while concentrations are calculated on a fixed grid.

The initial version of HYSPLIT used only rawinsonde observations for meteorological data (Draxler et al., 1982), but in the most recent version, HYSPLIT 4, the rawinsonde data was replaced by gridded meteorological data from either analyses or short-term forecasts from routine numerical weather prediction models (Draxler et al., 1998). The meteorological data fields are linearly interpolated to a terrain-following (σ) coordinate system.

$$\sigma = 1 - z/Z_{top} \qquad (2\text{-}9)$$

where z is the height expressed relative to the terrain, and Ztop is the top of HYSPLIT's coordinate system.

At a minimum HYSPLIT requires U, V (the horizontal wind components), T (temperature), Z (height) or P (pressure), and the pressure at the surface, P0. Also, in most circumstances, the vertical velocity field (W) is relative to the meteorological model's native

terrain-following coordinate system. Once the basic (U, V, W) meteorological data are processed and interpolated to the internal model grid, trajectories can be computed by advection components. The advection of a particle is computed from the average of the three-dimensional velocity vectors for the initial-position P(t) and the first-guess position P'(t+Δt). The velocity vectors are linearly interpolated in both space and time. The first guess position is

$$P'(t+\Delta t) = P(t) + V(P,t)\,\Delta t \qquad (2\text{-}10)$$

, and the final position is

$$P(t+\Delta t) = P(t) + 0.5\,[V(P,t) + V(P', t+\Delta t)]\,\Delta t \qquad (2\text{-}11)$$

where, V, here, represents the average of the three-dimensional velocity vectors. Trajectories are terminated if they reach the model top, but advection continues along the surface if trajectories intersect the ground (Draxler et al., 1998). Trajectories may be integrated both forward and backward in time. A measure of the integration may be obtained by computing a backward trajectory from the end-point-position of its forward counterpart.

2.6.2. Potential Source Contribution Function (PSCF)

PSCF, a trajectory-based model is a simple method that links residence time in upwind areas with high concentrations through a conditional probability field and originally developed by Ashbaugh et al. (1985). PSCF was extensively and successfully used in the past (Cheng et al., 1993; Lim et al., 2001; Poissant, 1999; Zeng and Hopke, 1989). The PSCF model counts each trajectory segment endpoint within a given grid cell. For an event at the receptor site, the probability is related to the number of endpoints in that cell associated with the total number of endpoints for all sampling dates. If N is the total number of trajectory segment endpoints over the study period, and if n is the number of trajectory segment endpoints fall into the *ij*-th cell, the probability of this events, A_{ij}, is calculated by

$$P[A_{ij}] = n_{ij} / N \qquad (2\text{-}12)$$

If the m_{ij} is the number of segment endpoints in the same grid cell (*ij*-th cell) when the concentrations are higher than a criterion value, the probability of this high concentration event, B_{ij}, is given by $P[B_{ij}]$,

$$P[B_{ij}] = m_{ij} / N \qquad (2\text{-}13)$$

The probability of high concentration event divided by the probability of total event in a fixed grid cell defines the PSCF value as

$$PSCF_{ij} = \frac{P[B_{ij}]}{P[A_{ij}]} = \frac{m_{ij}/N}{n_{ij}/N} = \frac{m_{ij}}{n_{ij}} \quad (2\text{-}14)$$

High PSCF values in that grid those grid cells are regarded as possible source locations. Cells including emission sources could be identified with conditional probabilities close to one if trajectories that have crossed the cells efficiently transport the released pollutant to the receptor site. Therefore, the PSCF model provides a tool to map the source potentials of geographical areas.

2.6.3. Lagrangian Particle Dispersion Model (LPDM)

Trajectories are typically calculated for samples collected over long time periods. However individual trajectories cannot represent the whole measurement time and do not consider the turbulent mixing and convection in the atmosphere. Specifically PSCF does not consider the reduction of the concentration of the species through diffusion, chemical transformation, and atmospheric scavenging during the transport between the source areas and the receptor (Cheng et al., 1993). It is insufficient to identify the source-receptor relationship using PSCF

based on backward trajectories and to represent the transport history of a sampling volume even if it is small (Stohl et al., 2002). For this reason, more elaborate models are needed, both of the planetary boundary layer (PBL), where an air mass quickly loses its identity due to strong mixing (Lyons et al., 1995), and at higher levels of the atmosphere when longer time scales are considered (Sutton, 1994). The LPDM contains no artificial numerical diffusion like Eulerian models (Nguyen et al., 1997) and hence has a greater potential to resolve fine-scale structures of the flow. The LPDM is based on the conditioned particle concepts (Smith, 1968) in which released particles with any specified release rate into the model domain are then advected by velocity components resolved by the model and subgrid-scale turbulent components. Therefore LPDM is physically and theoretically more correct than trajectory model. However trajectory model is still used because of convenience, availability of models and computational constraints (Stohl et al., 2002).

The source-receptor relationship can be linear or nonlinear. In this study, a linear source-receptor relationship was calculated using the HYSPLIT 4 dispersion model (LPDM) because standard LPDM cannot simulate nonlinear chemical reactions (Seibert and Frank, 2004). Thus, linear source-receptor relationships can be calculated simply with following equation.

$$y=Mx \quad (2\text{-}15)$$

where, y indicates the discrete observation (e.g. measured concentration) at receptor sites and x is the source emission term, which varied with locations and time. M is the source-receptor relationship including transport processes. In conventional PSCF, the number of end points in the ij-th cell which is expressed as a residence time (hr), is simply considered to be the source-receptor relationship of the *ij*-th cell (Han et al., 2005).

The output value of the dispersion model such as HYSPLIT 4 is regarded as source-receptor matrix. The HYSPLIT model gives gridded concentration fields (mass m^{-3}) as output. To obtain the residence time of each grid (e.g. transmission corrected residence time), a transformation is necessary (Seibert, 2004; Seibert and Frank, 2004; Han et al., 2005).

$$\tau = \frac{\Delta T_s V_s}{\mu_{tot}} \bar{c} \quad (2\text{-}16)$$

where ΔTs is the time during which the source is acting, Vs is the volume of grid and is the concentration in a grid cell as produced by HYSPLIT.

Once the transmission-corrected residence time is calculated, the

potential source contribution function (PSCF) can be applied. LPDM is more accurate in the prediction of the behavior of an air parcel, since the dispersion model can estimate precise standard deviations of atmospheric turbulence from calculated stability which changes at every grid and every time step through a meteorological model and dry and wet deposition using a meteorological model and measured or estimated precipitation rate (Draxler and Hess, 2005; Han et al., 2005).

References

Alberts, J. J., Schindler, J. E., Miller, R.W., Nutter, D. E., 1974. Elemental mercury evolution mediated by humic acid. Science, USA 184, 895–897.

Allard, B. and Arsenie, I., 1991. Abiotic reduction of mercury by humic substances in aquatic system - an important process for the mercury cycle. Water, Air, and Soil Pollution 56, 457-464.

Amyot, M., Mierle, G., Lean, D. R. S., McQueen, D. J., 1994. Sunlight-induced formation of dissolved gaseous mercury in lake waters. Environmental Science and Technology 28, 2366-2371.

Amyot, M., Gill, G. A., Morel, F. M. M., 1997. Production and loss of dissolved gaseous mercury in coastal seawater. Environmental Science and Technology 31, 3606-3611.

Amyot, M., Lean, D. R. S., Poissant, L., Doyon, M.-R., 2000. Distribution and transformation of elemental mercury in the St. Lawrence River and Lake Ontario. Canadian Journal of Fisheries and Aquatic Sciences 57(Suppl. 1), 155-163.

Ashbaugh, L. L., Malm, W. C., Sadeh, W. Z., 1985. A residence time probability analysis of sulfur concentrations at Grand Canyon National Park, Atmospheric Environment 19, 1263-1270.

Barkay, T., Miller, S.M., Summers, A. O., 2003. Bacterial mercury resistance from atoms to ecosystems. FEMS Microbiology Reviews 23, 355-384.

Boutron, C. 1986. Atmospheric toxic metals and metalloids in the snow and ice layers deposited in Greenland and Antarctica from prehistoric times to present. Toxic Metals in the Atmosphere 467, 217.

Bullock, O. R., Benjey, W. G., Keating, M. H., 1997. Modeling of regional scale atmospheric mercury transport and deposition using RELMAP. In: Baker, J.E. (Ed.), Atmospheric deposition of contaminants to the great lakes and coastal waters. SETAC press, Florida, pp. 323-347.

Bullock, O. R., Brehme, K. A., Mapp, G. R., 1998. Lagrangian modeling of mercury air emission, transport and deposition: an

analysis of model sensitivity to emissions uncertainty. Science of the Total Environment 213, 1-12.

Burke, J. B., Hoyer, M. E., Keeler, G. J., Scherbatskoy, T., 1995. Wet deposition of mercury and ambient mercury concentrations at a site in the Lake Champlain Basin. Water, Air, and Soil Pollution 50, 353-362.

Carpi, A. and Lindberg, S. E., 1997. Sunlight-mediated emission of elemental mercury from soil amended with municipal sewage sludge. Environmental Science and Technology 31, 2085-2091.

Carpi, A. and Lindberg, S. E., 1998. Application of a teflon^{TM} dynamic flux chamber for quantifying soil mercury flux: Tests and results over background soil. Atmospheric Environment 32, 873-882.

Chen, H., Yang, X., Perkins, C., 2004. Trend and variability of total gaseous mercury (TGM) in the state of Connecticut, U.S.A. during 1997-1999. Water, Air, and Soil Pollution 151, 103-116.

Cheng, M. D., Hopke, P. K., Zeng, Y., 1993. A receptor-oriented methodology for determining source regions of particle sulfate composition observed at Dorset, Ontario. Journal of Geophysical Research Atmospheres 98, 16839-16849.

Choi, A. L. and Grandjean, P. 2008. Methylmercury exposure and health effects in humans. Environmental Chemistry 5**,** 112-120.

Cohen, M., Artz, R., Draxler, R., Miller, P., Niemi, D., Ratte, D., Deslauriers, M., Duvar, R., Laurin, R., Slotnick, J., Nettesheim, T., McDonald, J., 2004. Modeling the atmospheric transport and deposition of mercury to the Great Lakes. Environmental Research 95, 247-265.

Costa, M. and Liss, P., 1999. Photoreduction of mercury in sea water and its possible implications for Hg^0 air-sea fluxes. Marine Chemistry 68, 87-95.

Costa, M. and Liss, P., 2000. Photoreduction and evolution of mercury from seawater. Science of the Total Environment 261, 125-135.

Dastoor, A. P. and Larocque, Y., 2004. Global circulation of atmospheric mercury: a modelling study. Atmospheric Environment 38, 147-161.

Draxler, R. R. and Hess, G. D., 1998. An overview of the HYSPLIT_4 modelling system for trajectories, dispersion and deposition. Australian Meteorological Magazine 47, 295-308.

Draxler, R. R. and Hess, G. D., 2005. HYSPLIT 4 USER's Guide. NOAA Technical Memorandum ERL ARL-230.

Driscoll, C. T., Blette, V., Yan, C., Schofield, C. L., Munson, R., Holsapple, J., 1995. The role of dissolved organic carbon in the chemistry and bioavailability of mercury in remote Adirondack lakes. Water, Air, and Soil Pollution 80, 499-508.

Dvonch, J., Graney, J., Marsik, F., Keeler, G., Stevens, R. 1998. An investigation of source-receptor relationships for mercury in south Florida using event precipitation data. Science of the Total Environment 213, 95-108.

Engle, M. A., Gustin, M. S., Zhang, H. 2001. Quantifying natural source mercury emissions from the Ivanhoe Mining District, north-central Nevada, USA. Atmospheric Environment 35, 3987-3997.

Engle, M. A. and Gustin, M. S., 2002. Scaling of atmospheric mercury emissions from three naturally enriched areas: Flowery Peak, Nevada; Peavine Peak, Nevada; and Long Valley Caldera, California. Science of the Total Environment 290, 91-104.

Ericksen, J. A., Gustin, M. S., Schorran, D. E., Johnson, D. W., Lindberg, S. E., Coleman, J. S., 2003. Accumulation of atmospheric mercury in forest foliage. Atmospheric Environment 37, 1613−1622.

Finlayson-Pitts, B. J. and Pitts, Jr., J. N., 1986. Atmospheric chemistry: Fundamentals and experimental techniques, Wiley, New York

Fitzgerald, W. F., Mason, R. P., Vandal, G. M., 1991. Atmospheric cycling and air-water exchange of mercury over mid-continental lacustrine regions. Water, Air, and Soil Pollution 56, 745-768.

Fitzgerald, W. F., 1995. Is mercury increasing in the atmosphere? The need for an atmospheric mercury network (AMNET). Water, Air, and Soil Pollution 80, 245-254.

Fthenakis, V., Lipfert, F., Moskowitz, P., Saroff, L., 1995. An assessment of mercury emissions and health risks from a coal-fired power plant. Journal of Hazardous Materials 44, 267-283.

Fu, X. W., Feng, X., Dong, Z. Q., Yin, R. S., Wang, J. X., Yang, Z. R., Zhang, H., 2010a. Atmospheric gaseous elemental mercury (GEM) concentrations and mercury depositions at a high-altitude mountain peak in south China. Atmospheric Chemistry and Physics 10, 2425-2437.

Fu, X., Feng, X., Zhu, W., Rothenberg, S., Yao, H., Zhang, H., 2010b. Elevated atmospheric deposition and dynamics of mercury in a remote upland forest of Southwestern China. Environmental Pollution 158, 2324–2333.

Gabriel, M. C., Williamson, D. G., Zhang, H., Brooks, S., Lindberg, S., 2006. Diurnal and seasonal trends in total gaseous mercury flux from three urban ground surfaces. Atmospheric Environment 40, 4269-4284.

Gauchard, P. A., Ferrari, C.P., Dommergue, A., Poissant, L., Pilote, M., Guehenneux, G., Boutron, C.F., Baussand, P., 2005. Atmospheric particle evolution during a nighttime atmospheric mercury depletion event in sub-Arctic at Kuujjuarapik/ Whapmagoostui, Que´bec, Canada . Science of the Total Environment 336, 215-224.

Gill G. A. and Bruland, K. W., 1990. Mercury speciation in surface freshwater systems in California and other areas. Environmental Science and Technology 24, 1392-1400.

Glass, G. E. and Sorensen, J. A., 1999. Six-year trend (1990-1995) of wet mercury deposition in the Upper Midwest, USA. Environmental Science and Technology 33, 3303-3312.

Gratz, L. E., Keeler, G. J., Miller, E. K. 2009. Long-term relationships between mercury wet deposition and meteorology. Atmospheric Environment 43**,** 6218-6229.

Gratz, L. E. and Keeler, G. J. 2011. Sources of mercury in precipitation to Underhill, VT. Atmospheric Environment 45**,** 5440-5449.

Guentzel, J. L., Landing, W. M., Gill, G. A., Pollman, C. D., 1995. Atmospheric deposition of mercury in Florida: The FAMS Project (1992-1994). Water, Air, and Soil Pollution 80, 393-402.

Guentzel, J. L., Landing, W. M., Gill, G. A., Pollman, C. D., 2001. Processes influencing rainfall deposition of mercury in Florida. The FAMS Project (1992-1996). Environmental Science and Technology 35, 863-873.

Guo, Y., Feng, X., Li, Z., He, T., Yan, H., Meng, B., Zhang, J., Qiu, G., 2008. Distribution and wet deposition fluxes of total and methyl mercury in Wujiang River Basin, Guizhou, China. Atmospheric Environment 42, 7096-7103.

Gustin, M. S., Taylor, G. E., Maxey, R. A., 1997. Effect of temperature and air movement on the flux of elemental mercury from substrate to the atmosphere. Journal of Geophysical Research 102, 3891–3898.

Gustin, M. S., Lindberg, S., Marsik, F., Casimir, A., Ebinghaus, R., Edwards, G., Hubble-Fitzgerald, C., Kemp, R., Kock, H., Leonard, T., London, J., Majewski, M., Montecinos, C., Owens, J., Pilote, M., Poissant, L., Rasmussen, P., Schaedlich, F., Schneeberger, D., Schroeder, W., Sommar, J., Turner, R., Vette, A., Wallschlaeger, D., Xiao, Z., Zhang, H., 1999. Nevada STORMS project: Measurement of mercury emissions from naturally enriched surfaces Journal of Geophysical Research 104, 21831-21844.

Gustin, M. S. and Lindberg, S. E., 2000. Assessing the contribution of natural sources to the global mercury cycle: The importance of intercomparing dynamic flux measurements. Fresenius Journal of Analytical Chemistry 366, 417-422.

Gustin, M. S., Lindberg, S. E., Austin, K., Coolbaugh, M., Vette, A., Zhang, H., 2000. Assessing the contribution of natural sources to regional atmospheric mercury budgets. Science of the Total Environment 259, 61-71.

Gustin, M. S., 2011. Exchange of mercury between the atmosphere and terrestrial ecosystems In Advances in Environmental Chemistry and Toxicology of Mercury; Liu, G., Cai, Y., O'Driscoll, N., Eds.; John Wiley and Sons: New York.

Hall, B. D., Olson, M. L., Rutter, A. P., Frontiera, R. R., Krabbenhoft, D. P., Gross, D. S., Yuen, M., Rudolph, T. M., Schauer, J. J., 2006. Atmospheric mercury speciation in Yellowstone National Park. Science of the Total Environment 367, 354-366.

Han, Y. J., Holsen, T. M., Hopke, P. K., Yi, S. M., 2005. Comparison between back-trajectory based modeling and Lagrangian backward dispersion modeling for locating sources of reactive gaseous mercury. Environmental Science and Technology 39, 1715-1723.

Hoyer, M., Burke, J., Keeler, G. J., 1995. Atmospheric sources, transport and deposition of mercury in Michigan: two years of event precipitation. Water, Air, and Soil Pollution 80, 199-208.

IPCS, 2000. International Chemical Safety Cards 0056, 0978, 0979, 0980, 0981, 0982 and 0984. Geneva, World Health Organization, International Programme on Chemical Safety. http://www.who.int/ipcs/publications/icsc/en/index.html.

Jones, R., Sinks, T., Schober, S., Pickett, M., 2004. Blood mercury levels in young children and childbearing-aged women-United States, 1999-2002. MMWR Morb Mortal Wkly Rep 53(43), 1018-1020.

Keeler, G. J., 1994. Lake Michigan urban air toxics study, Final Report. Atmospheric Research and Exposure Assessment Laboratory, Office of Research and Development. U. S. EPA. Research Triangle Park. N.C.

Keeler, G. J. and Dvonch, J. T., 2005. Atmospheric mercury: A decade of observations in the Great Lakes. In dynamics of mercury pollution on regional and global scales: atmospheric processes and human exposures around the world; Pirrone, N., Mahaffey, K., Eds.; Kluwer Ltd: Norwell, MA.

Keeler, G., Gilinsorn, G., Pirrone, N., 1995. Particulate mercury in the atmosphere: its significance, transport, transformation and sources. Water, Air, and Soil Pollution 80, 159-168.

Keeler, G. J., Landis, M. S., Norris, G. A., Christianson, E. M., Dvonch, J. T., 2006. Sources of mercury wet deposition in eastern Ohio, USA. Environmental Science and Technology 40, 5874-5881.

Kim, K. H., Lindberg, S. E., Meyers, T. P., 1995. Micrometeorological measurements of mercury vapor fluxes over background forest soils in eastern Tennessee. Atmospheric Environment 29, 267-282.

Kobayashi, T., 1987. Oxidation of metallic mercury in aqueous solution by hydrogen peroxide and chlorine, Journal of Japan Society for Air Pollution 22, 230-236.

Krabbenhoft, D. P., Hurley, J. P., Olson, M. L., Cleckner, L. B., 1998. Diel variability of mercury phase and species distributions in the Florida Everglades. Biogeochemistry 40, 311-325.

Lalonde, J. D., Amyot, M., Kraepiel, A. M. L., Morel, F. M. M., 2001. Photooxidation of Hg(0) in artificial and natural waters. Environmental Science and Technology 35, 1367-1372.

Lalonde, J. D., Amyot, M., Orvoine, J., Morel, F. M.. M., Auclair, J.-C., Ariya, P.A., 2004. Photoinduced oxidation of Hg0(aq) in the waters from the St. Lawrence Estuary. Environmental Science and Technology 38, 508-514.

Landis, M. S. and Keeler, G. J., 1997. Critical evaluation of a modified automatic wet-only precipitation collector for mercury and trace element determinations. Environmental Science and Technology 31, 2610-2615.

Landis, M. S., Stevens, R. K., Schaedlich, F., Prestbo, E. M., 2002. Development and characterization of an annular denuder methodology for the measurement of divalent inorganic reactive gaseous mercury in ambient air. Environmental Science and Technology 36, 3000–3009.

Leonard, T. L., Taylor, G. E., Gustin, M. S., Fernandez, G. C. J., 1998. Mercury and plants in contaminated soils: 1. Uptake, partitioning, and emission to the atmosphere. Environmental Toxicology and Chemistry 17, 2063– 2071.

Lim, C., Cheng, M., Schroeder, W., 2001. Transport patterns and potential sources of total gaseous mercury measured in Canadian high Arctic in 1995, Atmospheric Environment 35, 1141-1154.

Lin, C.-J. and Pehkonen, S. O., 1997. Aqueous free radical chemistry of mercury in the presence of iron oxides and ambient aerosol, Atmospheric Environment 31, 4125-4137

Lin, C.-J. and Pehkonen, S. O., 1999. The chemistry of atmospheric mercury: a review. Atmospheric Environment 33, 2067-2679.

Lin, C.-J., Pongprueksa, P., Lindberg, S. E., Pehkonen, S. O., Byun, D., Jang, C., 2006. Scientific uncertainties in atmospheric mercury models I: Model science evaluation. Atmospheric Environment 40, 2911-2928.

Lin, C.-J., Pongprueksa, P., Bullock, O. R., Lindberg, S. E., Pehkonen, S. O., Jang, C., Braverman, T., Ho, T. C., 2007. Scientific uncertainties in atmospheric mercury models II: Sensitivity analysis in the CONUS domain. Atmospheric Environment 41, 6544-6560.

Lindberg, S. E. and Turner R. R., 1977. Mercury emission from chlorine-production and solid waste deposits. Nature 268, 133-136.

Lindberg, S. E., Meyers, G. E., Taylor, Jr. R. R., Schroeder, W. H., 1992. Atmosphere surface exchange of Hg in a forest: results of modeling and gradient approaches. Journal of Geophysical Research 97, 2519-2528.

Lindberg, S. E., Kim, K. H., Munthe, J., 1995. The precise measurement of concentration gradients of mercury in air over soils: A review of past and recent measurements. Water, Air, and Soil Pollution 80, 383-392.

Lindqvist, O. and Rodhe, H., 1985. Atmospheric mercury - a review. Tellus. 37B, 136-159.

Lindqvist, O., Aastrup, M., Andersson, A., Bringmark, L., Hovsenius, G., Hakanson, L., Iverfeldt, Å., Meili, M. and Timm, B. 1991. Mercury in the Swedish environment: recent research on causes, consequences and corrective methods. Water, Air, and Soil Pollution 55, 143-177.

Lu, J. Y. and Schroeder, W. H., 2004. Annual time-series of total filterable atmospheric mercury concentrations in the Arctic. Tellus 56B, 213–222.

Lynam, M. M. and Keeler, G. J., 2002. Comparison of methods for particulate phase mercury: sampling and analysis. Analytical and Bioanalytical Chemistry 374, 1009-1014.

Lyons, W.A., Pielke, R.A., Tremback, C.J., Walko, R. L., 1995. Modeling impacts of mesoscale vertical motions upon coastal zone air pollution dispersion. Atmospheric Environment 29, 283-301.

Mason, R. P., Vandal, G.M., Fitzgerald, W.F., 1992. The sources and composition of mercury in Pacific Ocean rain. Journal of Atmospheric Chemistry 14, 489-500.

Mason, R. P., Fitzgerald, W. F., Morel, F. M. M., 1994. The biogeochemical cycling of elemental mercury: Anthropogenic influences. Geochimica et Cosmochimica Acta 58, 3191-3198.

Mason, R. P., Lawson, N. M., Sullivan, K. A., 1997. Atmospheric deposition to the Chesapeake Bay watershed-regional and local sources. Atmospheric Environment 31, 3531-3540.

Mason, R. P., Lawson, N. M., Sheu, G. R., 2000. Annual and seasonal trends in mercury deposition in Maryland. Atmospheric Environment 34, 1691-1701.

Mason, R. P., Abbott, M. L., Bodaly, R. A., Bullock, O. R., Driscoll, T. D., Ever, D., Lindberg, S. E., Murray, M., Swain, E. B., 2005. Monitoring the response to changing mercury deposition. Environmental Science and Technology 39, 14A–22A.

Miller, E. K., Vanarsdale, A., Keeler, G. J., Chalmers, A., Poissant, L., Kamman, N. C., Brulotte, R., 2005. Estimation and Mapping of dry mercury deposition across northeastern North America. Ecotoxicology 14, 53-70.

Moore, C. and Carpi, A., 2005. Mechanisms of the emission of mercury from soil: Role of UV radiation. Journal of Geophysical Research 110, D24302.

Morel, F. M. M., Draepiel, A. M. L., Amyot, M., 1998. The chemical cycle and bioaccumulation of mercury, Annual Review of Ecology and Systematics 29, 543-566.

Mukherjee, A.B., Melanen, M., Ekqvist, M., Verta, M., 2000. Assessment of atmospheric mercury emission in Finland. Science of the Total Environment 259, 73-83.

Munthe, J., 1992. The aqueous oxidation of elemental mercury by ozone, Atmospheric Environment 26A, 1461-1468.

Nater, E. A. and Grigal, D. F., 1992. Regional trends in mercury distribution across the Great Lakes states, north central USA. Nature 358, 139 - 141.

Nriagu, J. O. and Pacyna, J. M., 1988. Quantitative assessment of worldwide contamination of air, water and soils with trace metals. Nature 333, 134-139.

Nriagu, J. O., 1989. A global assessment of natural sources of atmospheric trace metals. Nature 338, 47-49.

Nriagu, J. O., 1990. Global metal pollution: Poisoning the biosphere?. Environment: Science and Policy for Sustainable Development 32, 7- 33.

Nguyen, K. C., Noonan, J. A., Galbally, I. E., Physick, W. L., 1997. Predictions of plume dispersion in complex terrain: Eulerian versus Lagrangian models. Atmospheric Environment 31, 947-958.

O'Driscoll, N. J., Siciliano, S. D., Lean, D. R. S., 2003. Continuous analysis of dissolved gaseous mercury in freshwater lakes, Science of the Total Environment 304, 285-294.

Pacyna, E. G. and Pacyna, J. M., 2002. Global emission of mercury from anthropogenic sources in 1995. Water, Air, and Soil Pollution 137, 149-165.

Pacyna, E. G., Pacyna, J. M., Steenhuisen, F., Wilson, S., 2006. Global anthropogenic mercury emission inventory for 2000. Atmospheric Environment 40, 4048–4063.

Pacyna, J. M., Pacyna, E. G., Steenhuisen, F., Wilson, S., 2003. Mapping 1995 global anthropogenic emissions of mercury. Atmospheric Environment 37, 109–117.

Pai, P., Niemi, D., Powers, B., 2000. A North America inventory of anthropogenic mercury emissions. Fuel Processing Technology 65-66, 101-115.

Pehkonen, S. O. and Lin, C.-J., 1998. Aqueous photochemistry of divalent mercury with organic acids, Journal of Air and Waste Management Association 48, 144-150.

Petersen, G., Iverfeldt, A., Munthe, J.,1995. Atmospheric mercury species over central and northern Europe - model calculations and comparison with observations from the Nordic air and precipitation network for 1987 and 1988, Atmospheric Environment 29, 46-67.

Pirrone, N., Keeler, G. J., Nriagu, J. O., 1996. Regional differences in worldwide emissions of mercury to the atmosphere. Atmospheric Environment 30, 2981-2987.

Pirrone, N., Allegrini, I., Keeler, G. J., Nriagu, J. O., Rossmann, R., Robbins, J. A., 1998. Historical atmospheric mercury emissions and depositions in North America compared to mercury accumulations in

sedimentary records, atmospheric Transport, Chemistry and Deposition of Mercury. Atmospheric Environment 32, 929–940.

Pirrone, N., Costa, P., Pacyna, J.M., Ferrara, R., 2001. Mercury emissions to the atmosphere from natural and anthropogenic sources in the Mediterranean region. Atmospheric Environment 35, 2997-3006.

Pirrone, N., Cinnirella, S., Feng, X., Finkelman, R. B., Friedli, H. R., Leaner, J., Mason, R. P., Mukherjee, A. B., Stracher, G. B., Streets, D. G., Telmer, K., 2010. Global mercury emissions to the atmosphere from anthropogenic and natural sources. Atmospheric Chemistry and Physics 10, 5951-5964.

Pizzichini, M., Fonzi, M., Sugherini, L., Fonzi, L., Gasparoni, A., Ccomporti, M., Pompella, A. 2002. Release of mercury from dental amalgam and its influence on salivary antioxidant activity. Science of the Total Environment, 284**,** 19-25.

Pleijel, K. and Munthe, J., 1995. Modeling the atmospheric chemistry of mercury - The importance of a detailed description of the chemistry of cloud water. Water, Air, and Soil Pollution 80, 317-324.

Poissant, L., 1999. Potential sources of atmospheric total gaseous mercury in the St. Lawrence River valley, Atmospheric Environment 33, 2537-2547.

Poissant, L., Pilote, M., Beauvais, C., Constant, P., Zhang, H., 2005. A year of continuous measurements of three atmospheric mercury species (GEM, RGM, and Hg_p) in southern Quebec, Canada. Atmospheric Environment 39, 1275-1287.

Prestbo, E. M. and Gay, D. A. 2009. Wet deposition of mercury in the US and Canada, 1996-2005: Results and analysis of the NADP mercury deposition network (MDN). Atmospheric Environment 43**,** 4223-4233.

Quig, D. 1998. Cysteine metabolism and metal toxicity. Alternative Medicine Review 3**,** 262-270.

Risch, M. R., Gay, D. A., Fowler, K. K., Keeler, G. J., Backus, S. M., Blanchard, P., Barres, J. A., Dvonch, J. T., 2011. Spatial pattern and temporal trends in mercury concentrations, precipitation depth, and mercury wet deposition in the North American Great Lakes region, 2002-2008. Environmental Pollution 161, 261-271.

Risch, M. R., Gay, D. A., Fowler, K. K., Keeler, G. J., Backus, S. M., Blanchard, P., Barres, J. A.,Dvonch, J. T. 2012. Spatial patterns and temporal trends in mercury concentrations, precipitation depths, and mercury wet deposition in the North American Great Lakes region, 2002–2008. Environmental pollution 161**,** 261-271.

Rogers, R. D., 1979. Volatility of Hg from soils amended with various Hg compounds. Soil Science Society of America Journal 43, 289-291.

Rogers, R. D. and McFarlane, J. C., 1979. Factors influencing the volatilization of mercury from soil. Journal of Environmental Quality 8, 255-260.

Sakata, M. and Marumoto, K., 2002. Formation of atmospheric particulate mercury in the Tokyo metropolitan area. Atmospheric Environment 36, 239–246.

Sakata, M. and Marumoto, K., 2005. Wet and dry deposition fluxes of mercury in Japan. Atmospheric Environment 39, 3139-3146.

Sanemasa, I., 1975. The solubility of elemental mercury vapor in water. Bulletin of the Chemical Society of Japan 48, 1795 –1798.

Schroeder, W. H., Yarwood, G., Niki, H., 1991. Transformation processes involving mercury species in the atmosphere - results from a literature survey. Water Air and Soil Pollution 56, 653-666.

Schroeder, W. Lindqvist, O., Munthe, J., Xiao, Z., 1992. Volatilization of mercury from lake surfaces. Science of the Total Environment 125, 47-66.

Schroeder, W. H. and Munthe, J., 1998. Atmospheric mercury - An overview. Atmospheric Environment 32, 809-822.

Schlüter, K., 2000. Review: evaporation of mercury from soils. An integration and synthesis of current knowledge. Environmental Geology 39, 249-271.

Seibert, P., 2004. Inverse modeling with a Lagrangian particle dispersion model: application to point releases over limited time intervals, edited by Schiermeier, F.A. and Gryning, S.E., *Air*

Pollution Modeling and its Application XIV, Kluwer Academic/Plenum Publishers, New York, 381-389.

Seibert, P. and Frank, A., 2004. Source-receptor matrix calculation with a Lagrangian particle dispersion model in backward mode. Atmospheric Chemistry and Physics 4, 51-63.

Seigneur, C., Wrobel, J., Constantinou, E., 1994. A chemical kinetic mechanism for atmospheric inorganic mercury. Environmental Science and Technology 28, 1589- 1597.

Seinfeld, J. H. and Pandis, S. N., 1998. Atmospheric Chemistry and Physics, John Wiley &Sons, INC., New York.

Sellers, P., Kelly, C. A., Rudd, J. W. M., MacHutchon, A. R.,1996. Photodegradation of methylmercury in lakes. Nature 380, 694-697.

Seo, Y. S., Han, Y. J. Choi, H. D., Holsen, T. M., Yi, S. M., 2012. Characteristics of total mercury (TM) wet deposition: Scavenging of atmospheric mercury species. Atmospheric Environment 49, 69-76.

Skogerboe, R. K. and Wilson, S. A., 1981. Reduction of ionic species by fulvic acid. Analytical Chemistry 53, 228–232.

Slemr, F., Schuster, G., Seiler, W., 1985. Distribution, speciation and budget of atmospheric mercury, Journal of Atmospheric Chemistry 3, 407-434.

Slemr, F. and Langer, E., 1992. Increase in global atmospheric concentrations of mercury inferred from measurements over the Atlantic Ocean, Nature 355, 434-437.

Smith, F. B., 1968. Conditioned particle motion in a homogeneous turbulent field. Atmospheric Environment 2, 491–508.

Sorensen, J.A., Glass, G.E., Schmidt, K.W., 1994. Regional patterns of wet mercury deposition. Environmental Science and Technology 28, 2025-2032.

Steding, D. J. and Flegal, A. R. 2002. Mercury concentrations in coastal California precipitation: evidence of local and trans-Pacific fluxes of mercury to North America. Journal of Geophysical Research 107, 4764.

Stein, E. D., Cohen, Y., Winer, A. M., 1996. Environmental distribution and transformation of mercury compounds. Critical Reviews in Environmental Science and Technology 26, 1-43.

Stohl, A. 1998. Computation, accuracy and applications of trajectories-a review and bibliography. Atmospheric Environment 32, 947-966.

Stohl A., Eckhardt, S., Forster, C., James, P., Spichtinger, N., Seibert, P., 2002. A replacement for simple back trajectory calculations in the interpretation of atmospheric trace substance measurements. Atmospheric Environment 36, 4635-4648.

Sutton, R., 2006. Lagrangian flow in the middle atmosphere. Quarterly Journal of the Royal Meteorological Society 120, 1299-1321.

Thornhill, M. H., Pemberton, M. N., Simmons, R. K., Theaker, E. D. 2003. Amalgam-contact hypersensitivity lesions and oral lichen planus. Oral Surgery, Oral Medicine, Oral Pathology, Oral Radiology, and Endodontology 95**,** 291-299.

Tokos, J. J., Hall, B., Calhoun, J., Prestbo, E., 1998. Homogeneous gas-phase reaction of Hg^0 with H_2O_2, O_3, CH_3I, and $(CH_3)_2S$: Implications for atmospheric Hg cycling, Atmospheric Environment 32, 823-827.

Travnikov, O., 2005. Contribution of intercontinental atmospheric transport to mercury pollution in the Northern Hemisphere. Atmospheric Environment 39, 7541-7548.

UNEP, 2002. Global Mercury Assessment. United Nations Environment Programme (UNEP) Chemicals, Geneva, Switzerland.

U.S. DOE, 1996. A comprehensive assessment of toxic emissions from coal-"red power plants: Phase I results from US DOE study. Energy and Environmental Research Center, September 1996.

U.S. EPA, 1993. National Emissions inventory for mercury and mercury compounds. US EPA-453/R-93-048, Research Triangle Park, NC.

U.S. EPA, 1996. Study of hazardous air pollutant emissions from electric utility steam generating units } Interim Final Report. EPA-453/R-96-013a, O$ce of Air Quality, Research Triangle Park, NC.

U.S. EPA, 1997. Mercury Reports to Congress. Office of Air Quality and Standards. Washington, DC: U.S. Environmental Protection Agency.

Varekamp, J. C. and Buseck, P. R., 1986. Global mercury flux from volcanic and geothermal sources. Applied Geochemistry 1, 65-73.

Vermette, S., Lindberg, S., Bloom, N., 1995. Field tests for a regional mercury deposition network-sampling design and preliminary test results. Atmospheric Environment 29, 1247-1251.

Walcek, C., Santis, S.D., Gentile, T., 2003. Preparation of mercury emissions inventory for eastern North America. Environmental Pollution 123, 375-381.

Wallschläger, D.,1996. Speziesanalytische Untersuchungen zur Abschätzung des Remobilisierungspotentials von Quecksilber aus kontaminierten Elbauen, Doctoral dissertation, University of Bremen, Bremen, Germany.

Wallschläger, D., Turner, R. R., London, J., Ebinghaus, R., Kock, H. H., Sommar, J., Xiao, Z., 1999. Factors affecting the measurement of mercury emissions from soils with flux chambers. Journal of Geophysical Research. 104, 21859 - 21871.

Wallschläger, D., Kock, H., Schroeder, W. H., Lindberg, S. E., Ebinghaus, R., Wilken, R. D., 2000. Mechanism and significance of mercury volatilization from contaminated floodplains of the German river Elbe. Atmospheric Environment 34, 3745-3755.

Wan, Q., Feng, X., Lu, J., Zheng, W., Song, X., Li, P., Han, S., Xu, H., 2009. Atmospheric mercury in Changbai Mountain area, northeastern China II. The distribution of reactive gaseous mercury and particulate mercury and mercury deposition fluxes. Environmental research 109, 721-727.

Wang, S., Feng, X., Qiu, G., Wei, Z., Xiao, T., 2005. Mercury emission to atmosphere from Lanmuchang Hg-Tl mining area, Southwestern Guizhou, China. Atmospheric Environment 39, 7459-7473.

Wängberg, I., Munthe, J., Pirrone, N., Iverfeldt, Å., Bahlman, E., Costa, P., Ebinghaus, R., Feng, X., Ferrara, R., Gårdfeldt, K., Kock, H., Lanzillotta, E., Mamane, Y., Mas, F., Melamed, E., Osnat, Y., Prestbo, E., Sommar, J., Schmolke, S., Spain, G., Sprovieri, F., Tuncel, G., 2001. Atmospheric mercury distribution in Northern

Europe and in Mediterranean region. Atmospheric Environment 35, 3019-3025.

Watras, C. J., Morrison, R. J. M., Frost, T. M., Kratz, T. K., 2000. Decreasing mercury in Northern Wisconsin: Temporal patterns in bulk precipitation and a precipitation-dominated lake. Environmental Science and Technology 34, 4051-4057.

White, E. M., Keeler, G. J., Landis, M. S. 2009. Spatial variability of mercury wet deposition in eastern Ohio: summertime meteorological case study analysis of local source influences. Environmental science and technology 43**,** 4946-4953.

Zahir, F., Rizwi, S. J., Haq, S. K., Khan, R. H. 2005. Low dose mercury toxicity and human health. Environmental toxicology and pharmacology, 20**,** 351-360.

Zeng, Y. and Hopke, P. K., 1989. A study of the sources of acid precipitation in Ontario, Canada. Atmospheric Environment 23, 1499-1509.

Zepp, R.G, Hoigne, J., Bader, H., 1987. Nitrate induced photooxidation of trace organic chemicals in water. Environmental Science and Technology 21, 443-450.

Zhang, H. and Lindberg, S. E., 1999. Processes influencing the emission of mercury from soils: A conceptual model. Journal of Geophysical Research 104, 21889-21896.

Zhang, H.and Lindberg, S. E., 2001. Sunlight and iron(III)-Induced photochemical production of dissolved gaseous mercury in freshwater. Environmental Science and Technology 35, 928-935.

Zielonka, U., Hlawiczka, S., Fudala, J., Wängberg, I., Munthe, J., 2005. Seasonal mercury concentrations measured in rural air in Southern Poland **:** contribution from local and regional coal combustion. Atmospheric Environment 39, 7580-7586.

Chapter 3

Characteristics of total mercury (TM) wet deposition: Scavenging of atmospheric mercury species[1]

Abstract

Total mercury (TM) in precipitation samples were collected with a modified MIC-B sampler on the roof of Graduate School of Public Health building in Seoul, Korea from January 2006 to December 2007 to determine the seasonal variations in TM wet deposition and to identify the contribution of gaseous oxidized mercury (GOM) and particulate bound mercury (PBM) scavenging to mercury wet deposition. The volume weighted mean (VWM) TM concentrations in 2006 and 2007 were 10.1 ± 17.0 ng L^{-1} and 16.3 ± 16.5 ng L^{-1}, respectively and the TM wet deposition flux in 2006 and 2007 were 16.8 μg m^{-2} and 20.2 μg m^{-2}, respectively. Seasonal VWM TM concentrations in 2006 were highest in fall followed by winter, spring, and summer. In 2007, VWM TM concentrations were greatest in winter, followed by spring, summer, and fall. Nonparametric Mann-Whitney test revealed that there was no statistical difference between fall and

[1]This chapter was published in Atmospheric Environment (2012), vol. 49, p69-76.

summer in 2006 (p=0.10), however, there was a statistical difference between winter and fall in 2007 (p<0.01). The high VWM TM concentration in spring was probably due to the yellow sand events suggesting that GOM and PBM present in the rain were long-range transported from China during this period. The large wet deposition fluxes observed in summers were possibly due to the intense rainfall. Overall there was a significant positive correlation between rainfall depth and wet deposition flux (r^2 = 0.22) ($p<0.01$) and a significant negative correlation between rainfall depth and TM concentration in precipitation (r^2 = 0.20) ($p<0.01$) due to dilution effects. In addition, a weak positive correlation between TM concentration and wet deposition flux was shown (r^2 = 0.10) (p<0.05). Multiple linear regression showed that scavenging coefficient (SC) for GOM was much higher than SC for PBM suggesting that GOM was more effectively scavenged by wet deposition than PBM (SC_{GOM} = 750 and SC_{PBM} = 380).

3.1. Introduction

Mercury (Hg), a well-known environmental toxic pollutant, is among the most highly bioaccumulative trace metals in the food chain (Meili, 1991) and is now classified as a persistent bioaccumulative and toxic (PBT) chemical by the United States Environmental Protection Agency (U.S. EPA, 1997). Mercury continuously goes through the emission and deposition cycle after its release, and therefore the atmosphere plays an important role in the environmental cycling of mercury. Mercury can be distributed long distances from sources through atmospheric transport in its gaseous elemental form (Bullock et al., 1998; Mason et al., 1994; Mason and Sheu, 2002; Petersen et al., 1995) so the relationship between source and environmental effects is complex.

Mercury is emitted from natural sources such as volcanoes, geothermal sources and topsoil enriched in mercury but also from anthropogenic sources such as fossil fuel combustion, ferrous and non-ferrous metals manufacturing facilities, ore processing facilities, incinerators and chemical production facilities (Pirrone et al., 2010). Deposition of natural and anthropogenic mercury is its main pathway to most aquatic systems, either as direct deposition to the water surface or as indirect deposition in runoff from the watershed (Mason et al., 1994;

Miller et al., 2005; Pirrone et al., 2001; Pirrone et al., 2010; Risch et al., 2011). Mercury has various physical and chemical forms including different oxidation states making its behavior complex. Mercury is capable of existing in three oxidation states, namely, 0, +1, and +2. Elemental mercury (oxidation state 0) is the predominant species in ambient air (> 95%) and its residence time is 0.5 ~ 2 years due to its inertness and low solubility (Schroeder and Munthe, 1998) which does not allow it to be efficiently incorporated into wet deposition. On the other hand, gaseous oxidized mercury (GOM) (oxidation state +2) is very water soluble, with relatively strong surface adhesion properties (Han et al., 2005) and can be scavenged by rain within precipitating clouds and below clouds (Lin and Pehkonen, 1999). Particulate bound mercury (PBM) can be wet deposited relatively efficiently if its host particles are in or below precipitating clouds (Cohen et al., 2004). As a result, the predominant species of mercury in wet deposition is in the oxidized or particulate forms.

There is a significant portion of Hg in wet deposition which originates from the global transport of elemental mercury through its chemical conversion to the divalent form, aerosol scavenging and subsequent incorporation into precipitation (Dastoor and Larocque, 2004). Therefore, estimating the importance of precipitation scavenging

of GOM and PBM is important to improve our understanding of the causes of regional and seasonal variations in mercury wet deposition.

Many studies have attempted to characterize mercury wet deposition (Glass and Sorensen, 1999; Guo et al., 2008; Keeler et al., 2006; Lai et al., 2007; Mason et al., 2000; Prestbo and Gay, 2009; Risch et al., 2011; Sakata and Marumoto, 2005; Selin and Jacob, 2008). The TM wet deposition flux is currently monitored at 109 active Mercury Deposition Network (MDN) sites in the United States and Canada. The TM wet deposition flux at MDN sites in 2006 and 2007 ranged from 1.2 to 21.8 $\mu g\ m^{-2}\ yr^{-1}$ (National Atmospheric Deposition Program, 2006; National Atmospheric Deposition Program, 2007). Even though mercury wet deposition research is very important, there are only limited studies outside the US and Europe.

The objectives of this study were to characterize the seasonal variations in atmospheric TM wet deposition in Seoul, Korea and to identify the contribution of gaseous oxidized mercury (GOM) and particulate bound mercury (PBM) to TM wet deposition in Korea using scavenging ratios.

3.2. Materials and methods

3.2.1. Sampling program

Between January 2006 and December 2007 event-based precipitation samples were collected on the roof (~ 17 m above ground) of the Graduate School of Public Health in Seoul, Korea (latitude : 37.514, longitude : 127.001) (Figure 3-1).

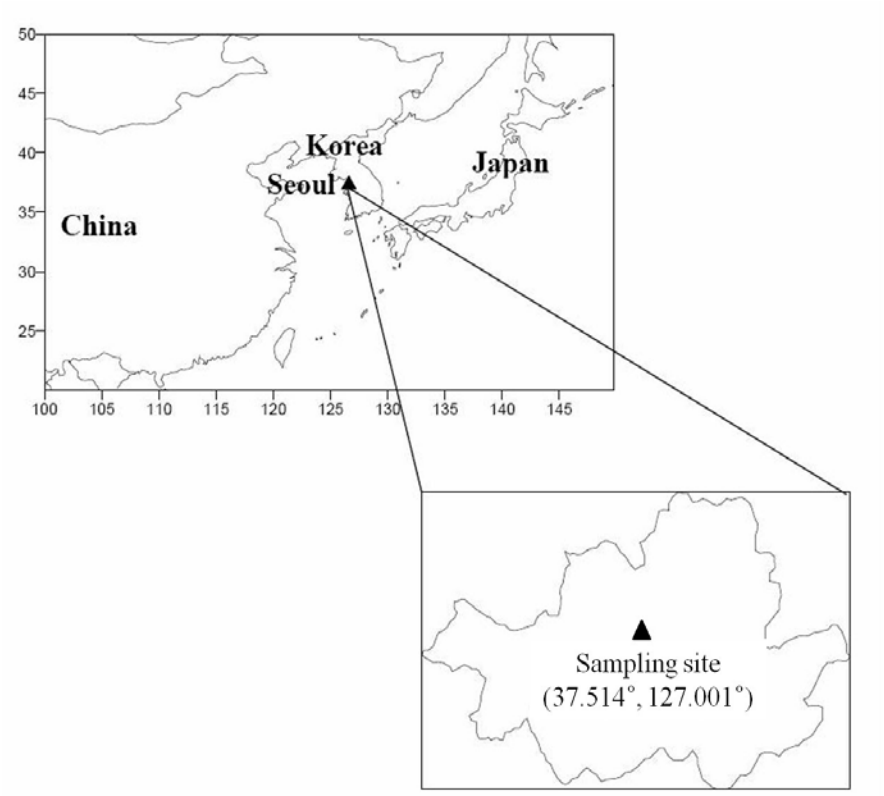

Figure 3-1. Location of sampling site in this study (Seoul, Korea)

Seoul is a diverse urban metropolis, and has a high population density as well as a massive traffic volume. The sampling site is surrounded by residential and commercial buildings and surface roads.

There are four waste incineration facilities located approximately 13 km northeast, 14 km southwest, 15 km southwest and 18 km southeast of the sampling site.

Wet-only precipitation samples were collected using a modified MIC-B (MIC, Thornhill, Ontario) automatic precipitation collector composed of four discrete precipitation sampling systems that allows for two mercury sampling trains and two trace elements as was used and validated in a previous study (Landis and Keeler, 1997). Briefly, the mercury sampling train consists of a borosilicate glass funnel, a Teflon adapter, a glass vapor lock and a Teflon bottle that were acid-cleaned prior to field use as is described below. Sampling trains were manually deployed only when precipitation was forecast and were retrieved after precipitation stopped. All field sampling and analytical supplies which came into contact with the samples were cleaned in an 11-day acid cleaning procedure outlined in the U.S. EPA Lake Michigan Mass Balance Methods Compendium (LMMBMC) (U.S. EPA, 1994b). Each precipitation sample volume was determined gravimetrically and the precipitation depth was calculated by dividing the precipitation volume by the funnel area.

In addition, samples for atmospheric speciated mercury concentrations (GOM and PBM) were collected on the same site as was samples for wet-only precipitation to identify the relationship between atmospheric GOM or PBM and TM concentration in precipitation (n=

72 for GOM, n=69 for PBM in 2006, and n=144 for GOM, n=130 for PBM in 2007). GOM and PBM concentrations were measured manually from January 2006 to December 2007, simultaneously during the daytime (10:00-16:00) and the nighttime (18:00-24:00) (except some data; samples were measured from midnight to midnight for 24 h). The manual sampling method for GOM and PBM followed the procedures outlined in previous studies (Landis et al., 2002a; Han et al., 2004b; Kim et al., 2009). In summary GOM and PBM (d_p < 2.5 μm) were collected using a KCl-coated annular denuder and quartz filter, respectively, at a flow rate 10 L min^{-1}. The sampling system included a coupler, elutriator, impactor, filter holder (URG Inc.), dry gas meter, pump, and a sampling box maintained at 50 ℃ to prevent hydrolysis of KCl. The quartz annular denuders were cleaned, coated and conditioned prior to GOM sampling. Once the denuder was coated and dried, it was thermally conditioned to ensure that the KCl coating was preserved in place and that any residual mercury was eliminated (Landis et al., 2002a). The quartz filters were used to collect PBM less than 2.5 μm in size and were baked in a tube furnace at 900 ℃ for one hour before use.

Meteorological data (temperature and wind speed) were obtained from the Korea Meteorological Administration (KMA) located approximately 1 km from the site to identify the type of precipitation

and extreme meteorological occurrences such as yellow sand events or typhoons that might influence the measured wet deposition.

3.2.2. Analytical Methods

TM in precipitation was measured using a Tekran Series 2600 equipped with cold vapor atomic fluorescence spectrometry (CVAFS) (Tekran Inc., Toronto, Canada) followed the procedures outlined in the U.S. EPA Method 1631 version E (U.S. EPA, 2002) and the U.S. EPA LMMBMC (U.S. EPA, 1994a). Before being analyzed, the samples were oxidized with BrCl to a 1% solution (v/v) and were stored in a refrigerator (4℃) for at least 12 hours. Mercury was then purged from solution in Hg-free argon streams after reduction of BrCl with $NH_2OH \cdot HCl$ and reduction of divalent Hg by $SnCl_2$ to Hg^0 and concentrated onto a gold-coated bead trap (Fitzgerald and Gill, 1979; Landis and Keeler, 1997). Stock mercury standard solutions (SRM 3133, mercury standard solution) were purchased from the National Institute of Standards and Technology (NIST). The analytical method for GOM and PBM followed the procedures outlined in previous studies (Landis et al., 2002a; Han et al., 2004b; Kim et al., 2009). Briefly, denuders and quartz filters were thermally desorbed for about 30 min using a tube furnace (Lindberg 55035C) at 525 ℃ and 900 ℃ to convert GOM or PBM to Hg^0 in a carrier gas of zero air, respectively.

The heated air was transported into a CVAFS analyzer (Tekran Model 2537A) for quantification (Kim et al., 2009).

3.2.3. Quality Assurance and Quality Control (QA/QC)

Quality assurance and quality control procedures for TM in precipitation were based on modified U.S. EPA Method 1631 version E (U.S. EPA., 2002) and LMMBMC (U.S. EPA, 1994a). The standard curve was used when the coefficient of determination (r^2) was greater than 0.995 (linear) over a mercury concentration range from 0.5 to 100 ng L^{-1}. Initial (IPR) and ongoing precision and recovery (OPR) solution (5 ppt) analyzed prior to the analysis of any samples and subsequently every 20 samples ranged between 93% and 106%, and 90% and 117%, respectively. These values were within the quality control acceptance criteria for performance in the EPA Method 1631 E (IPR: 79–121% and OPR: 77–123%).

To quantify method precision, duplicate samples are collected from the sampling site during the study and the relative percent difference (RPD) between the duplicate samples (n=94) was 9.6 ± 7.3 %. In addition standard reference materials (SRMs) (DORM2, National Research Council of Canada and SRM 1641d, NIST) were analyzed to demonstrate the accuracy and precision and to monitor for matrix interferences. SRMs were diluted to the required concentration before being measured following the same procedures as was used for field

samples. Recovery measured in the beginning of the experiments ranged between 90 and 110 % (100.2 ± 4.6 % in average). The method detection limit (MDL) was calculated as three times the standard deviation of seven sequential reagent blanks. MDLs for the total mercury was 0.06 ng L^{-1}. Field blanks (n=24) were collected by deploying the sampling assembly inside the MIC-B to demonstrate that samples were not contaminated by the sample collection and transport activities during non-precipitation conditions. The average field blank concentration in precipitation was 0.06 ± 0.04 ng L^{-1}. All samples were corrected by the associated monthly field blank. The actual sample concentrations ranged from 1.4 to 74.4 ng L^{-1}.

In addition, overall precision of GOM and PBM were calculated using a RPD between duplicate samples. Included in RPD analysis were 12 of 216 samples for GOM and 13 of 199 samples for PBM. RPDs were 11.9 ± 10.7 % for GOM (n=12, r^2=0.96) and 8.1 ± 5.8 % for PBM (n=13, r^2=0.98). Lab blank values < 2pg were required before the denuders were used for sampling. A field blank was taken for every twenty samples, and the average value for GOM and PBM were 1.1 ± 0.6 pg (n=14) and 0.9 ± 0.6 pg (n=14), respectively. The method detection limits (MDLs) for GOM and PBM calculated using the average field blank multiplied by three times the standard deviation of field blanks were 1.9 and 1.8 pg m^{-3}, respectively.

3.3. Results and discussion

3.3.1. Monthly and Seasonal variations of TM Wet deposition

For 2006 (n = 44), the rainfall depth, volume weighted mean (VWM) TM concentration and wet deposition flux were 1645 mm (37.4 ± 57.8 mm) and 10.1 ± 17.0 ng L^{-1}, and 16.8 μg m^{-2}, respectively. The VWM TM concentration in precipitation was highest in fall (28.0 ± 20.1 ng L^{-1}) and lowest in summer (6.8 ± 9.6 ng L^{-1}) while the wet deposition flux was highest in summer (8.3 μg m^{-2}) and lowest in winter (1.4 μg m^{-2}) (Figure 3-2a). For 2007 (n = 52), the rainfall depth, VWM TM concentration, and wet deposition flux were 1235 mm (23.8 ± 21.3 mm), 16.3 ± 16.5 ng L^{-1}, and 20.2 μg m^{-2}, respectively. The VWM TM concentration in precipitation was highest in winter (38.5 ± 17.2 ng L^{-1}) and lowest in fall (8.6 ± 9.9 ng L^{-1}) while the wet deposition flux was highest in summer (9.7 μg m^{-2}) and lowest in winter (1.2 μg m^{-2}) (Figure 3-2b).

The high VWM TM concentrations in spring were probably related to the yellow sand events between 2006 and 2007. Yellow sand events occurred immediately prior to wet deposition events in 2006 (16 March, 29 March, 7 April and 18 April) and in 2007 (7 March, 28 March, 2 April and 9 May). During those periods GOM and PBM concentrations were elevated (50.8 pg m^{-3} for GOM and 27.2 pg m^{-3} for PBM on 15 March in 2006; 6.9 pg m^{-3} for GOM and 12.3 pg m^{-3} for PBM on 28

March; 12.0 pg m^{-3} for GOM and 14.0 pg m^{-3} for PBM on 2 April; and 14.8 pg m^{-3} for GOM and 67.0 pg m^{-3} for PBM on 8 May in 2007) resulting in high VWM TM concentrations (55.3 ng L^{-1} on 16 March, 36.1 ng L^{-1} on 29 March, 32.8 ng L^{-1} on 18 April in 2006 and 59.1 ng L^{-1} on 7 March, 34.2 ng L^{-1} on 28 March, 23.0 ng L^{-1} on 9 May in 2007).

(a)

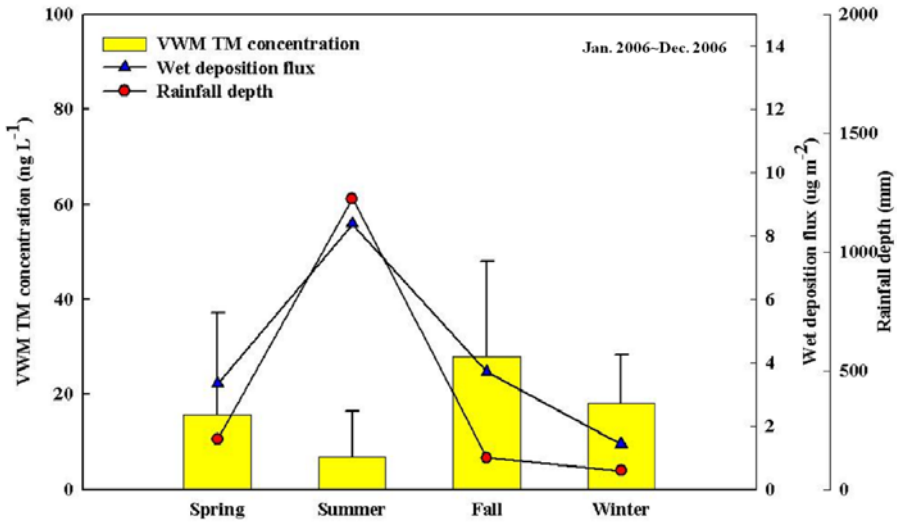

(b)

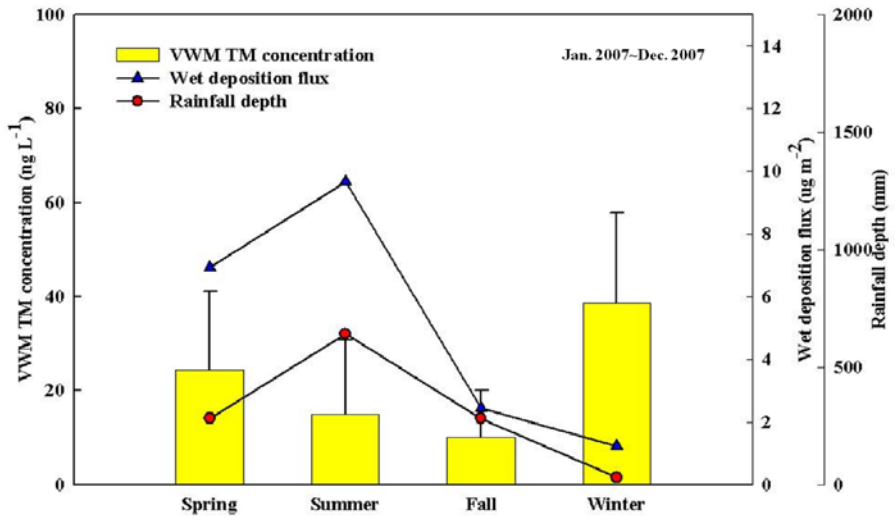

Figure 3-2. Seasonal variation of VWM TM concentration, wet deposition flux, and rainfall depth in 2006 (a) and 2007 (b)

In spring 2006, the VWM TM concentration during yellow sand events (39.1 ± 19.5 ng L^{-1}) (n=4) were much higher than during non-yellow sand events (10.4 ± 22.4 ng L^{-1}) (n=8). Similarly in spring 2007, the VWM TM concentration during yellow sand events (33.2 ± 22.0 ng L^{-1}) (n=4) was much higher than that during non-yellow sand events (23.4 ± 15.9 ng L^{-1}) (n=13). A nonparametric Mann-Whitney test (SPSS) was used to identify statistical difference in concentrations between yellow sand and non-yellow sand events between 2006 and 2007. There was statistically a significant difference between two groups between 2006 and 2007 ($p<0.05$). Previous studies reported that the concentrations of trace elements were higher during yellow sand events than during non-yellow sand events, indicating that the trace elements were being transported from China during yellow sand events (Han et al., 2004a; Yi et al., 2001). It should be noted that the rainfall depth in March and April 2006 (40 mm) was low. As will be discussed later there was a significant negative correlation between rainfall depth and TM concentration in precipitation ($r^2=0.20$) ($p<0.01$) in this study which could also be a factor in the high concentrations seen in spring 2006. In 2007, the VWM TM concentration was highest in winter, especially January (57.5 ± 9.7 ng L^{-1}), when the TM concentration observed on 1 January (44.6 ng L^{-1}) was high probably due to the low rainfall depth (1.0 mm). The TM concentration measured on 6 January

during a mixed rain and snow event was also very high (58.3 ng L^{-1}). This is because the atmospheric PBM concentration measured on 5 January in 2007 was higher (13.1 pg m^{-3}) than the average PBM concentration in January 2007 (9.1 ± 4.1 pg m^{-3}). On the other hand, the atmospheric GOM concentration measured on 5 January in 2007 was not higher (5.2 pg m^{-3}) than the average GOM concentration in January 2007 (7.4 ± 4.9 pg m^{-3}). This result suggests that atmospheric PBM was also effectively scavenged by snow as well as rain. Previous studies reported that TM concentrations in snow are generally smaller than those in rain owing to lower scavenging efficiencies and slower atmospheric reactions at low temperatures (Landis et al., 2002b; Mason et al., 2000). Other studies, however, reported that TM concentrations in precipitation were enhanced in winter due to the increased combustion of fossil fuels (Brosset; 1987; Iverfeldt, 1991). Unfortunately, none of these studies have investigated the importance of mercury species such as GOM or PBM concentrations in precipitation. Therefore, it is important to determine how efficiently atmospheric GOM and PBM is scavenged by different precipitation types (rain or snow). Murakami et al. (1983) proposed that particles (not Hg particles specifically) were more efficiently scavenged by snow than by rain, and Miller and Wang (1991) also indicated that the crystal shape of snow was proven to provide the effective filtering effect for particles because of their porosity. These results suggest that PBM may

be effectively scavenged by snow. Gases such as GOM enter cloud droplets or ice crystals (in-cloud process) or dissolve into falling raindrops (below-cloud process). In cold cloud processes (snow; e.g. accretion, vapor deposition) GOM might not be incorporated into precipitation formed as efficiently as in warm cloud processes (rain; e.g. water vapor diffusion, collision-coalescence) (Landis et al., 2002b). Therefore, the relative significance of snow scavenging to rain scavenging is probably different for GOM and PBM, and the scavenging by snow is likely to be more significant than by rain at least for PBM. A recent research (Ahn et al., 2011) also showed that the high scavenging efficiency of snow for PBM resulted in a large wet deposition flux during snow events.

The single largest wet deposition event (wet deposition flux: 2.4 μg m^{-2}, TM concentration: 7.7 ng L^{-1}, rainfall depth: 305 mm) was observed on 27 July, 2006. This exceptional event was associated with a tropical depression, typhoon Kaemi, which formed on 18 July, 2006 near the Caroline Islands impacting Korea with heavy rains and high winds. Large wet deposition events were also observed on 5 November, 2006 (wet deposition flux: 2.1 μg m^{-2}, TM concentration: 56.9 ng L^{-1}, rainfall depth: 37 mm) and on 14 August, 2007 (wet deposition flux: 2.1 μg m^{-2}, TM concentration: 52.5 ng L^{-1}, rainfall depth: 39 mm) probably due to the combined effects of a large rainfall depth and high TM concentrations. High TM wet deposition flux in summer 2006 and

2007 (50% and 48%, respectively, of total TM wet deposition flux) was primarily due to the high precipitation rate in summer (77% and 40%, respectively, of total rainfall depth).

Table 3-1 shows the atmospheric speciated mercury concentrations (GOM and PBM) measured between 2006 and 2007. The average PBM concentration was higher than that of GOM during two years. GOM concentrations were high in spring (21.7 ± 24.0 pg m^{-3}) and winter (20.3 ± 22.7 pg m^{-3}) in 2006, and were high in spring (14.8 ± 13.0 pg m^{-3}) and winter (10.2 ± 6.0 pg m^{-3}) in 2007. Similarly, PBM concentrations were high in spring (18.1 ± 10.9 pg m^{-3}) and winter (24.0 ± 15.1 pg m^{-3}) in 2006. However, the highest PBM concentration was observed in summer 2006. The high PBM concentration in summer 2006 was primarily due to very high concentration events measured from 4 June 2006 to 5 June 2006 (137.6 pg m^{-3}), from 8 June 2006 to 9 June 2006 (257.4 pg m^{-3}), and 16 June 2006 to 17 June 2006 (225.1 pg m^{-3}). If these samples were excluded, PBM concentration in summer 2006 decreased to 15.3 ± 17.2 pg m^{-3}. The monthly GOM and PBM concentration in winter between 2006 and 2007 was significantly correlated (r^2=0.58, $p<0.01$) suggesting that the high VWM TM concentration in winter was due to the high atmospheric mercury concentrations.

Table 3-1. Summary of atmospheric speciated mercury concentrations

Year			Total	Spring	Summer	Fall	Winter
2006	GOM ($pg\ m^{-3}$)	N	72	14	28	5	25
		Mean	14.0 ± 18.6	21.7 ± 24.0	6.1 ± 4.8	4.8 ± 2.9	20.3 ± 22.7
		Range	1.2 - 94.8	3.5 - 94.8	1.2 - 21.9	1.7 - 8.6	1.8 - 80.3
	PBM ($pg\ m^{-3}$)	N	69	13	28	4	24
		Mean	26.3 ± 42.6	18.1 ± 10.9	35.8 ± 64.7	5.8 ± 2.1	24.0 ± 15.1
		Range	1.7 - 257.4	4.8 - 45.2	1.7 - 257.4	3.5 - 9.1	3.7 - 57.8
2007	GOM ($pg\ m^{-3}$)	N	144	58	22	26	38
		Mean	11.5 ± 10.3	14.8 ± 13.0	7.8 ± 7.0	9.3 ± 9.0	10.2 ± 6.0
		Range	0.9 - 57.3	2.2 - 57.3	0.9 - 27.4	1.2 - 36.4	2.3 - 27.8
	PBM ($pg\ m^{-3}$)	N	130	58	23	18	31
		Mean	13.9 ± 13.1	14.0 ± 11.6	8.6 ± 5.5	17.9 ± 20.7	15.5 ± 13.4
		Range	2.5 - 72.4	2.7 - 67.0	2.5 - 23.0	3.4 - 66.8	2.8 - 72.4

To compare the TM wet deposition fluxes with previous studies the study sites were divided into the following three categories: (1) MDN sites located at similar latitudes Edmonson County, Kentucky (KY10) (latitude; 37.132) and Gloucester County, Virginia (VA98) (latitude; 37.531) with Seoul (latitude; 37.514) (2) rural sites (Eagle Harbor, Pellston, Dexter, Potsdam, Steubenville, Hokkaido, Guizhou), and (3) urban sites (Aichi, Hyogo, Tokyo) (Table 3-2). Annual TM wet deposition fluxes measured in 2006 (16.8 μg m^{-2}) and 2007 (20.2 μg m^{-2}) in Seoul were much higher than those at the MDN sites (KY10: 10.2 μg m^{-2}) and VA98: 7.6 μg m^{-2}), rural (Eagle Harbor: 5.2 μg m^{-2}, Pellston: 7.4 μg m^{-2}, Dexter: 10.7 μg m^{-2}, Potsdam: 5.9 μg m^{-2} Steubenville: 13.5 μg m^{-2}, and Hokkaido: 7.1 μg m^{-2}) and other urban sites (Aichi: 10.7 μg m^{-2}, Hyogo: 14.0 μg m^{-2} and Tokyo: 16.7 μg m^{-2}). The TM wet deposition flux in Wujiang, River basin, Guizhou, China (34.7 μg m^{-2}), however, was much higher than that found in this study. This is mainly because the annual TM concentration in Guizhou (36.0 ng L^{-1}) was much higher than that in this study even though annual rainfall depth (963 mm) in Guizhou was much lower than in this study. Significantly higher TM concentrations in Guizhou resulted in a wet deposition flux that was almost two times higher than those measured in this study. China is the largest mercury emitting country in the world, contributing 50% of the total anthropogenic emissions (Jiang et al.,

2006; Zhang and Wong, 2007). Therefore, much larger mercury emissions in Guizhou, China (Streets et al., 2005) probably results in both high atmospheric mercury concentrations and high wet deposition compared in Korea.

Table 3-2. Comparisons with previous studies for TM wet deposition flux

Site	Location	Sampling period	Precipitation depth (mm)	VWM conc. (ng L^{-1})	Wet deposition flux (μg m^{-2})	Representation	Reference
Kentucky (KY10), MDN	USA	Jan. 2006 ~ Dec. 2006	1286	8.8	10.2	Rural	National Atmospheric Deposition Program (2007)
Virginia (VA98), MDN	USA	Jan. 2006 ~ Dec. 2006	1446	7.7	7.6	Rural	National Atmospheric Deposition Program (2007)
Eagle Harbor, Michigan	USA	Jan. 2003 ~ Dec. 2003	645	8.3	5.2	Rural	Keeler and Dvonch (2005)
Pellston, Michigan	USA	Jan. 2003 ~ Dec. 2003	787	9.4	7.4	Rural	Keeler and Dvonch (2005)
Dexter, Michigan	USA	Jan. 2003 ~ Dec. 2003	896	11.9	10.7	Rural	Keeler and Dvonch (2005)
Potsdam, New York	USA	Jan. 2004 ~ Dec. 2004	1100	5.5	5.9	Rural	Lai et al. (2007)
Steubenville, Ohio	USA	Jan. 2003 ~ Dec. 2003	948	14.0	13.5	Rural	Keeler et al. (2006)
Hokkaido	Japan	Dec. 2002 ~ Nov. 2003	882	8.0	7.1	Rural	Sakata and Marumoto (2005)
Aichi	Japan	Dec. 2002 ~ Nov. 2003	1679	7.8	13.1	Urban	Sakata and Marumoto (2005)
Hyogo	Japan	Dec. 2002 ~ Nov. 2003	1481	9.5	14.0	Urban	Sakata and Marumoto (2005)
Tokyo	Japan	Dec. 2002 ~ Nov. 2003	1912	8.7	16.7	Urban	Sakata and Marumoto (2005)
Wujiang River, Guizhou	China	Jan. 2006 ~ Dec. 2006	963	36.0	34.7	Rural	Guo et al. (2008) and reference cited therein
Seoul	Korea	Jan. 2006 ~ Dec. 2006	1645	10.1	16.8	Urban	This study (2006)
Seoul	Korea	Jan. 2007 ~ Dec. 2007	1235	16.3	20.2	Urban	This study (2007)

3.3.2. Relationship between rainfall depth, VWM TM concentration and TM wet deposition flux

A negative correlation was observed between rainfall depth and VWM TM concentrations between 2006 and 2007 (r^2=0.20) (p<0.01) (Figure 3-3) indicating that TM concentrations in precipitation decreased as rainfall depth increased. This was probably due to "wash-out" of GOM and PBM from the atmosphere during the early stage of rain event (Hall et al., 2005).

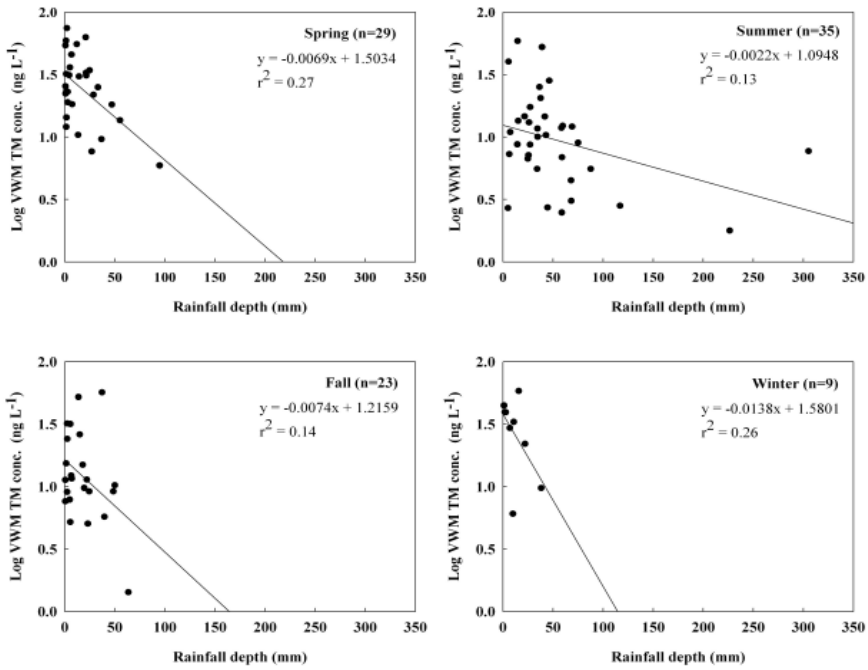

Figure 3-3. Relationship between rainfall depth and VWM TM concentration by season

This negative correlation between rainfall depth and TM concentrations in precipitation has been also found by previous studies

(Guo et al., 2008; Landis et al., 2002b; Watras et al., 2000). Because TM concentrations in precipitation were influenced by the volume of precipitation collected, the rainfall depth could partly explain the variance in TM concentrations. Other factors, however, such as the season, type of precipitation, and meteorological transport history may also strongly influence TM concentrations (Keeler et al., 2005). Briefly, atmospheric GOM and PBM concentrations generally have seasonal variations, causing seasonal variation in TM concentrations in precipitation. The type of precipitation is likely to affect the TM concentration in precipitation because of the different scavenging efficiencies. In addition, the prevailing meteorological transport pattern generally influences the TM concentration. The TM concentration is likely to be enhanced when the winds pass through an urban or industrial area.

There was statistically significant positive correlation between rainfall depth and TM wet deposition flux between 2006 and 2007 ($p<0.01$) (Figure 3-4). This result indicates that the TM wet deposition flux increased during large events even though continuous rain diluted the TM concentration in precipitation

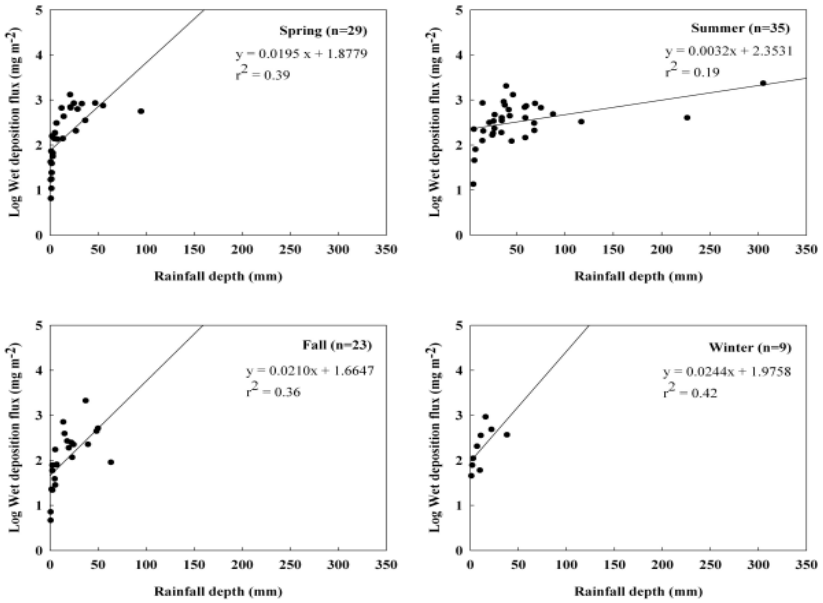

Figure 3-4. Relationship between rainfall depth and TM wet deposition flux by season

3.3.3. Scavenging ratios of GOM and PBM

The TM concentration in precipitation depends on the relative amounts of mercury species (e.g. GOM or PBM) in the air that is available for scavenging. To identify the contribution of mercury species to the TM concentration in precipitation and determine the association between TM concentration in precipitation and atmospheric concentration of mercury species (GOM and PBM), multiple linear regression was performed with by solving the following equation (3-1). For the GOM and PBM data, we used the data which was obtained within 24h before wet deposition event. GOM (n=21) and PBM

concentrations (n=21) measured before wet deposition events were used as independent variables and TM concentration (n=21) was used as the dependent variable.

$$TM_{\text{in precipitation}} = SC_{GOM}\, C_{GOM} + SC_{PBM}\, C_{PBM} \qquad (3\text{-}1)$$

where SC_{GOM} and SC_{PBM} (m^3 rain / m^3 air) are scavenging coefficient (SC) for GOM and PBM, and C_{GOM} (ng m^{-3}) and C_{PBM} (ng m^{-3}) are atmospheric concentrations for GOM and PBM, respectively. This analysis yielded the following equation:

$$TM_{\text{in precipitation}} = 747.12\, C_{GOM} + 382.46\, C_{PBM} + 1.49 \qquad (3\text{-}2)$$

The multiple linear model fit the data well (r^2=0.37) and was statistically significant (p<0.05). As shown in equation (3-2), SC_{GOM} (750) is much higher than SC_{PBM} (380), suggesting that GOM was more effectively scavenged by wet deposition than was PBM. Since there are no reported values for SC_{GOM} in the literature it was compared with other soluble species such as SO_4^{2-} and found to be reasonable. A previous study (Lindberg, 1982) reported that scavenging coefficient of SO_4^{2-} ranged from about 430 to 1900.

In addition, SC_{PBM} was within the range of values (200 to 2000) that is indicative of particle scavenging (Guentzel et al., 1995; Sakata and Asakura, 2007). It should be noted that Sakata and Asakura (2007) determined the amount of PBM in the precipitation samples by filtration. GOM, however, strongly adheres to surfaces and could have been sorbed to the particles or the filters resulting in a positive artifact which would increase SC_{PBM}. In addition, only particle sizes < 2.5 μm in the air were collected whereas rainfall collects all particle sizes. Particle scavenging depends on the particle size distribution with the larger particles more efficiently scavenged than smaller sizes (Kim et al., 2007).

3.4. Conclusions

In this study, atmospheric TM wet deposition was measured to characterize monthly and seasonal variations in Seoul, Korea. VWM TM concentrations in precipitation in 2006 and 2007 were 10.1 ± 17.0 ng L^{-1} and 16.3 ± 16.5 ng L^{-1}, respectively. The TM wet deposition flux in 2006 and 2007 were 16.8 μg m^{-2} and 20.2 μg m^{-2}, respectively. For the complete sampling period VWM TM concentrations were high in spring and winter. In particular VWM TM concentrations during yellow sand events were much higher than during non-yellow sand events resulting in high VWM TM concentrations in spring. These

results suggest that mercury species (GOM and PBM) are being transported from China during yellow sand events. There was a statistically significant positive correlation between rainfall depth and wet deposition flux (r^2=0.22) (*p<0.01*), while there was a significant negative correlation between rainfall depth and TM concentration in precipitation (r^2=0.20) (*p<0.01*). TM wet deposition flux was highest during summer 2007 (9.7 μg m^{-2}) and lowest during winter 2007 (1.2 μg m^{-2}). Multiple linear regression revealed that SC_{GOM} (750) was much higher than SC_{PBM} (380) suggesting that GOM was more effectively scavenged by wet deposition than PBM.

References

Ahn, M. C., Yi, S. M., Holsen, T. M., Han, Y. J., 2011. Mercury wet deposition in rural Korea: concentrations and fluxes. Journal of Environmental Monitoring 13, 2748-2754.

Brosset, C., 1987. The behaviour of mercury in the physical environment. Water, Air, and Soil Pollution 17, 37-50.

Bullock, R. O., Brehme, K. A., Mapp, G. R., 1998. Lagrangian modeling of mercury air emission, transport and deposition: an analysis of model sensitivity to emissions uncertainty. Science of the Total Environment 213, 1-12.

Cohen, M., Artz, R., Draxler, R., Miller, P., Niemi, D., Ratte, D., Deslauriers, M., Duvar, R., Laurin, R., Slotnick, J., Nettesheim, T., McDonald, J., 2004. Modeling the atmospheric transport and deposition of mercury to the Great Lakes. Environmental Research 95, 247-265.

Dastoor, A. P., Larocque, Y., 2004. Global circulation of atmospheric mercury: a modelling study. Atmospheric Environment 38, 147-161.

Fitzgerald, W. F., Gill, G. A., 1979. Subnanogram determination of mercury by two-stage gold amalgamation and gas phase detection applied to atmospheric analysis. Analytical Chemistry 51, 1714-1720.

Glass, G. E., Sorensen, J. A., 1999. Six-year trend (1990-1995) of wet mercury deposition in the Upper Midwest, U. S. A. Environmental Science and Technology 33, 3303-3312.

Guentzel, J. L., Landing, W. M., Gill, G. A., Poliman, C. D., 1995. Atmospheric deposition of mercury in Florida: The FAMS project (1992-1994). Water, Air, and Soil Pollution 80, 393–402.

Guo, Y., Feng, X., Li, Z., He, T., Yan, H., Meng, B., Zhang, J., Qiu, G., 2008. Distribution and wet deposition fluxes of total and methyl mercury in Wujiang River Basin, Guizhou, China. Atmospheric Environment 42, 7096-7103.

Hall, B., Monolopoulos, H., Hurley, J. P., Schauer, J. J., Louis, V. L. St., Kenski, D., Graydon, J., Babiarza, C. L., Clecknera, L. B., Keeler, G. J., 2005. Methyl and total mercury in precipitation in the Great Lakes

region. Atmospheric Environment 39, 7557-7569.

Han, Y. J., Holsen, T. M., Hopke, P. K., Cheong, J. P., Kim, H., Yi, S. M., 2004a. Identification of source locations for atmospheric dry deposition of heavy metals during yellow-sand events in Seoul, Korea in 1998 using hybrid receptor models. Atmospheric Environment 38, 5353-5361.

Han, Y. J., Holsen, T. M., Lai, S. O., Hopke, P. K., Yi, S. M., Liu, W., Pagano, J., Falanga, L., Milligan, M., Andolina, C., 2004b. Atmospheric gaseous mercury concentrations in New York State: relationships with meteorological data and other pollutants. Atmospheric Environment 38, 6431–6446.

Han, Y. J., Holsen, T. M., Hopke, P. K., Yi, S. M., 2005. Comparison between back-trajectory based modeling and Lagrangian backward dispersion modeling for locating sources of reactive gaseous mercury. Environmental Science and Technology 39, 1715-1723.

Iverfeldt, Å., 1991. Occurrence and turnover of atmospheric mercury over the Nordic countries. Water, Air and Soil Pollution 56, 251–265.

Jiang, G.B., Shi, J. B., Feng, X. B., 2006. Mercury pollution in China. Environmental Science and Technology 40, 3672–3678.

Keeler, G. J., Dvonch, J. T., 2005. Atmospheric mercury: A decade of observations in the Great Lakes. In dynamics of mercury pollution on regional and global scales: atmospheric processes and human exposures around the world; Pirrone, N., Mahaffey, K., Eds.; Kluwer Ltd: Norwell, MA.

Keeler, G. J., Gratz, L. E., Al-Wali, K., 2005. Long-term atmospheric mercury wet deposition at Underhill, Vermont. Ecotoxicology 14, 71-83.

Keeler, G. J., Landis, M. S., Norris, G. A., Christianson, E. M., Dvonch, J. T., 2006. Sources of mercury wet deposition in eastern Ohio, USA. Environmental Science and Technology 40, 5874-5881.

Kim, J., Jung, C. H., Choi, B. C., Oh, S. N., Brechtel, F. J., Yoon, S. C., Kim, S. W, 2007. Number size distribution of atmospheric aerosols during ACE-Asia dust and precipitation events. Atmospheric

Environment 41, 4841-4855.

Kim, S. H., Han, Y. J., Holsen, T. M., Yi, S. M., 2009. Characteristics of atmospheric speciated mercury concentrations (TGM, Hg(II) and Hg(p)) in Seoul, Korea. Atmospheric Environment 43, 3267-3274.

Lai, S. O., Holsen, T. M., Hopke, P. K., Liu, P., 2007. Wet deposition of mercury at a New York state rural site: Concentrations, fluxes, and source areas. Atmospheric Environment 41, 4337-4348.

Landis, M. S., Keeler, G. J., 1997. Critical evaluation of a modified automatic wet-only precipitation collector for mercury and trace element determinations. Environmental Science and Technology 31, 2610-2615.

Landis, M. S., Stevens, R. K., Schaedlich, F., Prestbo, E. M., 2002a. Development and characterization of an annular denuder methodology for the measurement of divalent inorganic reactive gaseous mercury in ambient air. Environmental Science and Technology 36, 3000–3009.

Landis, M. S., Vette, A. F., Keeler, G. J., 2002b. Atmospheric mercury in the Lake Michigan Basin: Influence of the Chicago/Gary urban Area. Environmental Science and Technology 36, 4508-4517.

Lin, C.-J., Pehkonen, S.O., 1999. The chemistry of atmospheric mercury: a review. Atmospheric Environment 33, 2067–2679.

Lindberg, S. E., 1982. Factors influencing trace metal, sulfate and hydrogen ion concentrations in rain. Atmospheric Environment 16, 1701-1709.

Mason, R. P., Fitzgerald, W. F., Morel, F. M. M., 1994. The biogeochemical cycling of elemental mercury: Anthropogenic influences. Geochimica et Cosmochimica Acta 58 3191-3198, 1994.

Mason, R. P., Lawson, N. M., Sheu, G. R., 2000. Annual and seasonal trends in mercury deposition in Maryland. Atmospheric Environment 34, 1691-1701.

Mason, R. P., Sheu, G.-R., 2002. Role of the ocean in the global mercury cycle. Global Biogeochemical Cycles 16, 1093. doi:10.1029/2001GB001440.

Meili, M, 1991. The coupling of mercury and organic matter in the biogeochemical cycle - towards a mechanistic model for the boreal zone. Water, Air, and Soil Pollution 56, 333-347.

Miller, E. K., Vanarsdale, A., Keeler, G. J., Chalmers, A., Poissant, L., Kamman, N. C., Brulotte, R., 2005. Estimation and Mapping of dry mercury deposition across northeastern North America. Ecotoxicology 14, 53-70.

Miller, N. L., Wang, P. K., 1991. A theoretical determination of the collection rates of aerosol particles by falling ice crystal plates and columns. Atmospheric Environment 25A, 2593-2606.

Murakami, M., Kimura, T., Magono, C., Kikuchi, K., 1983. Observations of precipitation scavenging for water-soluble particles. Journal of the Meteorological Society of Japan 61, 346-358.

National Atmospheric Deposition Program, 2006. 2006 Annual Summary. Mercury Deposition Network., pp.13-14. http://nadp.sws.uiuc.edu/lib/data/2006as.pdf.

National Atmospheric Deposition Program, 2007. 2007 Annual Summary. Mercury Deposition Network., pp.14-15. http://nadp.sws.uiuc.edu/lib/data/2007as.pdf.

Petersen, G., Iverfeldt, A., Munthe, J., 1995. Atmospheric mercury species over central and northern Europe - model calculations and comparison with observations from the Nordic air and precipitation network for 1987 and 1988. Atmospheric Environment 29, 47-67.

Pirrone, N., Pacyna, J. M., Barth, H., 2001. Atmospheric Mercury Research in Europe, Atmospheric Environment 35, 2997–3006.

Pirrone, N., Cinnirella, S., Feng, X., Finkelman, R.B., Friedli, H.R., Leaner, J., Mason, R., Mukherjee, A.B., Stracher, G.B., Streets, D.G., Telmer, K., 2010. Global mercury emissions to the atmosphere from anthropogenic and natural sources. Atmospheric Chemistry and Physics 10, 5951-5964.

Prestbo, E. M. and Gay, D. A., 2009. Wet deposition of mercury in the U.S and Canada, 1996-2005: Results and analysis of the NADP mercury deposition network (MDN).

Risch, M. R., Gay, D. A., Fowler, K. K., Keeler, G. J., Backus, S. M.,

Blanchard, P., Barres, J. A., Dvonch, J. T., 2011. Spatial pattern and temporal trends in mercury concentrations, precipitation depth, and mercury wet deposition in the North American Great Lakes region, 2002-2008. Environmental pollution 161, 261-271.

Sakata, M. and Marumoto, K., 2005. Wet and dry deposition fluxes of mercury in Japan. Atmospheric Environment 39, 3139-3146.

Sakata, M. and Asakura, K., 2007. Estimating contribution of precipitation scavenging of atmospheric particulate mercury to mercury wet deposition in Japan. Atmospheric Environment 41, 1669-1680.

Schroeder, W. H. and Munthe, J., 1998. Atmospheric mercury - An overview. Atmospheric Environment 32, 809-822.

Selin, N. E. and Jacob, D. J., 2008. Seasonal and spatial patterns of mercury wet deposition in the Unites States: Constraints on the contribution from North American anthropogenic sources. Atmospheric Environment 42, 5193-5204.

Streets, D. G., Hao, J., Wu, Y., Jiang, Y. W., Chan, M., Tian, H., Feng, X., 2005. Anthropogenic mercury emissions in China. Atmospheric Environment 39, 7789-7806.

U.S. EPA, 1994a. Lake Michigan Mass Balance Methods Compendium, Standard Operating Procedure for Analysis of Mercury in Precipitation,http://www.epa.gov/glnpo/lmmb/methods/umanalyt.pdf.

U.S. EPA, 1994b. Lake Michigan Mass Balance Methods Compendium, Standard Operating Procedure for Sampling of Mercury in Precipitation, http://www.epa.gov/glnpo/lmmb/methods/umfield.pdf.

U.S. EPA, 1997. Persistent, bioaccumulative and toxic chemical program, http://www.epa.gov/pbt.

U.S. EPA, 2002. Method 1631 (rev. E), Mercury in water by oxidation, purge and trap, and cold vapor atomic fluorescence spectrometry.

Watras, C. J., Morrison, K. A., Hudson, R. J. M., Frost, T. M., Kratz, T. K., 2000. Decreasing mercury in Northern Wisconsin: Temporal patterns in bulk precipitation and a precipitation-dominated lake. Environmental Science and Technology 34, 4051-4057.

Yi, S. M., Lee, E. Y., Holsen, T. M, 2001. Dry deposition fluxes and size distributions of heavy metals in Seoul, Korea during yellow sand events. Aerosol Science and Technology 35, 569–576.

Zhang, L., Wong, M.H., 2007. Environmental mercury contamination in China: sources and impacts. Environment International 33, 108-121.

Chapter 4

Source identification of total mercury (TM) wet deposition using a Lagrangian particle dispersion model (LPDM)[2]

Abstract

Precipitation samples for total mercury (TM) were collected with a modified MIC-B sampler concurrent with atmospheric gaseous oxidized mercury (GOM) and particulate bound mercury (PBM) concentrations on the roof of Graduate School of Public Health building in Seoul, Korea from January 2006 to December 2009. These samples were used to determine the seasonal variations in TM wet deposition, to determine the contribution of GOM and PBM scavenging to mercury wet deposition, and to identify source areas contributing to the high TM wet deposition using a Lagrangian particle dispersion model (LPDM).

During the sampling period, the VWM TM concentration was highest in winter, followed by spring, fall and summer, while the wet deposition flux was highest in summer, followed by spring, fall and winter. Multiple linear regression showed that the scavenging coefficient (SC) for GOM was much higher than the SC for PBM

[2] This chapter was submitted to *Environmental Science & Technology*.

indicating that GOM was more effectively scavenged by wet deposition than PBM (SC_{GOM} = 715 and SC_{PBM} = 407). Joint-probability LPDM (JP-LPDM) indicated that the main sources of TM wet deposition were Guizhou, Guangdong, Liaoning, Hunan, Shaanxi, Nei Mongol and Gobi Desert. This suggests that both anthropogenic sources such as industrial areas and natural source areas such as deserts contributed to the high TM concentration in Seoul, Korea.

4.1. Introduction

Gaseous elemental mercury (GEM) is the predominant form in ambient air (> 95%) and its residence time is relatively long (0.5 ~ 2 years) due to its low solubility and inertness (Schroeder and Munthe, 1998) which does not allow it to be efficiently incorporated into wet deposition. On the other hand, gaseous oxidized mercury (GOM) is very water soluble, with relatively strong surface adhesion properties (Han et al., 2005) and can be scavenged by rain within precipitating clouds and below clouds (Lin and Pehkonen, 1999). Particulate bound mercury (PBM) can be wet deposited relatively efficiently if it is associated with particles in or below precipitating clouds (Cohen et al., 2004).

As a result, the predominant form of mercury in wet deposition is in the oxidized (GOM) or particulate forms (PBM) (Seo et al., 2012). The GOM and PBM concentration is generally <5% of the total gas-phase mercury, however, their contribution to deposition is generally much higher than this because they are quickly deposited to the surface by wet and dry processes (U.S. EPA, 1997).

There have been several attempts to associate precipitation chemistry data with source locations (Lucey et al., 2001; Plaisance et al., 1996; Zeng and Hopke, 1989). Previous studies have also attempted to determine the annual total mercury (TM) wet deposition flux and

identified the likely source areas contributing to the high TM wet deposition flux using receptor models such as Potential Source Contribution Function (PSCF) (Lai et al., 2007; Huang and Gustin 2012). Trajectory calculations are often used for the interpretation of atmospheric trace elements measurements, however, two important factors are normally not considered. First, trace element samples are associated with air that is collected over a significant time interval, whereas back-trajectories track the path of an infinitesimally small particle; second, turbulence and convection are often ignored (Stohl et al., 2002). In this study backward simulation with a Lagrangian particle dispersion model (LPDM) was used in an attempt to reduce such errors associated with using a single trajectory. There have been a few prior studies that used LPDM to obtain source-receptor relationships (Han et al., 2005; Stohl et al., 2002; Seibert and Frank, 2004), but there have been no studies involving mercury wet deposition data. Additional complicating factors are that the chemical composition in precipitation is quite variable, not only from event to event, but also within an event (Seymour et al., 1978; Seymour and Stout, 1983; Davies; 1984). In addition, rain intensity is not always constant, and therefore it is not easy to identify the relationship between the source and the receptor.

The objectives of this study were to characterize the seasonal variations of atmospheric TM wet deposition and to identify the source

areas contributing to the high TM wet deposition using the LPDM receptor model which considers dispersion, reaction, and deposition.

4.2. Materials and methods

4.2.1. Sampling program

Wet-only precipitation samples (n=176) were collected using a modified MIC-B automatic precipitation collector (MIC, Thornhill, Ontario) on the roof (~ 17 m above ground) of the Graduate School of Public Health in Seoul, Korea between January 2006 and December 2009 (latitude : 37.514, longitude : 127.001) (Figure 4-1) (See Supporting Information (SI) for details). Seoul has a massive traffic volume as well as a high population density, and is a diverse urban metropolis. The sampling site is surrounded by residential and commercial buildings and surface roads. There are four waste incineration facilities located about 13 km northeast, 14 km southwest, 15 km southwest and 18 km southeast of the sampling site.

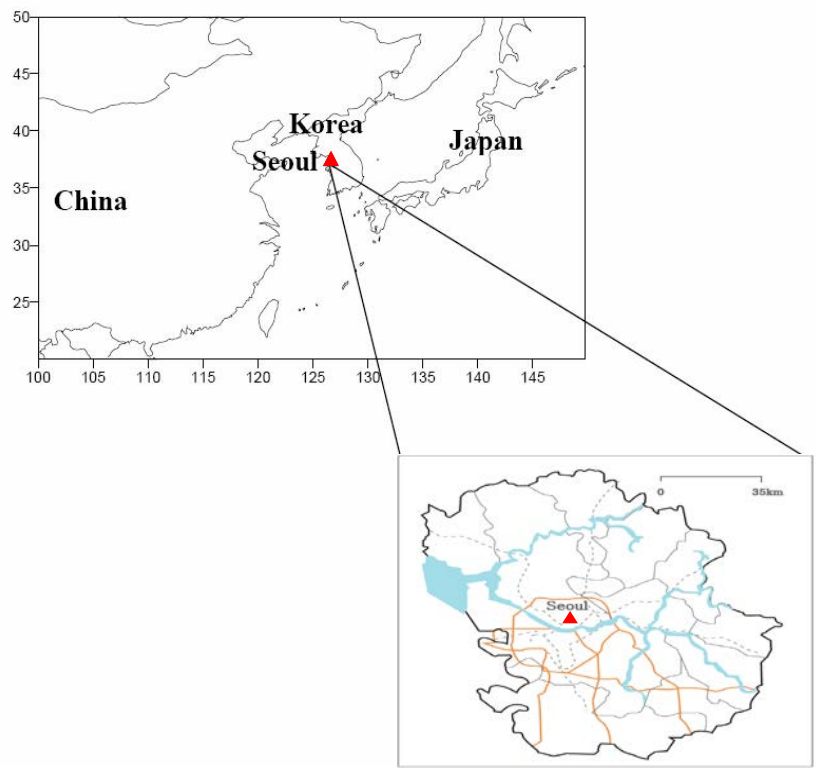

Figure 4-1. The location of sampling site in this study (Seoul, Korea)

All field sampling and analytical supplies which came into contact with the samples were cleaned in an 11-day acid cleaning procedures described in the U.S. EPA Lake Michigan Mass Balance Methods Compendium (LMMBMC) (U.S. EPA, 1994b). Teflon bottles were filled with 20 mL of 0.08 M HCl solution to minimize mercury loss in precipitation before field deployment. The precipitation sample volume was gravimetrically determined and the precipitation depth was calculated by dividing the precipitation volume by the funnel area.

In addition, samples for atmospheric speciated mercury concentrations (GOM and PBM) were collected at the same site as

were samples for wet-only precipitation (n= 390 for GOM, n=379 for PBM). GOM and PBM concentrations were measured manually from January 2006 to December 2009, simultaneously during the daytime (10:00-16:00) and the nighttime (18:00-24:00) (some samples were obtained from midnight to midnight for 24 h). The manual sampling method for GOM and PBM followed the procedures described in previous studies (Landis et al., 2002a; Han et al., 2004b; Kim et al., 2009) (See SI for details). Meteorological data (temperature and wind speed) were obtained from the Korea Meteorological Administration (KMA) located approximately 1 km from the site to identify the type of precipitation. Extreme meteorological occurrences such as yellow sand events or typhoons that might influence the measured wet deposition were also noted.

4.2.2. Analytical Methods

Total Mercury (TM) in precipitation was measured using a Tekran Series 2600 equipped with cold vapor atomic fluorescence spectrometry (CVAFS) (Tekran Inc., Toronto, Canada) followed the procedures outlined in the U.S. EPA Method 1631 version E (U.S. EPA, 2002) and the U.S. EPA LMMBMC (U.S. EPA, 1994a) (See SI for details).

The analytical method for GOM and PBM followed the procedures outlined in previous studies (Landis et al., 2002a; Han et al., 2004b; Kim et al., 2009). Briefly, denuders and quartz filters were thermally desorbed for about 30 min using a tube furnace (Lindberg 55035C) at 525℃ and 900℃ to convert GOM or PBM to Hg^0 in a carrier gas of zero air, respectively. The heated air was transported into a CVAFS analyzer (Tekran Model 2537A) for quantification (Kim et al., 2009).

4.2.3. QA/QC

Quality assurance and quality control procedures for TM in precipitation were based on the U.S. EPA Method 1631 version E (U.S. EPA., 2002) and Lake Michigan Mass Balance Methods Compendium (LMMBMC) (U.S. EPA, 1994a) (See SI for details).

RPD analyses (16 of 387 GOM samples and 18 of 376 PBM samples) were 11.4 ± 9.5 % for GOM (r^2=0.97) and 9.4 ± 6.3 % for PBM (r^2=0.98). Lab blank values < 2pg were required before the denuders were used for sampling. A field blank was taken for every twenty samples, and the average value for GOM and PBM were 1.1 ± 0.6 pg (n=17) and 0.8 ± 0.6 pg (n=14), respectively. The method detection limits (MDLs) for GOM and PBM calculated using the average field blank multiplied by three times the standard deviation of field blanks were 1.9 and 1.8 pg m^{-3}, respectively.

4.3. Model description

4.3.1. Potential Source Contribution Function (PSCF)

Trajectories are defined as the paths of small particles of air at a certain point in space at a given time and can be traced forward or backward in time (Stohl et al., 2002). The HYSPLIT (HYbrid Single-Particle Lagrangian Integrated Trajectory) model is a complete system for computing simple air parcel trajectories to complex dispersion and deposition simulations (Draxler and Hess, 2005). PSCF, a trajectory-based model is a simple method that links residence time in upwind areas with high concentrations through a conditional probability field, was originally developed by Ashbaugh et al. (1985). $PSCF_{ij}$ is the conditional probability that an air parcel that passed through the *ij*th cell had a high concentration upon arrival to the monitoring site and is defined as

$$\mathrm{PSCF}_{ij} = \frac{\mathrm{m}_{ij}}{\mathrm{n}_{ij}} \qquad (4\text{-}1)$$

where n_{ij} is the number of trajectory segment endpoints fall into the *ij*-th cell, and the m_{ij} is the number of segment endpoints in the same grid cell (*ij*-th cell) when the concentrations are higher than a criterion value.

PSCF has been extensively and successfully used in the past (Cheng et al., 1993; Poissant., 1999; Lin et al., 2001; Han et al., 2005; Hopke et al., 2005; Lai et al., 2007; Zeng and Hopke, 1989). A detailed description is outlined in the SI.

4.3.2. Lagrangian Particle Dispersion Model (LPDM)

Trajectories are typically calculated for samples collected over long time periods. However individual trajectories cannot represent the whole measurement time and do not consider turbulent mixing and convection in the atmosphere. Specifically traditional PSCF does not consider the reduction of the concentration of the species through diffusion, chemical transformation, and atmospheric scavenging during the transport between the source areas and the receptor (Cheng et al., 1993). It can be insufficient to identify the source-receptor relationship based on backward trajectories and to represent the transport history of a sampling volume even if it is small (Stohl et al., 2002). For this reason, more elaborate models are used, both of the planetary boundary layer (PBL), where an air mass quickly loses its identity due to strong mixing (Lyons et al., 1995), and at higher levels of the atmosphere when longer time scales are considered (Sutton, 1994). The LPDM contains no artificial numerical diffusion like Eulerian models (Nguyen

et al., 1997) and hence has a greater potential to resolve fine-scale structures of the flow.

The LPDM is based on the conditioned particle concepts (Smith, 1968; Park, 1990) in which released particles with any specified release rate into the model domain are advected by velocity components resolved by the model and subgrid-scale turbulent components. Therefore LPDM is physically and theoretically more correct than trajectory models. However trajectory models are still used because of convenience, availability of models and computational constraints (Stohl et al., 2002).

The source-receptor relationship can be linear or nonlinear. In this study, a linear source-receptor relationship was calculated using the HYSPLIT 4 dispersion model (LPDM) because standard LPDM cannot simulate nonlinear chemical reactions (Seibert and Frank, 2004). Linear source-receptor relationships can be calculated with following equation (4-2).

$$y=Mx \tag{4-2}$$

where, y indicates the discrete observation (e.g. measured concentration) at receptor sites and x is the source emission term, which varies with locations and time. M is the source-receptor relationship

including transport processes. In conventional PSCF, the number of end points in the *ij*-th cell which is expressed as a residence time (hr), is simply considered to be the source-receptor relationship of the *ij*-th cell (Han et al., 2005).

The output value of the dispersion model such as HYSPLIT 4 is regarded as source-receptor matrix. The HYSPLIT model gives gridded concentration fields (mass m^{-3}) as output. To obtain the residence time of each grid (e.g. transmission corrected residence time), a transformation is necessary (Han et al., 2005; Seibert, 2001; Seibert and Frank, 2004).

$$\tau = \frac{\Delta T_s V_s}{\mu_{tot}} \bar{c} \tag{4-3}$$

where ΔT_s is the time during which the source is acting, V_s is the volume of grid and $\bar{c}$ is the concentration in a grid cell as produced by HYSPLIT, and μ_{tot} is the total mass associated with particles released.

Once the transmission-corrected residence time is calculated, the potential source contribution function (PSCF) can be applied. LPDM is more accurate in the prediction of the behavior of an air parcel, since the dispersion model can estimate precise standard deviations of atmospheric turbulence from calculated stability which changes at

every grid and every time step through a meteorological model and dry and wet deposition using a meteorological model and measured or estimated precipitation rate (Draxler and Hess, 2005; Han et al., 2005). In this study, the LPDM were calculated with Global Data Assimilation System (GDAS) meteorological data.

LPDM cannot explain include transformations between multiple pollutant species. Therefore the LPDM results which considered only GOM are shown in this study. GOM is more effectively scavenged by wet deposition than is PBM. In addition, PBM has large uncertainties associated with size distributions which can change due to physical and chemical processes including adsorption, nucleation, and other gas-particle partitioning mechanisms, ambient particle concentrations and meteorological conditions (Kim et al., 2012).

All GOM was assumed to be $HgCl_2$ and the emission rate was set to a continuous 1 kg hr^{-1} in the source-receptor relationship. The molecular weight of $HgCl_2$, surface reactivity ratio, and Henry's constant were set to be 271.5 g, 1, and 1.4×10^6 M atm^{-1}, respectively. A detailed description is provided in a previous study (Han et al., 2005). The criterion value of LPDM for VWM TM concentration was set to the upper 20th percentile of the source concentration to provide a better estimation and resolution of source locations during the sampling period.

The VWM TM concentrations were used instead of wet deposition fluxes in the modeling analysis to avoid having the modeling results being driven by the amount of precipitation rather than the amount of Hg deposited (approximately 2/3 of total rainfall occurs during the summer season in Korea (Seo et al., 2012)). The geographic area covered by the computed trajectories was divided into an array of 0.5º latitude by 0.5º longitude grid cells.

The previous studies used Joint-probability PSCF (JP-PSCF) for multisite measurements (Han et al., 2005; Hsu et al., 2003). JP-PSCF combines measurements from multiple sites, thus providing information that cannot be obtained from single site measurements. In this study, joint-probability LPDM (JP-LPDM) was used at different starting heights. JP-LPDM incorporates probability from multiple starting heights, thus providing information that cannot be obtained from single starting height. The JP-LPDM value for a grid cell was defined with the following equation (4-4)

$$P(JP\text{-}LPDM_{ij}) = \frac{P(B_{ij})_{100m} + P(B_{ij})_{500m} + P(B_{ij})_{1000m}}{P(A_{ij})_{100m} + P(A_{ij})_{500m} + P(A_{ij})_{1000m}} \qquad (4\text{-}4)$$

where, $P(JP\text{-}LPDM_{ij})$ represent the value of joint probability of LPDM for the *ij*th cell.

4.4. Comparison between emission inventories and LPDM results

A spatial correlation index (r) (Haining, 1990), calculated using MATLAB was used to determine the statistical association between emission inventories and modeling results. A detailed description of this approach can be found in the previous studies (Han et al., 2005; Hopke et al., 2005; Lai et al., 2007). In this study, the anthropogenic mercury emission inventories estimated for China in 2000 was used (Street et al., 2005) although it should be noted that the China emission inventory is believed to have significant uncertainties in part because many of the activities that release large amounts of mercury occur in remote parts of the country.

4.5. Results and Discussion

4.5.1. Monthly and seasonal variations of TM wet deposition

The seasonal variations of volume weighted mean (VWM) TM concentrations, precipitation depth, and wet deposition flux from 2006 to 2009 (n=176) are summarized in Table 4-1.

Table 4-1. Summary of TM wet deposition in this study

Year		Total	Spring	Summer	Fall	Winter
2006	N	44	12	19	9	4
	Precipitation depth (mm)	1645.0	210.7	1223.6	132.8	77.9
	VWM TM conc. (ng L^{-1})	10.1 ± 17.0	15..8 ± 21.3	6.8 ± 9.6	28.0 ± 20.1	18.1 ± 10.3
	Wet deposition flux (μg m^{-2})	16.8	3.3	8.4	3.7	1.4
2007	N	52	17	16	14	5
	Precipitation depth (mm)	1235.7	281.5	641.7	281.0	31.5
	VWM TM conc. (ng L^{-1})	16.3 ± 16.5	24.4 ± 16.8	15.0 ± 15.7	8.6 ± 9.9	38.5 ± 17.2
	Wet deposition flux (μg m^{-2})	20.2	6.9	9.7	2.4	1.2
2008	N	39	10	18	5	6
	Precipitation depth (mm)	1290.8	180.8	909.3	142.8	57.9
	VWM TM conc. (ng L^{-1})	14.3 ± 11.9	16.1 ± 9.4	13.4 ± 9.9	12.4 ± 16.7	26.8 ± 13.1
	Wet deposition flux (μg m^{-2})	18.5	2.9	12.2	1.8	1.6
2009	N	41	10	16	10	8
	Precipitation depth (mm)	1556.6	235.2	1073.7	182.6	65.1
	VWM TM conc. (ng L^{-1})	10.2 ± 14.8	13.0 ± 6.6	7.3 ± 14.3	19.9 ± 11.1	31.9 ± 16.7
	Wet deposition flux (μg m^{-2})	16.4	2.3	8.0	3.8	2.3

The volume weighted mean (VWM) TM concentrations in 2006, 2007, 2008 and 2009 were 10.1 ± 17.0 ng L^{-1}, 16.3 ± 16.5 ng L^{-1}, 14.3 ± 11.9 ng L^{-1} and 10.2 ± 14.8 ng L^{-1}, respectively and the TM wet deposition flux in 2006, 2007, 2008 and 2009 were 16.8 μg m^{-2}, 20.2 μg m^{-2}, 18.5 μg m^{-2} and 16.4 μg m^{-2}, respectively. During the sampling period, the VWM TM concentration was highest in winter (27.0 ± 15.4 ng L^{-1}), followed by spring (18.2 ± 16.3 ng L^{-1}), fall (15.7 ± 13.6 ng L^{-1}), and summer (9.9 ± 12.5 ng L^{-1}) while the wet deposition flux was highest in summer (38.1 μg m^{-2}), followed by spring (15.4 μg m^{-2}), fall (11.7 μg m^{-2}), and winter (6.5 μg m^{-2}). Nonparametric Mann-Whitney test revealed that there were statistical differences in the VWM TM concentration between winter and other seasons ($p<0.01$) and there were statistical differences in wet deposition flux between summer and other seasons ($p<0.01$) except winter ($p=0.09$).

The high VWM TM concentration in winter was associated with the combined effect of the low rainfall depth and high speciated mercury (GOM and PBM) concentrations (Seo et al., 2012). As will be discussed later there was a statistically significant negative correlation between rainfall depth and TM concentration in precipitation ($r^2=0.19$) ($p<0.01$) which could be a factor in the high concentrations seen in winter in this study. The high TM wet deposition flux in summer (53% of total TM wet deposition flux) was primarily due to the high

precipitation rate in summer (77% of total rainfall depth). The high VWM TM concentration in spring was due to yellow sand events which occurred before wet deposition events, resulting in high speciated mercury concentrations. Yellow sand events occurred immediately prior to wet deposition events in 2006 (16 March, 29 March, 7 April and 18 April) and in 2007 (7 March, 28 March, 2 April and 9 May). During those periods GOM and PBM concentrations were elevated (50.8 pg m^{-3} GOM and 27.2 pg m^{-3} PBM on 15 March in 2006; 6.9 pg m^{-3} GOM and 12.3 pg m^{-3} PBM on 28 March; 12.0 pg m^{-3} GOM and 14.0 pg m^{-3} for PBM on 2 April; and 14.8 pg m^{-3} GOM and 67.0 pg m^{-3} PBM on 8 May in 2007) resulting in high VWM TM concentrations (55.3 ng L^{-1} on 16 March, 36.1 ng L^{-1} on 29 March, 32.8 ng L^{-1} on 18 April in 2006 and 59.1 ng L^{-1} on 7 March, 34.2 ng L^{-1} on 28 March, 23.0 ng L^{-1} on 9 May in 2007).

The VWM TM concentration during yellow sand events (34.4 ± 17.7 ng L^{-1}) (n=36) in spring were statistically higher than during non-yellow sand events in spring (15.4 ± 13.8 ng L^{-1}) (n=11) (nonparametric Mann-Whitney test, $p<0.05$). Other previous studies also suggested that the concentrations of trace elements were much higher during yellow sand events than during non-yellow sand events due to trace elements being transported from China (Kim et al., 2007; Han et al., 2004a; Seo, et al., 2012; Yi et al., 2001).

The average PBM concentrations were higher than those of GOM. The average GOM and PBM concentrations were higher in spring and winter compared to summer and fall (Table 4-2). The monthly GOM and PBM concentrations were significantly correlated (r^2=0.41, $p<0.01$) suggesting that the high VWM TM concentration in precipitation was due to the high atmospheric speciated mercury concentrations.

Table 4-2. Summary of atmospheric speciated mercury concentrations

Year			Total	Spring	Summer	Fall	Winter
2006	GOM ($pg\ m^{-3}$)	N	72	14	28	5	25
		Mean	14.0 ± 18.6	21.7 ± 24.0	6.1 ± 4.8	4.8 ± 2.9	20.3 ± 22.7
	PBM ($pg\ m^{-3}$)	N	69	13	28	4	24
		Mean	26.3 ± 42.6	18.1 ± 10.9	35.8 ± 64.7	5.8 ± 2.1	24.0 ± 15.1
2007	GOM ($pg\ m^{-3}$)	N	144	58	22	26	38
		Mean	11.5 ± 10.3	14.8 ± 13.0	7.8 ± 7.0	9.3 ± 9.0	10.2 ± 6.0
	PBM ($pg\ m^{-3}$)	N	130	58	23	18	31
		Mean	13.9 ± 13.1	14.0 ± 11.6	8.6 ± 5.5	17.9 ± 20.7	15.5 ± 13.4
2008	GOM ($pg\ m^{-3}$)	N	65	23	16	17	9
		Mean	10.6 ± 7.2	13.8 ± 7.4	9.0 ± 7.1	6.3 ± 4.0	13.8 ± 6.8
	PBM ($pg\ m^{-3}$)	N	69	23	16	21	9
		Mean	11.8 ± 9.0	11.0 ± 6.4	5.7 ± 3.3	13.7 ± 11.3	20.4 ± 8.2
2009	GOM ($pg\ m^{-3}$)	N	106	29	26	30	21
		Mean	11.1 ± 20.4	20.4 ± 33.9	8.0 ± 5.4	5.0 ± 5.2	12.4 ± 20.2
	PBM ($pg\ m^{-3}$)	N	108	26	27	28	27
		Mean	16.9 ± 21.6	24.8 ± 33.3	10.3 ± 13.0	10.6 ± 12.2	24.0 ± 19.9

Previous studies of TM wet deposition flux were divided into the following four categories for comparison: (1) MDN sites located at similar latitudes (Edmonson County, Kentucky (KY10) (latitude; 37.13) and Gloucester County, Virginia (VA98) (latitude; 37.531) with Seoul (latitude; 37.51)) because latitude is the single most important determining factor in meteorological phenomena (precipitation types, intensity and duration of sun exposure and temperature) (Hardy, 2003). In addition, a MDN site located at different latitude (Salt Lake County, Utah (UT97) (latitude; 40.71)) was also included. (2) rural sites (Eagle Harbor, Pellston, Dexter, Potsdam, Steubenville, Hokkaido, Guizhou), (3) urban sites (Aichi, Hyogo, Tokyo), and (4) remote site (Mt. Gongga, China) (Table 4-3). Annual TM wet deposition fluxes measured in 2006 (16.8 μg m^{-2}), 2007 (20.2 μg m^{-2}), 2008 (18.5 μg m^{-2}), and 2009 (16.4 μg m^{-2}) in Seoul were generally much higher than: 1) those at the MDN sites at similar latitude (KY10: 12.2 μg m^{-2} and VA98: 9.2 μg m^{-2}), and another MDN site (UT97: 8.9 μg m^{-2}) 2) rural sites (Eagle Harbor: 5.2 μg m^{-2}, Pellston: 7.4 μg m^{-2}, Dexter: 10.7 μg m^{-2} , Potsdam: 5.9 μg m^{-2}, Steubenville: 13.5 μg m^{-2} and Hokkaido: 7.1 μg m^{-2}) and 3) other urban sites (Aichi: 10.7 μg m^{-2} , Hyogo: 14.0 μg m^{-2} and Tokyo: 16.7 μg m^{-2}).

Table 4-3. Comparisons with previous studies for TM wet deposition flux

Site	Location	Sampling period	Precipitation depth (mm)	VWM conc. (ng L^{-1})	Wet deposition flux (μg m^{-2})	Representation	Reference
Kentucky(KY10), MDN	USA	Jan. 2009 ~ Dec. 2009	1544	7.8	12.2	Rural	National Atmospheric Deposition Program (2009)
Virginia (VA98), MDN	USA	Jan. 2009 ~ Dec. 2009	1346	6.8	9.2	Rural	National Atmospheric Deposition Program (2009)
Utah (UT97), MDN	USA	Jan. 2009 ~ Dec. 2009	460	19.5	8.9	Urban	National Atmospheric Deposition Program (2009)
Eagle Harbor, Michigan	USA	Jan. 2003 ~ Dec. 2003	645	8.3	5.2	Rural	Keeler and Dvonch (2005)
Pellston, Michigan	USA	Jan. 2003 ~ Dec. 2003	787	9.4	7.4	Rural	Keeler and Dvonch (2005)
Dexter, Michigan	USA	Jan. 2003 ~ Dec. 2003	896	11.9	10.7	Rural	Keeler and Dvonch (2005)
Potsdam, New York	USA	Jan. 2004 ~ Dec. 2004	1100	5.5	5.9	Rural	Lai et al. (2007)
Steubenville, Ohio	USA	Jan. 2003~ Dec. 2003	948	14.0	13.5	Rural	Keeler et al. (2006)
Hokkaido	Japan	Dec. 2002 ~ Nov. 2003	882	8.0	7.1	Rural	Sakata and Marumoto (2005)
Aichi	Japan	Dec. 2002 ~ Nov. 2003	1679	7.8	13.1	Urban	Sakata and Marumoto (2005)
Hyogo	Japan	Dec. 2002 ~ Nov. 2003	1481	9.5	14.0	Urban	Sakata and Marumoto (2005)
Tokyo	Japan	Dec. 2002 ~ Nov. 2003	1912	8.7	16.7	Urban	Sakata and Marumoto (2005)
Mt. Gongga	China	May 2006 ~ Apr. 2007	1818	14.3	26.1	Remote	Fu et al. (2010)
Wujiang River, Guizhou	China	Jan. 2006 ~ Dec. 2006	963	36.0	34.7	Rural	Guo et al. (2008) and reference cited therein
Seoul	Korea	Jan. 2006 ~ Dec. 2006	1645	10.1	16.8	Urban	This study
Seoul	Korea	Jan. 2007 ~ Dec. 2007	1235	16.3	20.2	Urban	This study
Seoul	Korea	Jan. 2008 ~ Dec. 2008	1291	16.1	18.5	Urban	This study
Seoul	Korea	Jan. 2009 ~ Dec. 2009	1822	10.2	16.4	Urban	This study

The TM wet deposition flux in Steubenville was quite low, however, the VWM TM concentration was high because of the influence of local and regional sources. There are five large coal-fired utility boilers within a 50 km radius of the site and seventeen within 100 km (Keeler et al., 2005).

In addition, the TM wet deposition flux in Mt. Gongga, China (26.1 $\mu g\ m^{-2}$) and Wujiang, River basin, Guizhou, China (34.7 $\mu g\ m^{-2}$) were much higher than those found in this study. Although Mt. Gongga is a remote area, the annual TM concentration there is very high probably because it is heavily impacted by industrial mercury emissions including non-ferrous smelting activities and coal combustion (Fu et al., 2010). The annual TM concentration in Guizhou (36.0 $ng\ L^{-1}$) was much higher than that in this study even though there was much lower annual rainfall depth (963 mm). Significantly higher TM concentrations in Guizhou result in a wet deposition flux that was about two times higher than those measured in this study. High mercury emissions in Guizhou are due to the high mercury content of raw coal in this province and the relatively large amount of uncontrolled coal combustion (Streets et al., 2005).

4.5.2. Relationship between rainfall depth, VWM TM concentration and TM wet deposition flux

There were statistically significant negative correlations between rainfall depth and log VWM TM concentrations (r^2=0.19) (p<0.01) (Figure 4-2), due to dilution effects during the later stage of precipitation event.

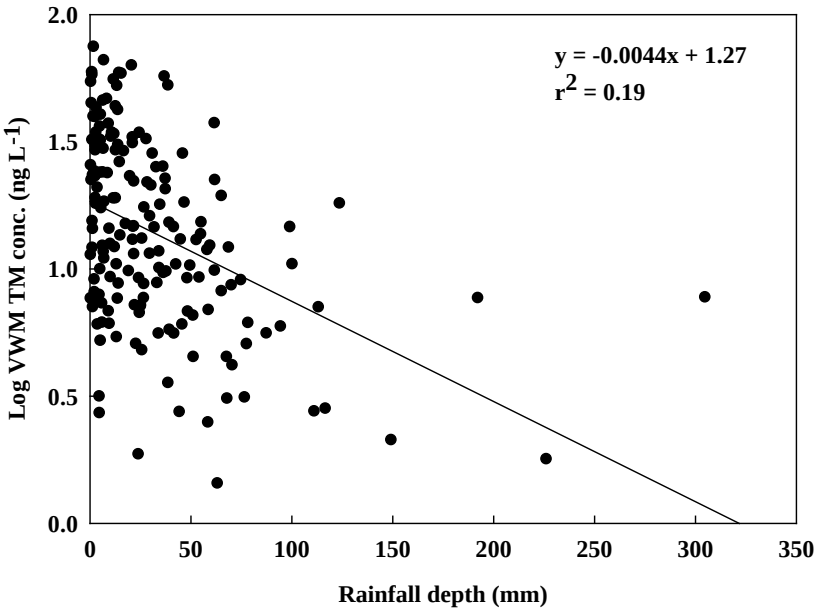

Figure 4-2. Relationship between rainfall depth and VWM TM concentration

This negative correlation has been also found by the previous studies (Guo et al., 2008; Landis et al., 2002b; Watras et al., 2000).

However, there were statistically significant positive correlations between rainfall depth and TM wet deposition flux (r^2=0.27) ($p<0.01$), suggesting that the TM wet deposition flux increased during large events even though continuous rain diluted the TM concentration in precipitation. Other factors such as the seasonal variation in atmospheric concentrations, the type of precipitation, and meteorological transport history, in particular transport through mercury source areas may also influence on the TM concentrations (Keeler et al., 2005).

4.5.3. Scavenging ratios of GOM and PBM

The TM concentration in precipitation depends on the relative atmospheric concentrations of mercury species such as GOM or PBM that are available for scavenging (Lindberg, 1982; Guentzel et al., 1995; Sakata and Asakura, 2007; Seo et al., 2012). In this study, the scavenging coefficient of GOM was calculated as $GOM_{in\ precipitation} / GOM_{in\ air}$, and the scavenging coefficient of PBM was calculated as $PBM_{in\ precipitation} / PBM_{in\ air}$. Since it is not possible to distinguish between mercury that was scavenged as GOM and that which was scavenged as PBM in precipitation samples the scavenging coefficient of each mercury species cannot be directly calculated. Instead, the

scavenging coefficients of each mercury species were estimated using multiple linear regression (SPSS) and compromise both in-cloud and below-cloud scavenging.

GOM (n=37) and PBM concentrations (n=37) measured 24 h before wet deposition events were used as independent variables, and TM concentration (n=37) was used as the dependent variable. Multiple linear regression was performed with by solving the following equation (4-5).

$$TM_{\text{in precipitation}} = SC_{GOM}\, C_{GOM} + SC_{PBM}\, C_{PBM} \qquad (4\text{-}5)$$

where SC_{GOM} and SC_{PBM} are scavenging coefficient (SC) for GOM and PBM, and C_{GOM} and C_{PBM} are atmospheric concentrations for GOM and PBM, respectively. This analysis yielded the following equation (4-6)

$$TM_{\text{in precipitation}} = 715\, C_{GOM} + 407\, C_{PBM} + 4 \qquad (4\text{-}6)$$

The multiple linear model fit the data well (r^2=0.59) and was statistically significant (p<0.01). As shown in equation (4-6), SC_{GOM} (714) is much higher than SC_{PBM} (407), suggesting that GOM was more effectively scavenged by wet deposition than was PBM. Seo et al.

(2012) determined that scavenging coefficient of GOM was about750, and Lindberg (1982) indicated that scavenging coefficient of other soluble species such as SO_4^{2-} ranged from about 430 to 1900. SC_{PBM} was within the range of values (200 to 2000) that is indicative of particle scavenging (Guentzel et al., 1995; Sakata and Asakura, 2007; Seo et al., 2012).

4.5.4. Identification of possible source location using LPDM

4.5.4.1. LPDM results at different starting heights

Previous studies reported that trajectories for long range transport (>24 h) that started at different heights may be considerably different because they traverse different distances and pathways (Hsu et al., 2003; Heo et al., 2009). According to Kim et al. (2007), mixing heights were generally < 300 m under stable conditions and about 2-3 km under well-mixed conditions in Seoul, Korea. In this study, two-day and three-day LPDM starting every hour at a height of 100 m (Approach 1), 500 m (Approach 2), 1000 m (Approach 3) above ground level were computed. LPDM starting at a height of one-half of mixing height (Approach 4) above ground level was also calculated with the HYSPLIT 4 model (Lai et al., 2007). The results for these four approaches (Figure 4-S1) suggest that VWM TM concentration in wet

deposition was regionally transported rather than globally transported. LPDM results that have started at different starting heights were similar and commonly indicate that the potential source areas included Nei Mongol, Gobi desert and industrial areas in southeast China.

4.5.4.2. LPDM result combined with different starting heights

In this study, the JP-LPDM result combined different starting heights using 72hr back-dispersion (Approach 5) is shown in Figure 4-3.

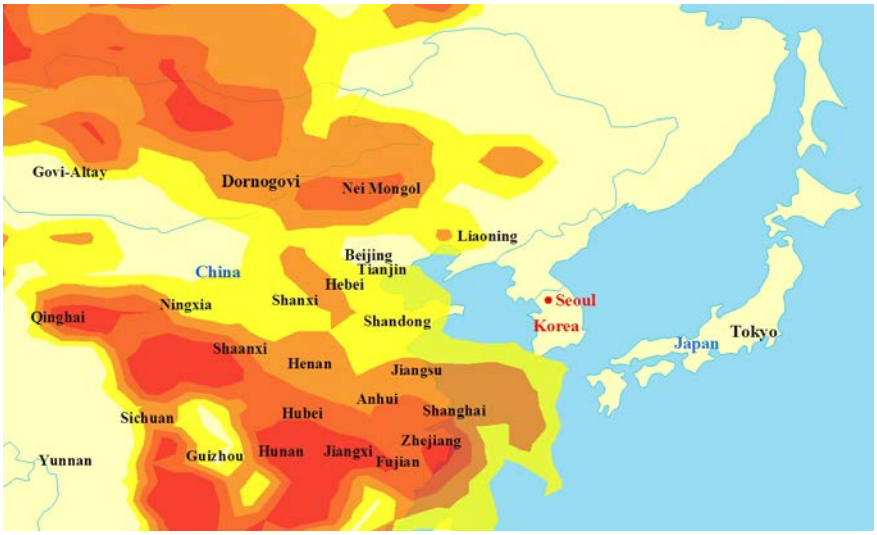

Figure 4-3. JP-LPDM result calculated from Approach 5 for VWM TM concentration

Sources contributing to the high VWM TM concentration of wet deposition at the sampling site were identified to be the major industrial area in China including Liaoning, Guangdong, Guizhou, similar to the locations identified using approaches 1-4. The spatial correlation index

(*r*) values between LPDM results and mercury emission inventories (Figure 4-S2) were compared using approaches 1-5 (Table 4-4). The indexes for LPDM using 72hr back-dispersion were consistently larger than those using 48hr back-dispersion. The largest *r* value (*r*=95.0) was obtained from the JP-LPDM that combined different starting heights using 72hr back-dispersion (Approach 5). This very large value indicates that the pairs of maps showed a very strong spatial correlation.

Table 4-4. Spatial correlation index (r) between LPDM results and emissions inventory

Approach	Starting height	Spatial correlation index (r)	
		LPDM using 48hr back-dispersion	LPDM using 72hr back-dispersion
Approach 1	100 m	64.0	92.0
Approach 2	500 m	47.6	88.3
Approach 3	1000 m	42.4	93.2
Approach 4	One-half of mixing height	45.6	48.7
Approach 5	Combined with different starting height	55.2	95.0

China is the largest mercury emitting country in the world, contributing 50% of the total anthropogenic emissions (Jiang et al., 2006; Zhang and Wong, 2007). According to the China mercury

emission inventory from 1995 to 2003 (UNEP, 2006), total mercury emissions from non-ferrous metal smelting was the largest mercury source followed by coal combustion and cement production. Streets et al. (2005) also reported that non-ferrous operations and coal are known to be large mercury emissions sources (non-ferrous metals ores generally contain higher mercury than other base metals (Pacyna and Munch, 1991)) and approximately 45% (242 ton yr^{-1}) of the mercury comes from non-ferrous metals smelting, 38% (202 ton yr^{-1}) from coal combustion, and 17% from miscellaneous activities in China.

Liaoning (54.1 t or 10.1% of total mercury emissions in China), Guangdong (44.2 t or 8.3%) and Guizhou (39 t or 7.3%) is the three highest mercury emitting provinces due to the non-ferrous metal smelters (e.g. large zinc smelting plants in Liaoning, and large zinc and lead smelting plants in Guangdong). In addition, high mercury emissions in Guizhou were due to the high mercury content of raw coal in this province and the relatively large amount of uncontrolled coal combustion. Sources contributing to the high VWM TM concentration of wet deposition at the sampling site were also identified to be the major coal supplying provinces in China including Hunan, Shaanxi, Nei Mongol. These provinces have little difference between the mercury content of coal because all, or nearly all, of the coal is obtained from within-province supplies (Streets et al., 2005). In

addition, all approaches commonly indicated that the Gobi Desert is a potential source. It is the second largest desert in China and was to be the main source of yellow sand transported to Korea. As described earlier, high VWM TM concentrations were mainly due to yellow sand events. Although the LPDM does not provide a quantitative apportionment of the amount of emissions, but it showed the specific source areas. Therefore it provides useful information on source-receptor relationships.

References

Ashbaugh, L. L., Malm, W. C., Sadeh, W. Z., 1985. A residence time probability analysis of sulfur concentrations at Grand Canyon National Park, Atmospheric Environment 19, 1263-1270.

Cheng, M.D., Hopke, P.K., Zeng, Y., 1993. A receptor-oriented methodology for determining source regions of particle sulfate composition observed at Dorset, Ontario. Journal of Geophysical Research Atmospheres 98, 16839-16849.

Cohen, M., Artz, R., Draxler, R., Miller, P., Niemi, D., Ratte, D., Deslauriers, M., Duvar, R., Laurin, R., Slotnick, J., Nettesheim, T., McDonald, J., 2004. Modeling the atmospheric transport and deposition of mercury to the Great Lakes. Environmental Research 95, 247-265.

Davis, T.D., 1984. Rainborne SO_2, precipitation pH and airborne SO_2 over short sampling times throughout individual events. Atmospheric Environment 18, 2499-2502.

Draxler, R.R. and Hess, G.D., 2005. HYSPLIT 4 USER's Guide. NOAA Technical Memorandum ERL ARL-230.

Fitzgerald, W. F. and Gill, G. A., 1979. Subnanogram determination of mercury by two-stage gold amalgamation and gas phase detection applied to atmospheric analysis. Analytical Chemistry 51, 1714-1720.

Fu, X., Feng, X., Zhu, W., Rothenberg, S., Yao, H., Zhang, H., 2010. Elevated atmospheric deposition and dynamics of mercury in a remote upland forest of Southwestern China. Environmental Pollution 158, 2324–2333.

Guentzel, J. L., Landing, W. M., Gill, G. A., Poliman, C. D., 1995. Atmospheric deposition of mercury in Florida: The FAMS project (1992-1994). Water, Air, and Soil Pollution 80, 393–402.

Guo, Y., Feng, X., Li, Z., He, T., Yan, H., Meng, B., Zhang, J., Qiu, G., 2008. Distribution and wet deposition fluxes of total and methyl mercury in Wujiang River Basin, Guizhou, China. Atmospheric Environment 42, 7096-7103.

Haining, R., 1990. Spatial Data Analysis in the Social and

Environmental Sciences. Cambridge University Press, Cambridge, UK.

Han, Y. J., Holsen, T. M., Hopke, P. K., Cheong, J. P., Kim, H., Yi, S. M., 2004a. Identification of source locations for atmospheric dry deposition of heavy metals during yellow-sand events in Seoul, Korea in 1998 using hybrid receptor models. Atmospheric Environment 38, 5353-5361.

Han, Y. J., Holsen, T. M., Lai, S. O., Hopke, P. K., Yi, S. M., Liu, W., Pagano, J., Falanga, L., Milligan, M., Andolina, C., 2004b. Atmospheric gaseous mercury concentrations in New York State: relationships with meteorological data and other pollutants. Atmospheric Environment 38, 6431–6446.

Han, Y.J., Holsen, T.M., Hopke, P.K., Yi, S.M., 2005. Comparison between Back-Trajectory Based Modeling and Lagrangian Backward Dispersion Modeling for Locating Sources of Reactive Gaseous Mercury. Environmental Science and Technology 39, 1715-1723.

Hardy, J.T, 2003. Climate change: causes, effects, and solutions. John Wiley & Sons Ltd.

Heo, J.B., Hopke, P.K., Yi, S.M., 2009. Source apportionment of $PM_{2.5}$ in Seoul, Korea. Atmospheric Chemistry and Physics 9, 4957-4971.

Hopke, P.K., Zhou, L., Poirot, R.L., 2005. Reconciling trajectory ensemble receptor model results with emissions. Environmental Science and Technology 39, 7980–7983.

Hsu, Y.K., Holsen, T.M., Hopke, P.K., 2003. Comparison of hybrid receptor models to locate PCB sources in Chicago. Atmospheric Environment 37, 545-562.

Huang, J. and Gustin, M. S., 2012. Evidence for a free troposphere source of mercury in wet deposition in the western United States. Environmental Science and Technology 46, 6621-6629.

Jiang, G.B., Shi, J. B., Feng, X. B., 2006. Mercury pollution in China. Environmental Science
and Technology 40, 3672–3678.

Keeler, G. J. and Dvonch, J. T., 2005. Atmospheric mercury: A decade

of observations in the Great Lakes. In dynamics of mercury pollution on regional and global scales: atmospheric processes and human exposures around the world; Pirrone, N., Mahaffey, K., Eds.; Kluwer Ltd: Norwell, MA.

Keeler, G. J., Gratz, L. E., Al-Wali, K., 2005. Long-term atmospheric mercury wet deposition at Underhill, Vermont. Ecotoxicology 14, 71-83.

Keeler, G. J., Landis, M. S., Norris, G. A., Christianson, E. M., Dvonch, J. T., 2006. Sources of mercury wet deposition in eastern Ohio, USA. Environmental Science and Technology 40, 5874-5881.

Kim, H.S., Huh, J.B., Hopke, P. K., Holsen, T. M., Yi, S.M., 2007. Characteristics of the major chemical constituents of $PM_{2.5}$ and smog events in Seoul, Korea in 2003 and 2004. Atmospheric Environment 41, 6762-6770.

Kim, S. H., Han, Y. J., Holsen, T. M., Yi, S. M., 2009. Characteristics of atmospheric speciated mercury concentrations (TGM, Hg(II) and Hg(p)) in Seoul, Korea. Atmospheric Environment 43, 3267-3274.

Kim, P. R, Han, Y. J., Holsen, T. M., Yi, S. M., 2012. Atmospheric particulate mercury: Concentrations and size distributions. Atmospheric Environment 61, 94-102.

Lai, S. O., Holsen, T. M., Hopke, P. K., Liu, P., 2007. Wet deposition of mercury at a New York state rural site: Concentrations, fluxes, and source areas. Atmospheric Environment 41, 4337-4348.

Landis, M. S. and Keeler, G. J., 1997. Critical evaluation of a modified automatic wet-only precipitation collector for mercury and trace element determinations. Environmental Science and Technology 31, 2610-2615.

Landis, M. S., Stevens, R. K., Schaedlich, F., Prestbo, E. M., 2002a. Development and characterization of an annular denuder methodology for the measurement of divalent inorganic reactive gaseous mercury in ambient air. Environmental Science and Technology 36, 3000–3009.

Landis, M. S., Vette, A. F., Keeler, G. J., 2002b. Atmospheric mercury in the Lake Michigan Basin: Influence of the Chicago/Gary urban

Area. Environmental Science and Technology 36, 4508-4517.

Lim, C., Cheng, M., Schroeder, W., 2001. Transport patterns and potential sources of total gaseous mercury measured in Canadian high Arctic in 1995, Atmospheric Environment 35, 1141-1154.

Lin, C.J. and Pehkonen, S.O., 1999. The chemistry of atmospheric mercury: a review. Atmospheric Environment 33, 2067-2679.

Lindberg, S. E., 1982. Factors influencing trace metal, sulfate and hydrogen ion concentrations in rain. Atmospheric Environment 16, 1701-1709.

Lucey, D., Hadjiiski, L., Hopke, P.K., Scudlark, J.R., Church, T., 2001. Identification of sources of pollutants in precipitation measured at the mid-Atlantic US coast using potential source contribution function (PSCF). Atmospheric Environment 35, 3979-3986.

Lyons, W.A., Pielke, R.A., Tremback, C.J., Walko, R. L., 1995. Modeling impacts of mesoscale vertical motions upon coastal zone air pollution dispersion. Atmospheric Environment 29, 283-301.

National Atmospheric Deposition Program, 2009. 2009 Annual Summary. Mercury Deposition Network, http://nadp.sws.uiuc.edu/lib/data/2009as.pdf.

Nguyen, K. C., Noonan, J. A., Galbally, I. E. and Physick, W. L., 1997. Predictions of plume dispersion in complex terrain: Eulerian versus Lagrangian models. Atmospheric Environment 31, 947-958.

Pacyna, J.M. and Munch, J., 1991. Anthropogenic mercury emission in Europe. Water, Air, and Soil Pollution 56, 51-61.

Park, S.U., 1990. Results of a three dimensional numerical model of land-sea breezes over South Korea. Journal of Korean Meteorological Society 26 (2), 78–103.

Poissant, L., 1999. Potential sources of atmospheric total gaseous mercury in the St.
Lawrence River valley, Atmospheric Environment 33, 2537-2547.

Plaisance, H., Coddeville, P., Guillermo, R., 1996. A qualitative determination of the source locations of precipitation constituents in

Morvan, France. Environmental Technology 17, 977-986.

Sakata, M. and Marumoto, K., 2005. Wet and dry deposition fluxes of mercury in Japan. Atmospheric Environment 39, 3139-3146.

Sakata, M. and Asakura, K., 2007. Estimating contribution of precipitation scavenging of atmospheric particulate mercury to mercury wet deposition in Japan. Atmospheric Environment 41, 1669-1680.

Schroeder, W. H. and Munthe, J., 1998. Atmospheric mercury - An overview. Atmospheric Environment 32, 809-822.

Seibert, P., 2004. Inverse modeling with a Lagrangian particle dispersion model: application to point releases over limited time intervals, edited by Schiermeier, F.A. and Gryning, S.E., *Air Pollution Modeling and its Application XIV*, Kluwer Academic/Plenum Publishers, New York, 381-389.

Seibert, P. and Frank, A., 2004. Source-receptor matrix calculation with a Lagrangian particle dispersion model in backward mode. Atmospheric Chemistry and Physics 4, 51-63.

Seo, Y.S., Han, Y.J. Choi, H.D., Holsen, T.M., Yi, S.M., 2012. Characteristics of total mercury (TM) wet deposition: Scavenging of atmospheric mercury species. Atmospheric Environment 49, 69-76.

Seymour, M.D., Schubert, S.A. Clayton, J.W., Fernando, J.Q, 1978. Variations in the acid content of rain water in the course of a single precipitation. Water, Air, and Soil Pollution 10, 147-161.

Seymour, M.D. and Stout, T., 1983. Observations on the chemical composition of rain using short sampling times during a single event. Atmospheric Environment 17, 1483-1487.

Smith, F.B., 1968. Conditioned particle motion in a homogeneous turbulent field. Atmospheric Environment 2, 491–508.

Stohl A., Eckhardt, S., Forster, C., James, P., Spichtinger, N., Seibert, P., 2002. A replacement for simple back trajectory calculations in the interpretation of atmospheric trace substance measurements. Atmospheric Environment 36, 4635-4648.

Streets, D. G., Hao, J., Wu, Y., Jiang, Y. W., Chan, M., Tian, H., Feng, X., 2005. Anthropogenic mercury emissions in China. Atmospheric Environment 39, 7789-7806.

Sutton, R., 2006. Lagrangian flow in the middle atmosphere. Quarterly Journal of the Royal Meteorological Society 120, 1299-1321.

UNEP, 2006. Improve the estimates of anthropogenic mercury emissions in China (accessed on August 28 2012 at http://www.chem.unep.ch/MERCURY/China%20emission%20inventory%20.pdf)

U.S. EPA, 1994a. Lake Michigan Mass Balance Methods Compendium, Standard Operating Procedure for Analysis of Mercury in Precipitation, http://www.epa.gov/glnpo/lmmb/methods/umanalyt.pdf.

U.S. EPA, 1994b. Lake Michigan Mass Balance Methods Compendium, Standard Operating Procedure for Sampling of Mercury in Precipitation, http://www.epa.gov/glnpo/lmmb/methods/umfield.pdf.

U.S. EPA, 1997. Mercury study report to Congress. Office of Air Quality Planning and Standards and Office of Research and Development; EPA-452/R-97-005; U.S. Government Printing Office: Washington, DC.

U.S. EPA, 2002. Method 1631 (rev. E), Mercury in water by oxidation, purge and trap, and cold vapor atomic fluorescence spectrometry.

Watras, C. J., Morrison, K. A., Hudson, R. J. M., Frost, T. M., Kratz, T. K., 2000. Decreasing mercury in Northern Wisconsin: Temporal patterns in bulk precipitation and a precipitation-dominated lake. Environmental Science and Technology 34, 4051-4057.

Yi, S. M., Lee, E. Y., Holsen, T. M, 2001. Dry deposition fluxes and size distributions of heavy metals in Seoul, Korea during yellow sand events. Aerosol Science and Technology 35, 569–576.

Zeng, Y. and Hopke, P.K., 1989. A study of the sources of acid precipitation in Ontario, Canada. Atmospheric Environment 23, 1499-1509.

Zhang, L. and Wong, M.H., 2007. Environmental mercury contamination in China: sources and impacts. Environment International 33, 108-121.

Supporting Information

Sampling program

The precipitation samples were collected using a modified MIC-B automatic precipitation collector (MIC, Thornhill, Ontario) equipped with four discrete precipitation sampling systems that allows for two mercury sampling trains and two trace elements sampling trains as was used and validated in previous studies (Lai et al., 2007; Landis and Keeler, 1997; Seo et al., 2012). Briefly, the mercury sampling train consists of a borosilicate glass funnel, a glass vapor lock, a Teflon adapter and a Teflon bottle that was acid-cleaned before field use. The sampling trains were manually deployed only when precipitation was forecast and were retrieved after precipitation stopped.

GOM and PBM (dp < 2.5 μm) were collected using a KCl-coated annular denuder and quartz filter, respectively, at a flow rate 10 L min^{-1}. The sampling system included a coupler, elutriator, impactor, filter holder (URG Inc.), dry gas meter, pump, and a sampling box maintained at 50 ℃ to prevent hydrolysis of KCl. The quartz annular denuders were cleaned, coated and conditioned prior to GOM sampling. Once the denuder was coated and dried, it was thermally conditioned to ensure that the KCl coating was preserved in place and that any

residual mercury was eliminated (Landis et al., 2002a). The quartz filters were used to collect PBM less than 2.5 μm in size and were baked in a tube furnace at 900 ℃ for one hour before use.

Analytical Methods

Total Mercury (TM) in precipitation was measured using a Tekran Series 2600 equipped with cold vapor atomic fluorescence spectrometry (CVAFS) (Tekran Inc., Toronto, Canada) followed the procedures outlined in the U.S. EPA Method 1631 version E (U.S. EPA, 2002) and the U.S. EPA LMMBMC (U.S. EPA, 1994a). Prior to being analyzed, the samples were oxidized with BrCl to a 1% solution (v/v) and were stored in a refrigerator (4℃) for at least 12 hours. Mercury was then purged from the solution with a high purity argon stream after reduction with $NH_2OH{\cdot}HCl$ and reduction of divalent mercury by $SnCl_2$ to Hg^0 and concentrated onto a gold-coated bead trap (Fitzgerald and Gill, 1979; Landis and Keeler, 1997). Calibration standards were prepared by diluting the mercury stock solution (SRM 3133, mercury standard solution) which was purchased from the National Institute of Standards and Technology (NIST).

QA/QC

Quality assurance and quality control procedures for TM in precipitation were based on the U.S. EPA Method 1631 version E (U.S. EPA., 2002) and Lake Michigan Mass Balance Methods Compendium (LMMBMC) (U.S. EPA, 1994a). The standard curve was deemed acceptable when r^2 was greater than 0.995 (linear) over a mercury concentration range from 0.5 to 100 ng L^{-1}. Initial precision and recovery (IPR) and ongoing precision and recovery (OPR) solution (5 ppt) analyzed prior to the analysis of any samples and subsequently every 20 samples ranged between 93% and 107%, and 90% and 117%, respectively. The relative percent difference (RPD) between duplicate samples (n=172) was 7.4 ± 6.3 %. Recovery (%) of diluted standard reference materials (SRMs) (DORM2, National Research Council of Canada and SRM 1641d, NIST) was measured at the start of the experiments and ranged between 90 and 110 % (100.1 ± 4.3 % in average). The MDL (three times the standard deviation of seven sequential reagent blanks) for total mercury was 0.06 ng L^{-1}. Field blanks (n=48) were collected by deploying the sampling assembly inside the MIC-B during non-precipitation conditions. The average field blank concentration was 0.26 ± 0.23 ng L^{-1}. All samples were corrected by the associated monthly field blank. The actual sample concentrations ranged from 1.4 to 74.4 ng L^{-1}.

Potential Source Contribution Function (PSCF)

The PSCF model counts each trajectory segment endpoint within a given grid cell. For an event at the receptor site, the probability is related to the number of endpoints in that cell associated with the total number of endpoints for all sampling dates. If N is the total number of trajectory segment endpoints over the study period, and if n is the number of trajectory segment endpoints fall into the *ij*-th cell, the probability of this events, A_{ij}, is calculated by

$$P[A_{ij}] = n_{ij} / N$$

If the m_{ij} is the number of segment endpoints in the same grid cell (*ij*-th cell) when the concentrations are higher than a criterion value, the probability of this high concentration event, B_{ij}, is given by $P[B_{ij}]$,

$$P[B_{ij}] = m_{ij} / N$$

The probability of high concentration event divided by the probability of total event in a fixed grid cell defines the PSCF value as

$$PSCF_{ij} = \frac{P[B_{ij}]}{P[A_{ij}]} = \frac{m_{ij}/N}{n_{ij}/N} = \frac{m_{ij}}{n_{ij}}$$

High PSCF values in that grid those grid cells are regarded as possible source locations. Cells including emission sources could be identified with conditional probabilities close to one if trajectories that have crossed the cells efficiently transport the released pollutant to the receptor site. Therefore, the PSCF model provides a tool to map the source potentials of geographical areas.

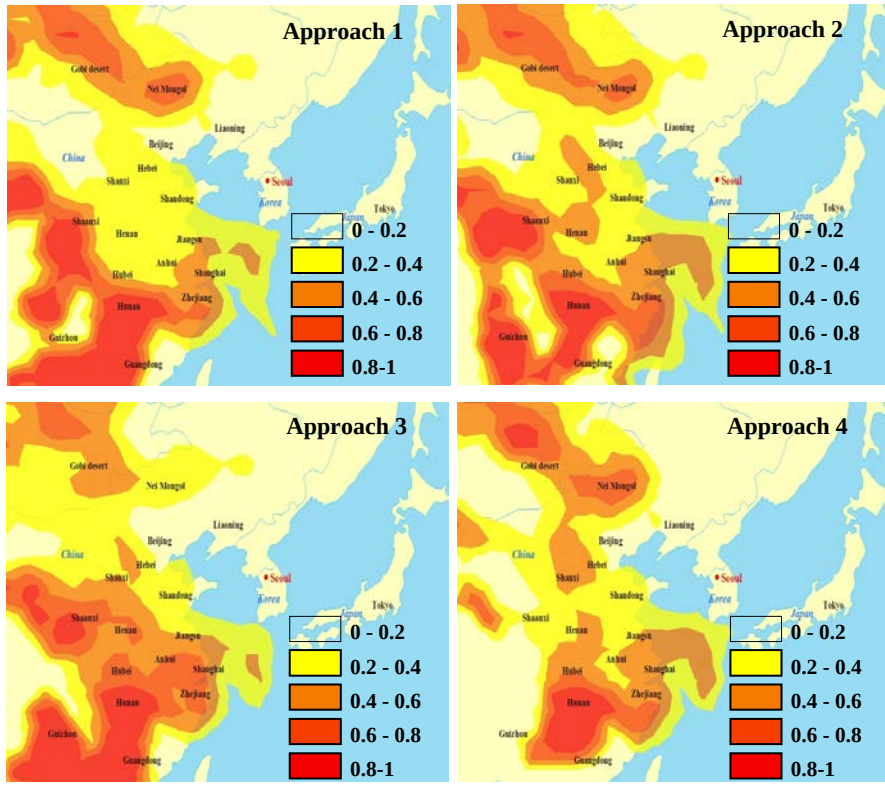

Figure 4-S1. LPDM results calculated from Approach 1 to 4 for VWM TM concentration at different starting heights.

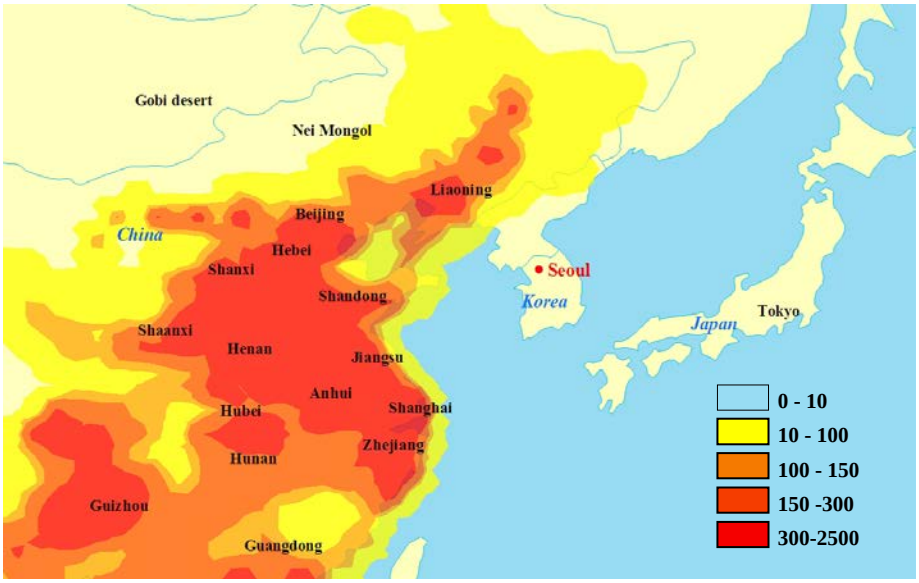

Figure 4-S2. GOM emission map of China (Units: kg/grid·year; Grid size: 0.5 degree; Reference year: 2000; Source: David Streets at Argonne National Lab)

Chapter 5
Conclusions

In this study, total mercury (TM) in precipitation samples was collected with a modified MIC-B sampler on the roof of Graduate School of Public Health building in Seoul, Korea from January 2006 to December 2009 to determine the seasonal variations and to identify the contribution of GOM and PBM scavenging to mercury wet deposition, and to identify the source areas contributing to the high TM wet deposition using a Lagrangian particle dispersion model (LPDM).

The volume weighted mean (VWM) TM concentrations in 2006, 2007, 2008 and 2009 were 10.1 ± 17.0 ng L^{-1}, 16.3 ± 16.5 ng L^{-1}, 14.3 ± 11.9 ng L^{-1} and 10.2 ± 14.8 ng L^{-1}, respectively and the TM wet deposition flux in 2006, 2007, 2008 and 2009 were 16.8 μg m^{-2}, 20.2 μg m^{-2}, 18.5 μg m^{-2} and 16.4 μg m^{-2}, respectively. During the sampling period, the VWM TM concentration was highest in winter (27.0 ± 15.4 ng L^{-1}), followed by spring (18.2 ± 16.3 ng L^{-1}), fall (15.7 ± 13.6 ng L^{-1}), and summer (9.9 ± 12.5 ng L^{-1}) while the wet deposition flux was highest in summer (38.1 μg m^{-2}), followed by spring (15.4 μg m^{-2}), fall (11.7 μg m^{-2}), and winter (6.5 μg m^{-2}).

The VWM TM concentration during yellow sand events (34.4 ± 17.7 ng L^{-1}) (n=36) in spring were statistically higher than during non-

yellow sand events in spring (15.4 ± 13.8 ng L^{-1}) (n=11) (nonparametric Mann-Whitney test, $p<0.05$).

There were statistically significant negative correlations between rainfall depth and log VWM TM concentrations ($r^2=0.19$) ($p<0.01$), due to dilution effects during the later stage of precipitation event. However, there were statistically significant positive correlations between rainfall depth and TM wet deposition flux ($r^2=0.27$) ($p<0.01$), suggesting that the TM wet deposition flux increased during large events even though continuous rain diluted the TM concentration in precipitation.

Multiple linear regression showed that the scavenging coefficient (SC) for GOM was much higher than the SC for PBM indicating that GOM was more effectively scavenged by wet deposition than PBM (SC_{GOM} = 715 and SC_{PBM} = 407).

Joint-probability LPDM (JP-LPDM) indicated that the main sources contributing to the high VWM TM concentration of wet deposition at the sampling site were identified to be the major industrial area in China including Guizhou, Guangdong, Liaoning, Hunan, Shaanxi, Nei Mongol and Gobi Desert. This suggested that both anthropogenic sources such as industrial areas and natural source areas such as deserts contributed to the high TM concentration in Seoul, Korea. The spatial correlation indexes (r) values for LPDM using 72hr back-dispersion were consistently larger than those using 48hr back-dispersion. The

largest r value was obtained from the JP-LPDM that combined different starting heights using 72hr back-dispersion. This very large value indicates that the pairs of maps showed a very strong spatial correlation.

국문초록

서울시 대기 중 총 수은의 습식침적량 특성에 관한 연구: 수용모델을 이용한 오염 가능 지역 위치 파악

서울대학교 대학원
보건학과 환경보건 전공
서용석

서울대학교 보건대학원 옥상에서 2006년 1월부터 2009년 12월까지 자동 강우 채취기를 이용하여 강수 중에 포함되어 있는 총 수은 시료를 채취 및 분석하고 동시에 대기 중 가스상 산화수은과 입자상 수은을 채취 및 분석하였다. 이들 시료를 이용하여 습식침적에 의한 총 수은의 계절적인 변화를 살펴보고 대기 중 가스상 수은과 입자상 수은의 습식침적에 대한 기여도를 알아보고 또한 수용모델을 이용하여 오염원의 위치를 파악하였다.

강수 내 총 수은의 부피가중 평균 농도는 2006년, 2007년, 2008년, 2009년이 각각 10.1 ± 17.0 ng L^{-1}, 16.3 ± 16.5 ng L^{-1}, 14.3 ± 11.9 ng L^{-1}, and 10.2 ± 14.8 ng L^{-1} 이었고, 총 수은의 습식침적량은 각각 16.8 μg m^{-2}, 20.2 μg m^{-2}, 18.5 μg m^{-2}, 16.4 μg m^{-2} 이었다. 시료채취 기간 동안 총 수은의 부피가중 평균 농도는 겨울, 봄, 가을, 여름의 순으로

나타났으나, 습식침적량은 여름, 봄, 가을, 겨울의 순으로 나타났다. 비모수 검정을 통해 겨울철의 총 수은의 농도가 다른 계절에 비해 통계적으로 유의하게 높았음을 알 수 있었고(p<0.01), 여름철의 총 수은의 습식침적량은 겨울철을 제외한(p=0.09) 나머지 계절에 비해 통계적으로 유의하게 높았음을 알 수 있었다(p<0.01).

강수 중 총 수은의 부피가중 평균 농도가 겨울철에 높은 이유는 적은 강수량과 대기 중 가스상 산화 수은과 입자상 수은의 농도가 높았기 때문인 것으로 보인다. 또한 봄철에 총 수은의 부피가중 평균 농도가 높은 이유는 황사의 영향이 큰 것으로 보이는데 이는 강수 중에 존재하는 가스상 산화수은과 입자상 수은이 중국으로부터 장거리 이동을 통해 우리나라에 영향을 미친 것으로 보인다. 비가 오기 전 황사가 발생했을 때, 대기 중 가스상 산화수은과 입자상 수은의 농도가 높은 것을 확인하였으며, 이로 인해 강수 중의 총 수은 농도가 높았다는 것을 알 수 있었다.

연구기간 중 여름철의 습식침적량은 총 습식침적량의 53%을 차지하였는데 이는 총 연구기간 중 빗물 양의 77%가 여름철에 집중되었기 때문인 것으로 보인다.

다중회귀 분석을 이용하여 입자상 수은의 소기계수(407)에 비해 가스상 산화 수은의 소기계수(715)가 더 크다는 것을 확인하였는데 이를 통해 가스상 산화수은이 입자상 수은에 비해 소기가 잘된다는 것을 알 수 있었다.

수용모델인 Joint-probability Lagrangian particle dispersion model (JP- LPDM)을 이용하여 습식침적에 의한 총 수은의

주요 오염원을 파악한 결과, 중국의 Guizhou, Guangdong, Liaoning, Hunan, Shaanxi, Nei Mongol 및 Gobi 사막이 주요 오염원으로 나타났다. 이는 서울 지역에 영향을 미치는 습식침적에 의한 총 수은의 오염원이 산업지역과 같은 인위적인 오염원뿐만 아니라, 자연적인 오염원도 기여한다는 것을 알 수 있었다.

주요어: 총 수은, 가스상 산화수은, 입자상 수은, 습식침적, 소기계수, Joint-probability Lagrangian particle dispersion model (JP-LPDM)

학번: 2005-31234